Medium Access Control, Packet Routing, and Internet Gateway Placement in Vehicular Ad Hoc Networks

by

Hassan Aboubakr Omar

A thesis
presented to the University of Waterloo
in fulfillment of the
thesis requirement for the degree of
Doctor of Philosophy
in
Electrical and Computer Engineering

Waterloo, Ontario, Canada, 2014

Author's Declaration

I hereby declare that I am the sole author of this thesis. This is a true copy of the thesis, including any required final revisions, as accepted by my examiners.

I understand that my thesis may be made electronically available to the public.

Abstract

Road accidents represent a serious social problem and are one of the leading causes of human death and disability on a global scale. To reduce the risk and severity of a road accident, a variety of new safety applications can be realized through wireless communications among vehicles driving nearby each other, or among vehicles and especially deployed road side units (RSUs), a technology known as a vehicular ad hoc network (VANET). Most of the VANET-enabled safety applications are based on broadcasting of safety messages by vehicles or RSUs, either periodically or in case of an unexpected event, such as a hard brake or dangerous road condition detection. Each broadcast safety message should be successfully delivered to the surrounding vehicles and RSUs without any excess delay, which is one of the main functions of a medium access control (MAC) protocol proposed for VANETs. This thesis presents VeMAC, a new multichannel time division multiple access (TDMA) protocol specifically designed to support the high priority safety applications in a VANET scenario. The ability of the VeMAC protocol to deliver periodic and event-driven safety messages in VANETs is demonstrated by a detailed delivery delay analysis, including queueing and service delays, for both types of safety messages. As well, computer simulations are conducted by using MATLAB, the network simulator ns-2, and the microscopic vehicle traffic simulator VISSIM, in order to evaluate the performance of the VeMAC protocol, in comparison with the IEEE 802.11p standard and the ADHOC MAC protocol (another TDMA protocol proposed for ad hoc networks). A real city scenario is simulated and different performance metrics are evaluated, including the network goodput, protocol overhead, channel utilization, protocol fairness, probability of a transmission collision, and safety message delivery delay. It is shown that the VeMAC protocol considerably outperforms the existing MAC schemes, which have significant limitations in supporting VANET safety applications.

In addition to enhancing road safety, in-vehicle Internet access is one of the main applications of VANETs, which aims at providing the vehicle passengers with a low-cost access to the Internet via on-road gateways. This thesis presents a new strategy for deploying Internet gateways on the roads, in order to minimize the total cost of gateway deployment, while ensuring that a vehicle can connect to an Internet gateway (using multihop communications) with a probability greater than a specified threshold. This cost minimization problem is formulated by using binary integer programming, and applied for optimal gateway placement in a real city scenario. To the best of our knowledge, no previous strategy for gateway deployment has considered the probability of multihop connectivity among the vehicles and the deployed gateways. In order to allow a vehicle to discover the existence of an Internet gateway and to communicate with the gateway via multihops, a novel data

packet routing scheme is proposed based on the VeMAC protocol. The performance of this cross-layer design is evaluated for a multichannel VANET in a highway scenario, mainly in terms of the end-to-end packet delivery delay. The packet queueing at each relay vehicle is considered in the end-to-end delay analysis, and numerical results are presented to study the effect of various parameters, such as the vehicle density and the packet arrival rate, on the performance metrics.

The proposed VeMAC protocol is a promising candidate for MAC in VANETs, which can realize many advanced safety applications to enhance the public safety standards and improve the safety level of drivers/passengers and pedestrians on roads. On the other hand, the proposed gateway placement strategy and packet routing scheme represent a strong step toward providing reliable and ubiquitous in-vehicle Internet connectivity.

Acknowledgements

I would like to express my deep appreciation to Prof. Weihua Zhuang for her exemplary supervision, great support, and valuable advice throughout my PhD program.

I sincerely would like to thank Prof. Sherman (Xuemin) Shen and all my colleagues at the Broadband Communications Research (BBCR) group for the beneficial discussions, research collaboration, and continuous exchange of knowledge.

I gratefully acknowledge my PhD committee members, Prof. Fakhri Karray, Prof. Nasser Azad, Prof. Sagar Naik, and Prof. Yi Qian, for their constructive comments and suggestions, which helped to improve the quality of the thesis. Also, it is a pleasure to truly acknowledge Prof. Jon Mark for accepting to serve as a delegate in my PhD thesis examining committee.

I would like to thank my colleague Usama Shahdah, a PhD student in the Transportation Systems Research group at the University of Waterloo, for his very useful guidance for conducting vehicle traffic computer simulations.

Sincere thanks go to Prof. Emad Al-Hussaini, Prof. Hany Abd El-Malek, and Prof. Nabila Seif, from the Faculty of Engineering at Cairo University, for providing supportive recommendation letters at the time of my application for a PhD program at the University of Waterloo.

Praise be to Allah

This PhD thesis is dedicated to my mother, Samia, my father, Aboubakr, and my sister, Dina.

Table of Contents

List of Figures

List of Tables

List of Abbreviations

AcS	Acceptance of Services.
AnS	Announcement of Services.
HPSA	High Priority Short Applications.
1PPS	One Pulse Per Second.
A-opt	ADHOC-optimal.
AC	Access Category.
AE	ADHOC-enhanced.
AIFS	Arbitrary Interfram Space.
BSM	Basic Safety Message.
CCH	Control Channel.
CDF	Cumulative Distribution Function.
CDMA	Code Division Multiple Access.
CPThresh	Capture Threshold.
CSThresh	Carrier Sensing Threshold.
CTS	Clear-To-Send.
CW	Contention Window.
DSRC	Dedicated Short Range Communications.
EDCA	Enhanced Distributed Channel Access.

ETSI European Telecommunications Standards Institute.

FCC Federal Communication Comission.

FCS Frame Check Sequence.

GDP Gateway Discovery Packet.

GPS Global Positioning System.

GPSR Greedy Perimeter Stateless Routing.

HOL Head of Line.

i.i.d. Independent and Identically Distributed.

ID Identifier.

ITS Intelligent Transportation System.

LTE-A Long Term Evolution Advanced.

MAC Medium Access Control.

MANET Mobile Ad Hoc Network.

MPDU MAC Layer Protocol Data Unit.

MSDU MAC Layer Service Data Unit.

MTU Maximum Transmission Unit.

OBU On-Board Unit.

OFDM Orthogonal Frequency Division Multiplexing.

PDF Probability Density Function.

PDU Protocol Data Unit.

PGF Probability Generating Function.

PLCP Physical Layer Convergence Procedure.

PMF Probability Mass Funciton.

PN Pseudo Noise.

QoS Quality-of-Service.

RSU	Road Side Unit.
RTS	Request-To-Send.
RxThresh	Receiving Threshold.
SCH	Service Channel.
SDMA	Space Division Multiple Access.
SRP	Slot Release Prevention.
TDMA	Time Division Multiple Access.
TH	Two Hop.
THS	Two-Hop Set.
THSO	Two-Hop Set Occupancy.
TTL	Time-To-Live.
USDoT	United States Department of Transportation.
UW	University of Waterloo.
V-inf	VeMAC with $\tau = \infty$.
V0	VeMAC with $\tau = 0$.
V2R	Vehicle-To-Road Side Unit.
V2V	Vehicle-To-Vehicle.
VANET	Vehicular Ad Hoc Network.
VSC	Vehicle Safety Communications.

List of Symbols

α_i	Minimum probability threshold required to a vehicle located at the i^{th} cell to connect to each of ν_i gateways
β_i	Index set of all gateways which can be reached by a vehicle located in cell i within ρ_{max} hops
η	Rate of the Poisson process which represents the distribution of the vehicles along a highway segment at any time instant
η_{lane}	Rate of the Poisson process which represents the distribution of the vehicles in each lane of a highway segment at any time instant
γ_j	Cost of deploying a gateway at the j^{th} location
λ	Arrival rate of event-driven safety messages (Chapter 4) or packet generation rate at the application layer of each vehicle (Chapter 5)
λ_r^m	Total packet arrival rate at the r^{th} vehicle in the m^{th} hop-region
λ_v	Rate of vehicle arrival from each possible entry of the road network in the VISSIM simulations
$\mathbb{E}(X)$	Expected value of a random variable X
$\mathcal{A}_x$	Set of time slots that node x can attempt to access on the control channel
$\mathcal{D}_x$	Set of one-hop neighbors of node x which have not successfully received a certain packet broadcasted on the control channel (possibly by node x itself)
$\mathcal{F}$	Set of time slots on the control channel associated with road side units
$\mathcal{J}$	Optimal set of gateway location indices

$\mathcal{L}$	Set of time slots on the control channel associated with vehicles moving to the left directions
$\mathcal{N}_x$	Set of one-hop neighbours of node x, from which node x has received VeMAC Type1 packets on the control channel in the previous L slots
$\mathcal{Q}_x$	Set of time slots acquired by node x on the control channel
$\mathcal{R}$	Set of time slots on the control channel associated with vehicles moving to the right directions
$\mathcal{R}_x$	Set of potential relays included by vehicle x in a broadcasted gateway discovery packet
$\mathcal{T}_x$	Set of time slots that node x must not use on the control channel in the next L time slots
$\mathcal{T}_x^m$	Set of time slots that node x must not use on channel c_m in the next l_m time slots
$\mathcal{E}$	Event (probability theory)
$\mathcal{G}_m$	Event that random variable G_m takes a value g_m
$\mathcal{H}_m$	Event that random variable H_m takes a value h_m
$\mathcal{N}_m$	Event that random variable N_m takes a value n_m
$\mathcal{U}_{i,r}^m$	Event that the i^{th} vehicle in the m^{th} hop-region exists and its communication range can reach the r^{th} vehicle in the $(m-1)^{\text{st}}$ hop-region
$\mathcal{V}_{i,r}^m$	Event that the i^{th} vehicle in the m^{th} hop-region exists and uses the r^{th} vehicle in the $(m-1)^{\text{st}}$ hop-region as a relay to a gateway
$\mathcal{W}_i^m$	Event that W_i^m takes a value w_i^m
$\min(x, y)$	Minimum of x and y
μ_n	Average number of contending nodes which acquire a time slot within n frames obtained from mathematical analysis
μ_n^{sim}	Average number of contending nodes which acquire a time slot within n frames obtained from computer simulations

ν_i	Number of gateways that a vehicle located at the i^{th} cell can connect to, each with a probability not less than a threshold α_i
$\overline{X^2}$	Second moment of a random variable X
$\overline{X}$	First moment of a random variable X
$\Pi(z)$	Probability generating function of the number of packets in the queue just before the start of the service time of a head of line batch
π_j	The $(j-1)^{\text{st}}$ constant among the b constants in $\Pi(z)$
ρ_{max}	Maximum allowed value of ρ_j for any j
ρ_j	Maximum number of hops that a gateway deployed at the j^{th} location can use to connect to a certain vehicle
σ_{ijk}	Probability that a vehicle at the i^{th} cell can reach a gateway at the j^{th} position within k hops
τ	VeMAC split up parameter
BX_{add}	Additive part of the safety distance
BX_{mult}	Multiplicative part of the safety distance
ID_k^x	VeMAC ID used by node x to access time slot k
Length_h	Length of the highway segment simulated in MATLAB
Length_s	Length of a street in the city scenario simulated in MATLAB
$\text{M/G}^{(b)}/1$	A queueing system with Poisson arrival of customers and independent time intervals between successive occasions of service, where the customers are served in batches of a maximum batch-size b
ϱ	Average number of packet arrivals to an $\text{M/G}^{(b)}/1$ between two successive occasions of service divided by the batch-size b
ϑ_x^m	Set of time slots over which a provider node x offers a service on service channel c_m
$\widetilde{N}_m$	Total number of vehicles in the m^{th} hop-region which can reach at least one vehicle in the $(m+1)^{\text{st}}$ hop-region

ξ_i	Packet arrival rate coming to a relay vehicle from its i^{th} one-hop neighbour
A_r^n	Number of ways of obtaining an ordered subset of r elements from a set of n elements
a_y^m	Time slot over which a user node x transmits an acknowledgement packet on service channel c_m
b	Batch-size, i.e., the maximum number of packets that a node can announce over a time slot on the control channel to be transmitted on the same service channel
c_i	Service channel number i
C_r^n	Number of ways of obtaining a subset of r elements from a set of n elements
$d_{\max}$	A delay threshold on the average packet delay required to be achieved at each vehicle
D_{r}^m	Average packet delay at a randomly chosen relay in the m^{th} hop-region
D_{v}^m	Average packet delay at a randomly chosen vehicle in the m^{th} hop-region
E^m	Average end-to-end delay from a randomly chosen vehicle in the m^{th} hop-region to a gateway
F_n	Probability that a specific node (among the contending ones) acquires a time slot within n frames
F_n^{all}	Probability that all the contending nodes acquire a time slot within n frames
F_X	Cumulative distribution function of a discrete random variable
f_X	Probability mass function of a discrete random variable
$G'_X(z)$	Derivative of $G_X(z)$ with respect to z
G_m	Gap between the first vehicle in the m^{th} hop-region and the farthest edge of the region with respect to the gateway
G_X	Probability generating function of a discrete random variable which takes non-negative integer values

H_m	Distance separating the first vehicle in the m^{th} hop-region and that in the $(m-1)^{\text{st}}$ hop-region
I	Inter-arrival time of periodic safety messages
$I_{(a<b)}$	Indicator variable which equals 1 if $a < b$ and equals 0 otherwise
$I_{i,r}^m$	Indicator variable which equals 1 whenever event $\mathcal{V}_{i,r}^m$ occurs, and equals 0 otherwise.
J	Index of a time slot at the start of which a safety message becomes the head of line
K	Total number of nodes which need to acquire a time slot on the control channel
k	Number of time slots that a node acquires per frame
$K(z)$	Probability generating function of the number of packet arrivals during S_r^m
k_e	Number of event-driven time slots that a node acquires per frame on the control channel
k_p	Number of periodic time slots that a node acquires per frame on the control channel
k_r^m	Number of time slots that the r^{th} vehicle in the m^{th} hop-region acquires per frame, over which the vehicle can transmit VeMAC Type1 packets
L	Number of time slots per frame on the control channel
l_m	Number of time slots per frame on channel c_m
M	Number of hop-regions which partition a highway segment
$M_{i,j}$	Entry of a matrix M, located at the i^{th} row and j^{th} column
N	Number of available time slots in a frame
N_{cells}	Total number of road cells under consideration
N_{gate}	Total number of potential gateway locations
N_{lanes}	Number of lanes of a highway segment

N_c	Number of contending nodes attempting to acquire a specific time slot
N_f	Number of periodic safety message fragments queued before a tagged fragment within a batch
n_f	Total number of fragments of a periodic safety message
N_m	Number of vehicles located in the m^{th} hop-region
N_q	Total number of vehicles successfully acquiring a time slot
N_s	Total number of streets in the city scenario simulated in MATLAB
N_v	Total number of vehicles used for MATLAB simulations in highway and city scenarios
N_{input}	Number of one-hop neighbours of a relay vehicle
N_{sch}	Number of service channels
N_{max}	Maximum number of nodes which can exist in a two-hop set
N_{succ}^{x}	Number of nodes in the two-hop neighbourhood of node x which have successfully acquired a time slot
O_m	Total number of time slots used by all the vehicles in the m^{th} hop-region
P	One-step transition probability matrix of a Markov chain
P^n	n-step transition probability matrix of a Markov chain
p_{acc}	Probability of accessing an available time slot in the ADHOC MAC protocol
p_{ij}	Transition probability from state i to state j in a Markov chain
p_{opt}	Optimal probability of accessing an available time slot
Q_r^m	Packet queueing delay at the r^{th} vehicle in the m^{th} hop-region
R	Communication range
r_x	Ratio of the number of safety messages transmitted by node x to the total number of safety messages transmitted by all nodes during the simulation time

S_r^m	Time duration (in the unit of a time slot) between successive occasions of announcement for a head of line batch on the control channel
s_x	Total number of safety messages generated at node x normalized by the total number of safety messages generated at all nodes during the simulation time
t	Duration of a time slot on the control channel
T_m	Total number of time slots used by all the vehicles in the m^{th} two-hop region
t_x	One of the time slots acquired by node x on the control channel
t_{in}	Total time of arrival of vehicles to the road network in the VISSIM simulations
t_w	Warm up period in the VISSIM simulations
V_m	Total number of time slots used by $\widetilde{N}_m$
W	Total delay (sum of the service delay and queueing delay)
$W(l, u, v)$	Number of ways by which l nodes can acquire a time slot given that there are u contending nodes each randomly choosing a time slot among v available time slots
W_b	Total service delay of a batch of fragments of a periodic safety message
W_i^m	Distance between the first vehicle in the m^{th} hop-region and the i^{th} vehicle (if exists) in the same region
W_q	Queueing delay
W_s	Service delay
W_{q_1}	Delay since a batch of fragments of a periodic safety enters the queue until the first fragment of the batch becomes the head of line
W_{q_2}	Service delay of all the periodic safety message fragments queued before a tagged fragment within a batch
x_j	Binary decision variable which equals 1 iff a gateway is deployed at the j^{th} potential gateway location
X_n	Total number of nodes which acquired a time slot within n frame

y_{jk}	Binary decision variable which equals 1 iff a gateway is deployed at the j^{th} location and has $\rho_j = k$
z_{ij}	Binary decision variable which equals 1 if [only if] a gateway is deployed at the j^{th} location and can reach a vehicle at the i^{th} cell within ρ_j hops with a probability greater than [greater than or equal to] α_i
AX	Average standstill distance

Chapter 1

Introduction

1.1 Vehicular Ad Hoc Networks

An ad hoc network is defined as a collection of nodes dynamically forming a network without any existing infrastructure or centralized administration. One special type of mobile ad hoc networks is the network among moving vehicles, which is known as vehicular ad hoc network (VANET). A VANET is an emerging technology which consists of a set of vehicles, each equipped with a communication device called on-board unit (OBU), and a set of stationary units along the road, referred to as road side units (RSUs). As shown in Fig. 1.1, some RSUs can act as a gateway for connectivity to other communication networks, such as the Internet. Each vehicle OBU has a wireless network interface which allows the vehicle to directly connect to other vehicles and RSUs within its communication range, as well as a wireless or wired interfaces to which application units can be attached. By employing vehicle-to-vehicle (V2V) and vehicle-to-RSU (V2R) communications, VANETs can support a wide variety of applications in road safety, passenger infotainment, and vehicle traffic optimization [2, 3, 4], which is the main reason that VANETs have received significant support from government, academia, and industrial organizations over the globe.

Motivated by the importance of vehicular communications, in 1999, the United States Federal Communication Comission (FCC) has allocated 75 MHz radio spectrum in the 5.9 GHz band for dedicated short range communications (DSRC) to be exclusively used by V2V and V2R communications. Similarly, in 2008, the European Telecommunications Standards Institute (ETSI) has allocated 30 MHz of spectrum (also in the 5.9 GHz band) for Intelligent Transportation System (ITS) applications. As shown in Fig. 1.2, the DSRC spectrum is divided into seven 10 MHz channels: six service channels for safety and non-safety related

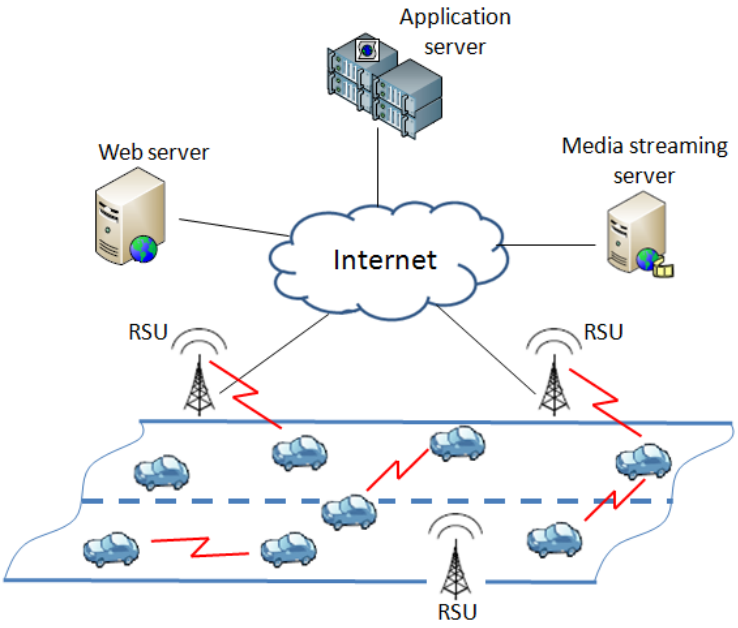

Figure 1.1: Illustration of a VANET.

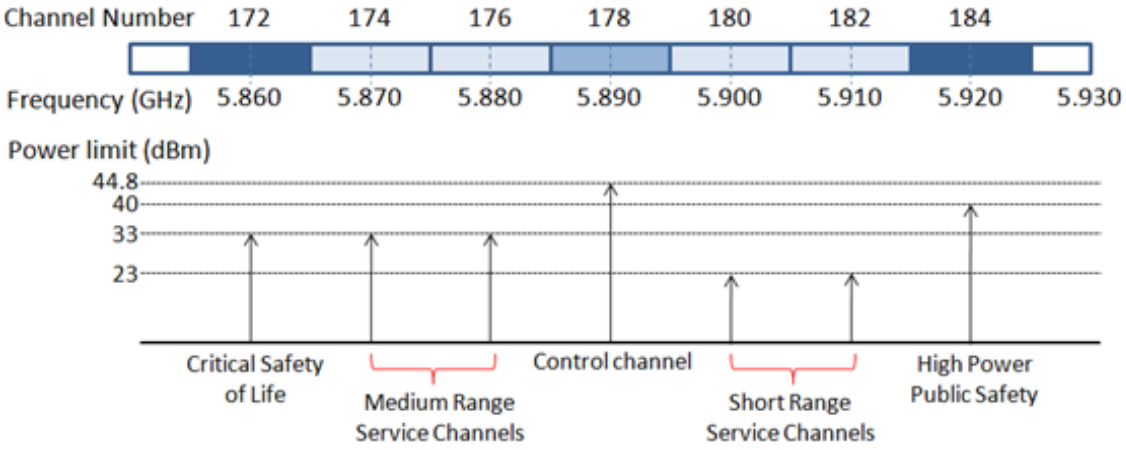

Figure 1.2: The DSRC spectrum allocated by the FCC, with the effective isotropically radiated power (EIRP) limits as specified in the ASTM E2213 standard [1] for public RSUs.

applications, and one control channel for transmission of control information and high priority safety messages. Such allocation of radio spectrum for vehicular communications has motivated the establishment of many national and international research projects, e.g., [5, 6, 7, 8, 9, 10, 11, 12, 13, 14], which are all dedicated to the research in VANETs. Every project has its unique objectives, focusing on safety related applications [11, 12], security of vehicular communications [7, 8], the development of a simulation platform for V2V and V2R communications [14], and so on.

1.2 VANET Applications

1.2.1 Safety Applications

The primary category of VANET applications is to enhance the public safety standards and provide a safer environment for drivers/passengers and pedestrians on road. For instance, at a signalized intersection as shown in Fig. 1.3a, an RSU can continuously broadcast to the approaching vehicles information about the traffic signal status and timing, stopping location, type of road surface, weather conditions, etc. Then, based on this broadcast information, the in-vehicle system can predict a traffic signal violation and give a warning to the driver, or advise him/her with an optimal speed to reach the traffic signal during the green light phase. Fig. 1.3b illustrates examples of safety applications that are based on V2V communications. As shown in Fig. 1.3b, if a vehicle suddenly breaks, it broadcasts information about its current status (i.e., position, speed, deceleration, etc.), which is used by the surrounding vehicles to early detect the sudden brake, even in limited visibility conditions, such as due to heavy fog. In case a vehicle senses that a crash is unavoidable, necessary actions such as extending the front bumper or pre-arming the airbags can be taken to reduce the severity of the crash.

In order to estimate the potential benefits of VANET safety applications and define their communication requirements, the Vehicle Safety Communications (VSC) project [2] has been established by seven car manufacturers (including GM, BMW, and Ford), in partnership with the United States Department of Transportation (USDoT). In the VSC project, the VANET safety applications are classified into periodic and event-driven safety applications, based on the way that the corresponding safety messages are transmitted by each node (i.e., vehicle or RSU). The periodic safety applications (e.g., blind spot warning) require automatic transmission of safety messages by each node at regular time intervals, while the event-driven safety applications (e.g., road condition warning [2]) require transmission of safety messages only in case of an event such as a hard brake, approaching an

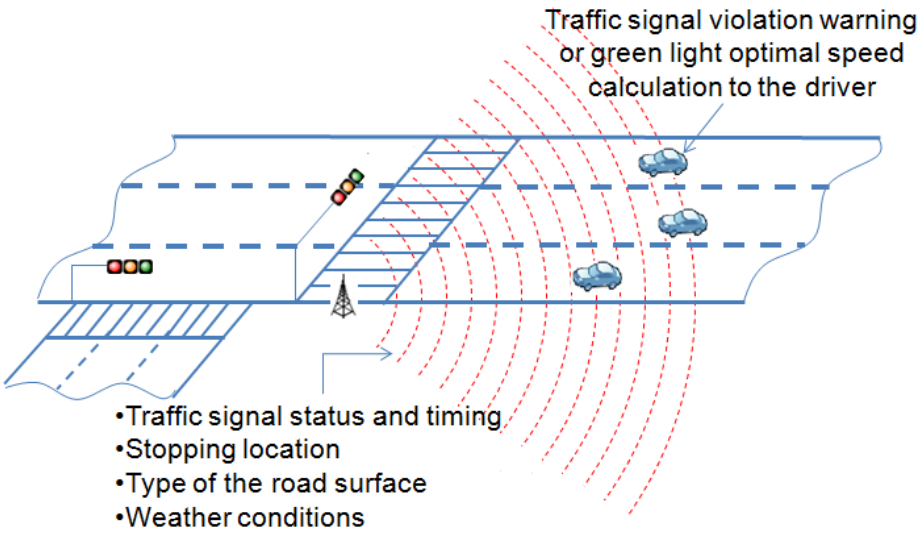

(a) Traffic signal violation warning and green light optimal speed advisory

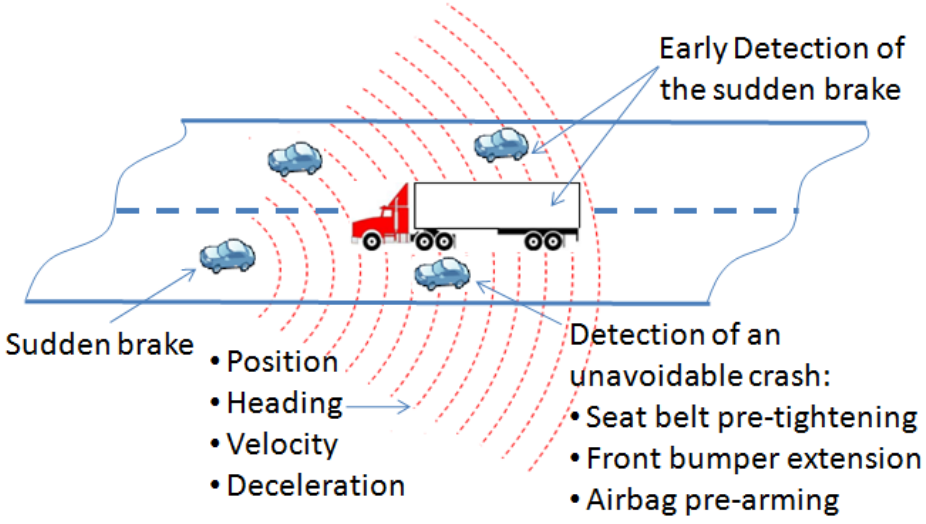

(b) Emergency electronic brake light and pre-crash sensing

Figure 1.3: Examples of safety applications based on V2R (Fig. 1.3a) and V2V (Fig. 1.3b) communications as defined in [2].

emergency vehicle, and dangerous road condition detection. The applications in Fig. 1.3a and 1.3b are examples of periodic and event-driven safety applications respectively [2].

Most (if not all) of the safety applications are based on broadcasting of safety messages, either periodic or event-driven, to all the nodes within the communication range. For instance, as shown in Fig. 1.3, the information broadcast by the RSU (Fig. 1.3a) or by the breaking vehicle (Fig. 1.3b) should be successfully delivered to all the surrounding vehicles with a high level of precision and without any excess delay. Given that any inaccuracy in the broadcast safety messages may result in serious consequences, such as damage of vehicles or injuries of drivers and passengers, it is necessary to develop a medium access control (MAC) protocol which provides an efficient broadcast service, in order to support the quality-of-service (QoS) requirements of the high priority safety applications in VANETs.

1.2.2 In-vehicle Internet Access

Although safety applications are the key motivation for VANETs, the applications targeting passenger infotainment have been gaining significant interests [4]. Infotainment improves the driving experience, makes the trips more enjoyable, and may accelerate the deployment of VANETs due to a small market penetration requirement as compared to that needed for most of the safety applications [15]. One of the main infotainment services of VANETs is in-vehicle Internet access, which allows a vehicle to connect to the Internet by communicating with Internet gateways deployed along the road sides [4]. A vehicle can communicate with a gateway either directly (when they are within the communication range of each other) or via multihop communications, i.e., by using other vehicles to relay data packets to/from the gateway. In order to support multihop in-vehicle Internet access, a routing protocol is required to allow a vehicle to discover the existence of an Internet gateway, and to deliver data packets between a vehicle and a gateway via multihop communications. Additionally, a gateway deployment strategy should be employed in order to determine optimal locations of Internet gateways, which ensure that a vehicle can connect to the Internet (i.e., can find a network path to an Internet gateway) with a probability greater than an acceptable threshold.

1.3 MAC in VANETs

Various MAC protocols have been proposed for VANETs, based either on IEEE 802.11 or on channelization such as space division multiple access (SDMA), code division multiple

access (CDMA), and time division multiple access (TDMA). In SDMA schemes, each vehicle decides whether or not it is allowed to access the channel based on its location on the road [16, 17]. An SDMA scheme consists of the following three components. First, a *discretization procedure* divides the road into small areas called cells. Each cell may contain one [16] or more vehicles [17] based on the size of the cell determined by the SDMA scheme. Second, a *mapping function* assigns to each of the cells a unique time slot. To avoid the hidden terminal problem, two cells are assigned the same time slot only if the distance between them is greater than twice of the communication range. Third, an *assignment rule* specifies which time slots a vehicle is allowed to access based on its current location. For any SDMA scheme, the vehicles should be able to correctly determine their current position, store the mapping of the cells into time slots, and synchronize to a common reference. One main problem of SDMA schemes is that, when most of the cells on a road are unoccupied by vehicles, the unused time slots assigned to these cells represent a waste of bandwidth.

Similarly, CDMA is proposed for MAC in VANETs due to its robustness against interference and noise [18, 19]. The main issue which arises with CDMA in VANETs is how to allocate the pseudo noise (PN) codes to different vehicles. Due to a large number of vehicles, if every vehicle is assigned a unique PN code, the length of these codes will become extremely long, and the required bit rates for VANET applications may not be attained. Consequently, it is mandatory that the PN codes be shared among different vehicles in a dynamic and fully distributed way. One solution for distributed PN code allocation is to provide each node with several filters matched to the available PN codes, which are shared by all nodes [18]. Then, each node attempts to select a PN code that is not used by other nodes within its communication range, by selecting the PN code corresponding to the matched filter which gives the minimal output. However, this scheme suffers from the hidden terminal problem, and its implementation is impractical due to its requirement of a matched filter for each PN code. Although the number of matched filters can be reduced by using a location based PN allocation scheme [19], the complexity of these matched filters increases since they need to be adaptive. That is, each filter should match to different PN codes based on the area where the vehicle is currently located. The complexity of implementation is the main disadvantage of CDMA schemes.

The ADHOC MAC is the most well known TDMA protocol proposed for inter-vehicle communication networks [20]. The ADHOC MAC protocol operates in a time slotted structure, where time slots are grouped into virtual frames, i.e., no frame alignment is needed. By letting each node report the status of all the time slots in the previous (sliding) virtual frame, the ADHOC MAC can support an acknowledged broadcast service without the hidden terminal problem [20]. However, the ADHOC MAC protocol has major limitations

which significantly degrades its performance, as will be discussed in details in Subsection 3.5.3. On the other hand, the main solution currently proposed for MAC in VANETs is the IEEE 802.11p standard [21]. The protocol is based on the legacy IEEE 802.11 standard [22] which is widely implemented, with new parameter values for the enhanced distributed channel access (EDCA) [22, 21] scheme to be used for communications over the control channel (CCH) (as recommended by the IEEE 1609.4 standard [23]). However, as will be explained in Section 4.3, the IEEE 802.11p standard does not provide a reliable broadcast service, which considerably reduces its ability to support the periodic and event-driven safety applications in VANETs.

1.4 Routing in VANETs

The routing protocols proposed for point-to-point communications in VANETs can be classified into topology-based and position-based protocols. Topology based protocols make the routing decisions relying mainly on information about the topology of the network. That is, they use the information about the existence of communication links among different nodes to determine which path a packet should be routed through. This class can be categorized into proactive and reactive protocols. In proactive protocols [24, 25], the next hop to a certain destination can be directly found from a routing table stored at each node, while in reactive protocols [26, 27, 28], a route discovery procedure is initiated before the start of transmission of data packets between the source and destination nodes. Also, there exist hybrid proactive-reactive protocols [29], which proactively maintain routing information in a local neighborhood, and reactively discover the paths to destinations beyond this local neighborhood. Most of the topology-based routing protocols are originally designed for mobile ad hoc networks (MANETs) and do not consider the special characteristics of a VANET. In VANETs, due to a large number and high mobility of nodes, link failures occur more frequently than in a regular MANET. Consequently, the control packets required to update the routing tables for proactive protocols [24, 25] or to find/repair the network routes for reactive protocols represent a great overhead which can degrade the VANET performance. Also, each time a link failure occurs, a certain delay is required until this failure information propagates throughout the network and updates the routing table stored at each node (for proactive protocols) or until a source node re-initiates a route discovery procedure to find a new route to a destination node (for reactive protocols). During this delay, each packet which is en route to a destination through an invalid route will potentially be lost.

The second class of routing protocols, known as the position-based protocols [30, 31, 32],

makes routing decisions based solely on position information, and without reliance on any topology information. Each relay node is aware of the positions of its one-hop neighbors as well as the position of the destination node. The position of the destination node is determined by the mean of a location service [33, 34, 35], while the positions of one-hop neighbors are determined by using a neighbor discovery algorithm, such as the exchange of Hello messages. Based on this position information, each relay node forwards a packet to a candidate among its one hop-neighbors, which is expected to deliver the packet closer or faster to the final destination. The position-based protocols have some disadvantages which may decrease their chances to be applied in a VANET. First, it is not guaranteed that a location service will exist in VANETs to inform the source node about the location of the destination node. Additionally, even if a location service exists, the query of this location service before the transmission of each packet represents a considerable routing overhead which is completely neglected in the evaluation of position based protocols: it is assumed that each packet header contains the correct position of the destination without considering any additional overhead. Second, the greedy forwarding strategy, which is employed by position-based protocols, is based on forwarding a packet to the one-hop neighbor closest to the destination (either the real destination [30] or the next road intersection [32]). By using this strategy, a packet can reach a node which cannot find other neighbors closer to the destination than itself. In this case the packet is said to have reached a local maximum, which is a likely situation in VANETs, especially in city scenarios. The position-based protocols deal with this situation by switching from the greedy forwarding to a recovery strategy. However, the proposed recovery strategies are inefficient in terms of the hop number and packet delivery delay, and some of which may even fail to deliver a packet to the destination [31, 36]. Note that, the long delivery delay decreases the probability of successful delivery of a packet since the destination position stored in the packet header becomes less accurate due to mobility of the destination.

1.5 Thesis Objectives and Outline

Motivated by the limitations of the current networking schemes proposed for VANETs, as discussed in Sections 1.3 and 1.4, this thesis has the following objectives:

1. to introduce a multichannel TDMA MAC protocol which can provide a reliable one-hope broadcast service, necessary to support the QoS requirements of VANET periodic and event-driven safety applications;

2. to present a strategy for deploying Internet gateways on the roads, in order to minimize the total cost of gateway deployment, and ensure multihop in-vehicle Internet access with a probability greater than a specified threshold;

3. to develop a data routing protocol, consisting of gateway discovery and packet forwarding schemes, to allow a vehicle to communicate with an Internet gateway by using multihop communications.

The rest of the thesis is organized as follows. Chapter 2 describes the system model under consideration, while Chapter 3 introduces a novel multichannel TDMA protocol, called VeMAC, and compares its performance with that of ADHOC MAC, via simulations in highway and city scenarios [37, 38, 39]. The ability of the VeMAC protocol to support periodic and event-driven safety messages is investigated in Chapter 4 in comparison with the IEEE 802.11p standard [40, 41]. This performance evaluation is done by presenting a detailed delivery delay analysis for periodic and event-driven safety messages, and conducting computer simulations in a realistic city scenario consisting of roads around the University of Waterloo (UW). Chapter 5 first explains a new strategy for deploying Internet gateways on the roads, then proposes a packet routing scheme, designed over the VeMAC protocol, for multihop in-vehicle Internet access [42, 43]. The gateway deployment strategy is applied for optimal placement of Internet gateways around the UW campus, while the proposed routing scheme is evaluated in a highway scenario, in terms of different performance metrics, including the end-to-end packet delivery delay. Finally, Chapter 6 concludes this thesis and suggests some further research topics.

Chapter 2

System Model

2.1 VANET Description: Elements and Applications

The VANET under consideration consists of a set of RSUs and a set of vehicles moving in opposite directions on two-way vehicle traffic roads. A vehicle is said to be moving in a left (right) direction if it is currently heading to any direction from north/south to west (east). Based on this definition, as shown in Fig. 2.1, if two vehicles are moving in opposite directions on a two-way road, regardless of the orientation of the road, it is guaranteed that one vehicle is moving in a left direction while the other vehicle is moving in a right one. The vehicles and RSUs broadcast periodic and event-driven safety messages for the purpose of safety applications. The periodic safety messages broadcast by different vehicles have the same (fixed) message size[1]. Similarly, the periodic safety messages broadcast by an RSU have equal message size, which may differ from the size of the periodic messages broadcast by another RSU depending on the application. Also, a set of gateways is placed along the road sides to provide Internet connectivity to the vehicles. The vehicles employ multihop communications to connect to the gateways, and a gateway can communicate only with the vehicles located within a maximum number of hops from the gateway. The location of each gateway and the maximum number of hops that it can use to communicate with a vehicle are determined as described in Chapter 5.

[1]A generic safety message format, called the Basic Safety Message (BSM), is specified in the SAE J2735 application layer standard [44] to be periodically broadcast by vehicles. The BSM exploits the large overlap among the vehicle state information required by various V2V applications in order to avoid using application-specific messages and wasting the wireless network resources [45].

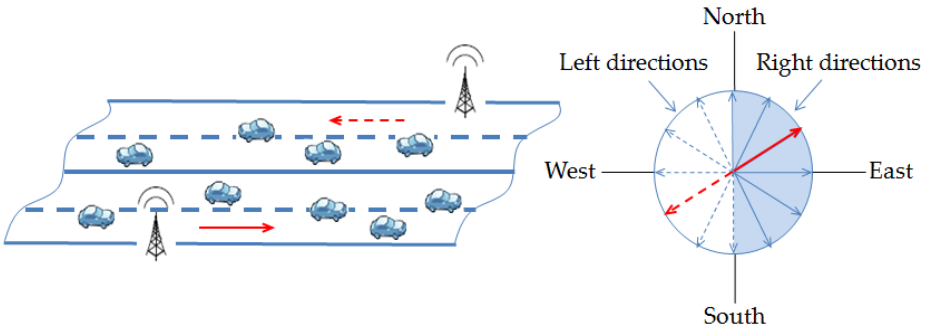

Figure 2.1: Right and left directions of vehicle movement.

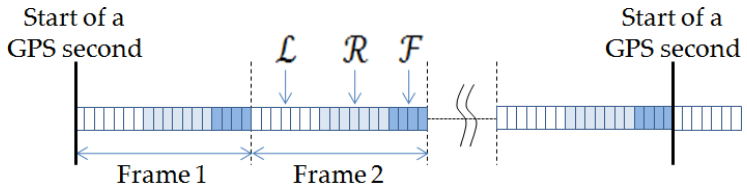

Figure 2.2: Partitioning of each frame on the CCH into $\mathcal{L}, \mathcal{R}$ and $\mathcal{F}$ sets.

2.2 Communications Channels

The VANET has one CCH and N_{sch} service channels (SCHs), denoted by $c_1, c_2, \ldots, c_{N_{sch}}$. The CCH is used for transmission of two kinds of information: high priority short applications (such as periodic or event driven safety messages), and control information required for the nodes to organize the communications over the service channels. The N_{sch} SCHs are used for transmission of safety or non-safety related application messages. It is assumed that the transmission power levels on all channels are fixed and known to all nodes. All channels are symmetric, in the sense that node x is in the communication range of node y if and only if node y is in the communication range of node x.

On the CCH, the time is partitioned to frames consisting of a constant number L of time slots of equal duration t. Each frame is partitioned into three sets of time slots: $\mathcal{L}$, $\mathcal{R}$, and $\mathcal{F}$, in that order, as shown in Fig. 2.2. The $\mathcal{F}$ set is associated with RSUs, while the $\mathcal{L}$ and $\mathcal{R}$ sets are associated with vehicles moving in left and right directions respectively. Each second contains an integer (fixed) number of frames, and each time slot is identified by the index (from 0 to $L-1$) of the time slot within a frame.

2.3 Node Equipment and Identification

Each node (i.e., vehicle or RSU) has two transceivers: Transceiver1 is always tuned to the CCH, while Transceiver2 switches among the SCHs. Also, each node is equipped with a global positioning system (GPS) receiver and can accurately determine its position and moving direction using GPS. The current position of each node is included in the header of each packet transmitted on the CCH. Each node is identified by a unique MAC address and a set of short identifiers (IDs), called VeMAC IDs, where each VeMAC ID corresponds to a certain time slot that the node is accessing per frame on the CCH (more details in Chapter 3). Each VeMAC ID is chosen by a node at random, included in the header of each packet transmitted in the corresponding time slot, and changed if the node detects that its ID is already in use by another node [20].

2.4 Time Slot Synchronization

Synchronization among nodes is performed using the one pulse per second (1PPS) signal provided by any GPS receiver. The rising edge of this 1PPS is aligned with the start of every GPS second with accuracy within 100 ns even for inexpensive GPS receivers. Consequently, this accurate 1PPS signal can be used as a common time reference among all the nodes. Hence, at any instant, each node can determine the index of the current slot within a frame on the CCH, and whether it belongs to the $\mathcal{L}$, $\mathcal{R}$, or $\mathcal{F}$ set. In case of a temporary loss of GPS signal, the synchronization among different nodes can still be maintained within a certain accuracy for a time duration which depends on the stability of the GPS receiver's local oscillator at each node [46]. If the GPS signal is lost in a certain area for a long duration (longer than a specified threshold), a distributed synchronization scheme, such as the one presented in [46], should be employed until the GPS signal is recovered. Details of such a back up synchronization scheme are out of scope of this thesis.

2.5 Definitions

For a certain node, x, set $\mathcal{N}_x$ denotes the set of one-hop neighbours of node x, from which node x has received VeMAC Type1 packets (defined in Section 3.1.3) on the CCH in the previous L slots. Set $\mathcal{T}_x$ is defined as the set of time slots that node x must not use on the CCH in the next L time slots. This set is used by node x to determine which time slots it

can access on the CCH without causing any hidden terminal problem. How each node x constructs and updates sets $\mathcal{N}_x$ and $\mathcal{T}_x$ is discussed in Chapter 3.

A two-hop set (THS) is defined as a set of nodes in which each node can reach any other node in two hops at most. The term 'message' refers to a MAC layer service data unit (MSDU), i.e., the unit of information arriving to the MAC layer entity from the layer above. On the other hand, the term 'packet' refers to either a MAC layer protocol data unit (MPDU) (in Chapters 3 and 4), or a network layer protocol data unit (PDU) (in Chapter 5).

Chapter 3

VeMAC: A TDMA MAC Protocol for Reliable Broadcast in VANETs

This chapter presents VeMAC, a novel multichannel TDMA protocol developed specifically for a VANET scenario [37, 38, 39]. The VeMAC supports an efficient one-hop broadcast services on the CCH, by using implicit acknowledgments and eliminating the hidden terminal problem, in order to successfully deliver both periodic and event-driven safety messages in VANETs. The protocol reduces transmission collisions due to node mobility on the control channel by assigning disjoint sets of time slots to vehicles moving in opposite directions and to road side units. Analysis and simulation results in highway and city scenarios are presented to evaluate the performance of VeMAC and compare it with ADHOC MAC [20]. It is shown that, due to its ability to decrease the rate of transmission collisions, the VeMAC protocol can provide significantly higher throughput on the CCH than ADHOC MAC.

3.1 VeMAC Basics

3.1.1 Safety Message Queueing and Service

As discussed in Section 2.1, the vehicles and RSUs broadcast periodic and event-driven safety messages on the CCH for the purpose of safety applications, and the periodic safety messages broadcast by different vehicles have the same (fixed) message size. As shown in Fig. 3.1, at each node, the periodic and event-driven safety messages are mapped to two

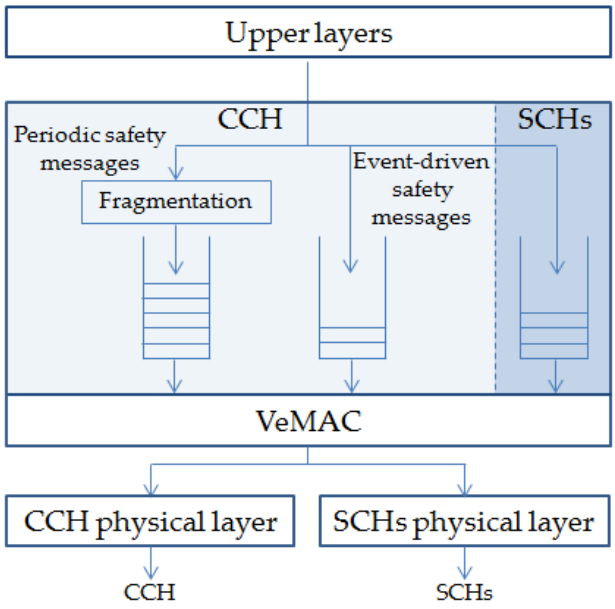

Figure 3.1: Safety message queues.

different queues, which are served independently by the VeMAC protocol, as described in details in Section 3.2.

Based on a given transmission rate determined by the physical layer, the VeMAC maximum transmission unit (MTU) is defined as the maximum amount of data (without the physical layer overhead) which can be transmitted in the duration of one time slot. The duration of a time slot, t, is chosen such that the MTU is equal to the size of a periodic safety message broadcast by a vehicle plus the maximum size of control information introduced by the VeMAC protocol. For RSUs, if the size of a periodic safety message plus the VeMAC control information exceeds the MTU, the message is fragmented to be transmitted as multiple VeMAC packets, as indicated in Fig. 3.1. This fragmentation is typical for applications such as curve speed warning and left turn assistant [2], in which the size of a periodic safety message broadcast by an RSU is considerably larger than that of the periodic messages broadcast by vehicles [2]. On the other hand, all the event-driven safety messages are assumed to be small enough to fit in a single VeMAC packet, without fragmentation. Each VeMAC packet carries at most one safety message and only one VeMAC packet can be transmitted per time slot.

In the VeMAC protocol, in order to serve the two safety message queues in Fig. 3.1, each node must acquire at least one time slot per frame on the CCH. A time slot acquired

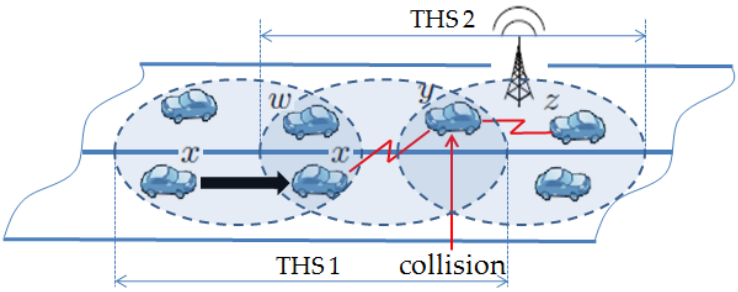

Figure 3.2: Merging collision caused by node mobility.

by a certain node is referred to as a periodic or event-driven slot, according to the type of the safety message transmitted during this time slot. The number of periodic slots that the node acquires per frame, denoted by k_p, depends on the fixed size and arrival rate of the periodic safety messages. Similarly, the number of event-driven slots that the node can access per frame, denoted by k_e, depends on the average arrival rate of the event-driven safety messages. A node should use a unique VeMAC ID to access each of the k_p and k_e slots. As mentioned in Section 2.3, each VeMAC ID is chosen by the node at random, included in the header of each packet transmitted in the corresponding time slot, and changed if the node detects that its VeMAC ID is already in use by another node [20]. The k_p and k_e values are chosen such as to satisfy the delay constraints of the periodic and event-driven safety messages based on the delay analysis in Chapter 4. Once a node acquires a periodic or event-driven slot, it keeps using the same slot in all subsequent frames unless there is no packet waiting for transmission in the corresponding queue or a transmission collision is detected.

3.1.2 Transmission Collision Types on The CCH

Two types of transmission collision can happen on the CCH: access collision and merging collision. An access collision happens when two or more members of the same THS attempt to acquire the same available time slot. On the other hand, a merging collision happens when two or more nodes acquiring the same time slot become members of the same THS due to node activation or node mobility. In VANETs, merging collisions are more likely to occur among vehicles moving in opposite directions or between a vehicle and a stationary RSU since they approach each other with a much higher relative velocity as compared to vehicles moving in the same direction. For example, in Fig. 3.2, if vehicle x moves to THS2 and if x is using the same time slot as z, then collision will occur at y. Upon detection of a

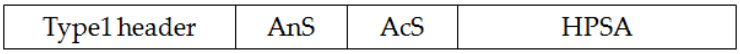

(a) Type1 packet

(b) Type2 packet

Figure 3.3: VeMAC packet types.

merging collision on the CCH, each colliding node should release its time slot and acquire a new one, which may generate more access collisions.

3.1.3 VeMAC Packet Types

Two different types of VeMAC packets can be transmitted on the CCH, as shown in Fig. 3.3. A Type1 packet is divided into four main fields: Type1 header, announcement of services (*AnS*), acceptance of services (*AcS*), and high priority short applications (*HPSA*). The *HPSA* field is to include the periodic and event-driven safety messages, while the *AnS* and *AcS* fields are used to control the communications over the SCHs. A Type2 packet does not contain any control information: it consists of an *HPSA* field and a short Type2 header (the difference between Type1 and Type2 headers will be discussed). Each node must transmit exactly one Type1 packet in each frame using one of its acquired periodic time slots, and if the node is accessing more than one time slot per frame, Type2 packets are transmitted over the rest of time slots. The transmission of one Type1 packet in each frame is mandatory since the information in the Type1 header, *AnS* and *AcS* fields, is necessary for other nodes to decide which time slots they can access on the CCH and SCHs. On the other hand, the transmission of Type2 packets is to decrease the protocol overhead by removing all the control information which needs to be transmitted only once per frame. As the event-driven safety messages are always transmitted using Type2 packets (i.e., without control information and with a large *HPSA* field in the packet), fragmentation is not considered for this type of safety messages.

3.2 CCH Access

For the purpose of time slot assignment on the CCH, in the header of each Type1 packet transmitted on the CCH, the transmitting node x should broadcast the VeMAC ID(s) and

the corresponding time slot(s) of each node in set $\mathcal{N}_x$. The short length of a VeMAC ID (9 bits as suggested in Chapter 4) serves to decrease the protocol overhead as compared to broadcasting the corresponding MAC address. The main difference between Type1 and Type2 headers is that the Type2 one is shorter as it does not contain the VeMAC IDs or the corresponding time slots of the nodes in set $\mathcal{N}_x$. Now, suppose node x is just powered on and needs to acquire a time slot. By listening to the CCH for L successive time slots (not necessarily in the same frame), node x can determine set $\mathcal{N}_x$ and the time slot(s) used by each node in $\mathcal{N}_x$. Also, since each one-hop neighbour $y \in \mathcal{N}_x$ announces (in the header of its transmitted Type1 packet) the time slot(s) used by each node in $\mathcal{N}_y$, node x can determine all the time slots used by each of its two-hop neighbours, $z \in \mathcal{N}_y, z \notin \mathcal{N}_x$, $\forall y \in \mathcal{N}_x$. Accordingly, node x sets $\mathcal{T}_x$ to the set of time slots used by all nodes within its two-hop neighbourhood. Then, sets $\mathcal{N}_x$ and $\mathcal{T}_x$ are updated by node x at the end of each time slot (always based on the packets received in the previous L slots).

Given $\mathcal{T}_x$, node x determines the set of accessible time slots, $\mathcal{A}_x$, (to be discussed) and then attempts to acquire a time slot by randomly accessing any time slot in $\mathcal{A}_x$, say time slot k. If no other node in the two-hop neighbourhood of node x simultaneously attempts to acquire time slot k, then no access collision happens. In this case, the attempt of node x is successful and each one-hop neighbour w of node x adds node x to set $\mathcal{N}_w$ and record the VeMAC ID used by node x to access time slot k, denoted by ID_k^x. On the other hand, if at least one node within the two-hop neighbourhood of node x accesses time slot k, then all the transmissions in the slot fail and time slot k is not acquired by any of the contending nodes. Node x will determine whether or not its attempt was successful by observing the $L-1$ time slots following k. The attempt of node x is considered successful iff the Type1 packet received from each node $w \in \mathcal{N}_x$ includes ID_k^x in its headers. Otherwise, node x re-accesses one of the time slots in $\mathcal{A}_x$ until it successfully acquires a time slot. Once node x acquires a time slot, it keeps using the same slot in all subsequent frames unless a merging collision happens. Similar to an access collision, a merging collision on time slot k is detected by node x as soon as it receives a Type1 packet from a node $w \in \mathcal{N}_x$ without including ID_k^x in its header. Upon detection of a merging collision, each colliding node should release its time slot and acquire a new one using the same procedure. In order to acquire more than one time slot per frame, node x employs the same procedure using a unique VeMAC ID for accessing each extra time slot.

At the end of each time slot, the collision detection by a certain node x should be done before updating set $\mathcal{N}_x$. Upon receiving a Type1 packet from a node y without including ID_k^x in its header, we stress on that, node x should approve this collision detection and release time slot k iff the transmitting node $y \in \mathcal{N}_x$. This condition is referred to as the slot release prevention (SRP) condition, and its main objective is to prevent node x from

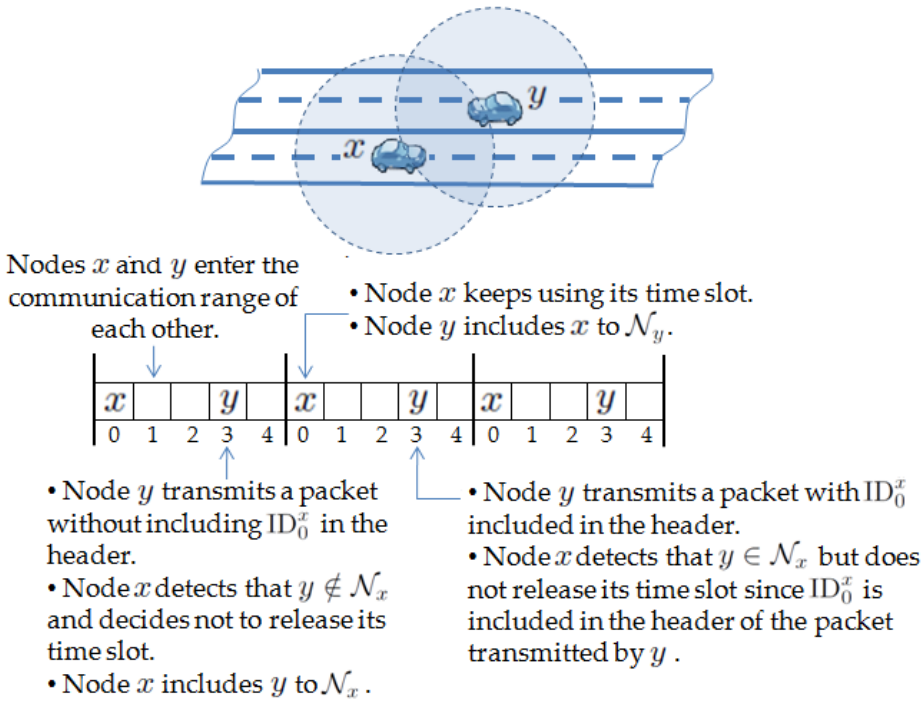

Figure 3.4: The SRP condition preventing node x from unnecessarily releasing its time slot.

unnecessarily releasing its time slot when it just enters the communication range of another node y. To illustrate that, consider the time slot assignment shown in Fig. 3.4 for the two nodes x and y. Note that, each of the nodes x and y is accessing one time slot per frame, and hence all the packets transmitted are of Type1 packets. When node x enters the communication range of node y, even if no collision happens, the first packet received by node x from node y will not include ID_0^x. The reason is that, by the time node y transmits its packet, node y has not yet received any packet from node x on time slot 0. By applying the SRP condition, when node x receives the first packet from node y, node x determines that node $y \notin \mathcal{N}_x$ and does not release its time slot (remember that collision detection by node x is done before updating $\mathcal{N}_x$). After node x's transmission, the subsequent packets transmitted by node y will include ID_0^x and, hence, the unnecessary release of node x's time slot is prevented. Note that, without the SRP condition, when two nodes enter the communication range of each other, one of them will eventually release the time slot over which it transmits the Type1 packets, even if no merging collision happens. This behaviour can significantly decrease the performance of a TDMA protocol as discussed in Subsection 3.5.4.

When a node, x, is attempting to acquire a time slot, a parameter called the split up parameter, denoted by τ, determines how node x accesses the time slots belonging to the $\mathcal{L}$, $\mathcal{R}$, and $\mathcal{F}$ sets. Consider that node x is moving in one of the right directions. Initially, node x limits the set $\mathcal{A}_x$ to the available time slots associated with the right directions, i.e., $\mathcal{A}_x = \overline{\mathcal{T}_x} \cap \mathcal{R}$. If after τ frames node x cannot acquire a time slot, then node x augments $\mathcal{A}_x$ by adding the time slots associated with the opposite direction, i.e., $\mathcal{A}_x = \overline{\mathcal{T}_x} \cap (\mathcal{R} \cup \mathcal{L})$. If, after τ more frames, node x still cannot acquire a time slot, node x will start to access any available time slot, i.e., $\mathcal{A}_x = \overline{\mathcal{T}_x}$. The same procedure applies for a vehicle moving in a left direction by replacing $\mathcal{R}$ with $\mathcal{L}$. Similarly, if node x is an RSU, for the first τ frames $\mathcal{A}_x = \overline{\mathcal{T}_x} \cap \mathcal{F}$, and then $\mathcal{A}_x = \overline{\mathcal{T}_x}$. Note that, when $\tau = \infty$, regardless of the number of access collisions that node x has encountered to acquire a time slot, it can only access the time slots reserved for its moving direction (i.e., in the $\mathcal{R}$ set). On the other extreme, when $\tau = 0$, node x can access any available time slot on the CCH even if it does not experience any access collision. Hence, the choice of the τ value can significantly affect the rates of access collision and merging collision. For example, when $\tau = 0$, all the vehicles and RSUs are accessing the same set of time slots. Hence, a merging collision is possible between any two nodes. However, when a merging collision happens, each colliding node x is free to access any time slot in $\overline{\mathcal{T}_x}$, which can decrease the probability of an access collision. On the other extreme, when $\tau = \infty$, the vehicles moving in opposite directions and the RSUs are accessing disjoint sets of time slots. However, when a merging collision happens, for example among vehicles moving in a right direction, there is a higher probability of an access collision (compared with the $\tau = 0$ case) since the choice of each colliding node x is limited to time slots in $\overline{\mathcal{T}_x} \cap \mathcal{R}$. A performance comparison between the $\tau = 0$ and $\tau = \infty$ cases is provided in Section 3.5, and the effect of the τ value on the delay of periodic and event-driven safety messages is investigated in Chapter 4 for these two extreme cases.

Using the proposed scheme, a reliable broadcast service can be provided on the CCH. That is, if node x transmits a broadcast packet on time slot k, by listening to the $L-1$ time slots following k, node x can determine the set $\mathcal{D}_x$ of one-hop neighbors which have not successfully received the packet, where $\mathcal{D}_x = \{y \in \mathcal{N}_x : \mathrm{ID}_k^x \text{ is not broadcast by node } y\}$. In other words, when node y includes ID_k^x in the header of its Type1 packet, it is considered as an implicit acknowledgement by node y of receiving the packet broadcast by node x on time slot k.

3.3 SCH Access

On the SCHs, time is partitioned to frames consisting of a constant number of fixed duration time slots. All the SCHs are slot synchronized with the CCH, and on each SCH, each second contains an integer number of frames. The number of time slots per frame on channel c_m is denoted by l_m, $m = 0, \ldots, N_{sch}$, and a time slot on channel c_m is identified by the index (from 0 to $l_m - 1$) of this time slot within a frame on channel c_m. Note that, the same time slot can have different indices on channels c_i and c_j, $i \neq j$, since l_i is not necessarily equal to l_j.

A *provider* is a node which announces on the CCH for a service offered on a specific SCH, while a *user* is a node which receives the announcement for a service and decides to make use of this service[1]. For a certain node x, let $\mathcal{T}_x^m$ denote the set of time slots that node x must not use on channel c_m in the next l_m time slots, $m = 0, \ldots, N_{sch}$. Set $\mathcal{T}_x^m$ is used by node x to determine which time slots it can access on channel c_m without causing any hidden terminal problem, as described in the following.

Consider that a node x has an MSDU to be delivered to a certain destination (assuming unicast) on SCH c_m. By using $\mathcal{T}_x^m$ (how node x constructs $\mathcal{T}_x^m$ will be explained), node x determines the set of time slots that it will access on channel c_m to offer the service, denoted by ϑ_x^m, such that $\vartheta_x^m \cap \mathcal{T}_x^m = \phi$. Accordingly, node x announces the following information in the *AnS* field of its next packet transmitted on the CCH: a) priority of the service, b) reliability of the service (i.e., acknowledged or not), c) MAC address of the intended destination y, d) the index m of the service channel, and e) ϑ_x^m. Once the provider x announces for the service, no further action is needed unless the destination accepts the service as described below.

Based on the information announced by provider x on the CCH, the destination y determines whether or not to make use of the announced service. If node y decides to use the service by provider x on channel c_m, it accepts the service by including ϑ_x^m in the *AcS* field of its next packet transmitted on the CCH. The announcement of ϑ_x^m by the user y is for each surrounding node, z, to update its $\mathcal{T}_z^m$ set as to be discussed. Also, for a reliable service, node y should include in the *AnS* field the time slot that will be used by node y to transmit the acknowledgement packet, denoted by a_y^m. Node y determines a_y^m such that $a_y^m \notin \mathcal{T}_y^m$. When provider x receives the acceptance of the service, it tunes its Transceiver2 to channel c_m and starts offering the service on the time slots announced in ϑ_x^m. As well, if the service is reliable, node x should include a_y^m in the *AcS* field of its next packet transmitted on the CCH. Again, the announcement of a_y^m by provider x is

[1]The term 'service' refers to the delivery of an MSDU on a certain service channel.

to avoid the collision of the acknowledgement packet by properly updating the $\mathcal{T}_z^m$ set of each surrounding node z. Node y should transmit the acknowledgement only after node x announces a_y^m on the CCH.

Each node, x, updates sets $\mathcal{T}_x^m$, $m = 1, \ldots, N_{sch}$, as follows. When node x receives a packet on the CCH from another node y, based on the position of node y which is included in the header of the packet, and the position of node x obtained from the GPS receiver, node x can estimate its distance to node y. Based on this estimated distance and on the fixed transmission power on all channels which is known to node x, node x can determine whether or not node y is in its communication range on channel c_m, $m = 1, \ldots, N_{sch}$ [2]. If node x decides that it can reach node y on a certain channel c_m, node x adds to set $\mathcal{T}_x^m$ the time slots indicated by each ϑ_y^m set and a_y^m slot included in the AcS field of the packet transmitted by y. The reason is that, each ϑ_y^m represents a set of time slots over which node y will receive a packet on channel c_m from a certain provider in the next l_m slots. Similarly, each a_y^m indicates a time slot over which node y will receive an acknowledgement packet on channel c_m from a certain user in the next l_m slots. Consequently, by updating $\mathcal{T}_x^m$ in the way described, collision at node y can be prevented since each node x in the one-hop neighbourhood of node y will avoid using the time slots over which node y will receive packets. At the end of time slot i_m on channel c_m, if $i_m \in \mathcal{T}_x^m$, node x removes i_m from $\mathcal{T}_x^m$, $m = 1, \ldots, N_{sch}$ and $i_m = 0, \ldots, l_m - 1$. Note that updating the $\mathcal{T}_x^m$, $m = 1 \ldots, N_{sch}$, sets for each node x is based on information in the AcS (not in the AnS) field, which eliminates any exposed terminal problem. The following example illustrates how the nodes access the service channels.

Consider the THS configuration shown in Fig. 3.5, node x has a reliable service to offer to node z on time slots numbered 1, 2, and 4 on channel c_1. Fig. 3.5 shows the sequence of actions taken by provider x, user z, and the surrounding nodes y and w. First, node x announces for the service and includes $\vartheta_x^1 = \{1, 2, 4\}$ in the AnS field of its packet transmitted on the CCH. Following this announcement, no action is taken by both surrounding nodes w and y. Once node z accepts the service and announces ϑ_x^1, node x starts offering the service on channel c_1 on time slots $\{1, 2, 4\}$ as announced in ϑ_x^1. When node y receives the packet transmitted by node z on the CCH, it adds ϑ_x^1 to $\mathcal{T}_y^1$ to avoid using the upcoming time slots $\{1, 2, 4\}$ over which node z will receive packets from node x (assume that node y can reach node z on channel c_1). Note that, node w is free to use the time slots in $\vartheta_x^1 = \{1, 2, 4\}$ since it did not receive the acceptance of service transmitted by node z on the CCH; hence, simultaneous transmissions from node w to v and from node x to z are allowed on channel c_1, i.e., no exposed terminal problem. However, in the absence of the exposed terminal problem, it is possible that node w announces a service to node

[2] It is assumed that each node has a path loss model for each service channel $c_m, m = 1, \ldots, N_{sch}$.

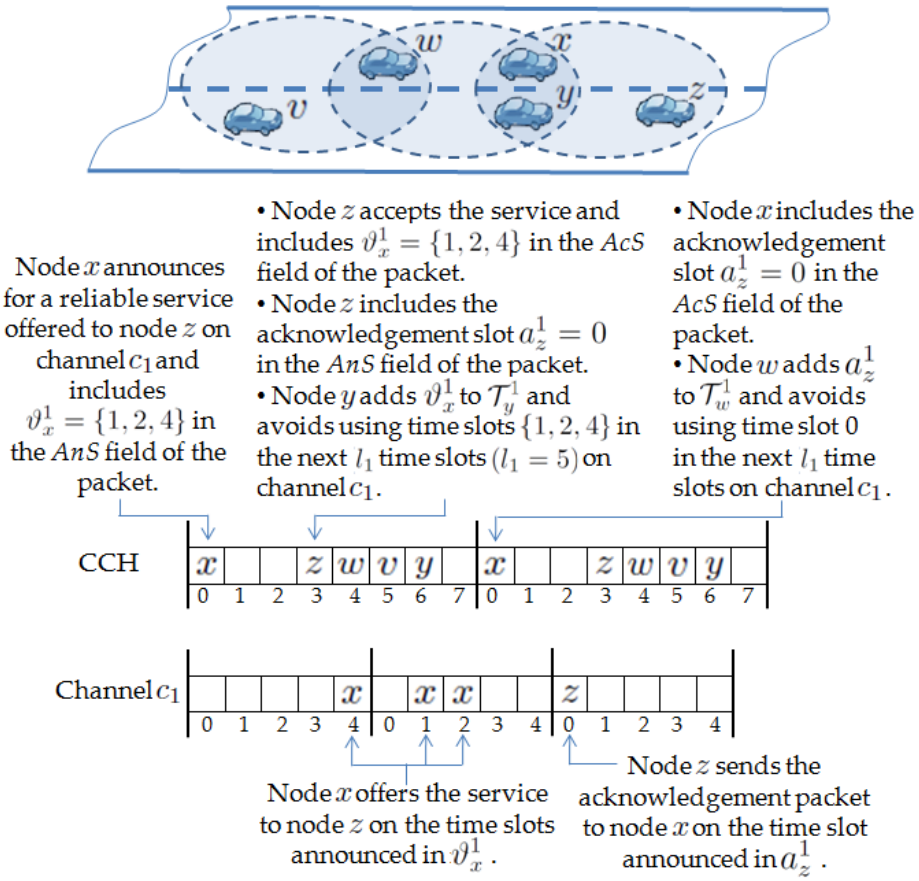

Figure 3.5: Node x offering a service to node z on channel c_1.

y on time slots $\{1, 2, 4\}$ after node x did the same announcement to node z (note that simultaneous transmissions from node w to y and from node x to z result in a collision at node y). In this case, if node y accepts the service and includes $\vartheta_w^1 = \{1, 2, 4\}$ in the AcS field of its packet transmitted on the CCH (on time slot $\{6\}$), node x will receive this packet transmitted by node y, includes ϑ_w^1 to $\mathcal{T}_x^1$, and avoids using the upcoming time slots $\{1, 2, 4\}$ on channel c_1 to prevent collision at node y (recall the definition of $\mathcal{T}_x^1$), although node x was supposed to transmit a packet to node z on the time slot $\{2\}$ following node y's acceptance of service. This missing packet, together with the other packets incorrectly received by node z, are (re)transmitted by node x after it receives the acknowledgment packet from node z. The acknowledgement packet is transmitted using the same procedure as illustrated in Fig. 3.5.

3.4 Analysis of Time Slot Acquisition

The objective of the analysis in this subsection is to investigate how fast the contending nodes can acquire a time slot on the CCH by using the VeMAC protocol. Let K denote the number of contending nodes, each of which needs to acquire a time slot on the CCH. We want to determine the average number of nodes which acquire a time slot within n frames, the probability that a specific node acquires a time slot within n frames, and the probability that all the nodes acquire a time slot within n frames. To simplify the analysis, the following assumptions are made: a) all the contending nodes belong to the same set of THSs, e.g., node w and node x in its final position in Fig. 3.2; b) the set of THSs to which the contending nodes belong does not change; c) when a node, x, fails to acquire a time slot after τ frames, the set $\mathcal{A}_x$ is not augmented, i.e., $\tau = 0$; d) at the end of each frame, each node, x, is aware of all acquired time slots during the frame, and updates the sets $\mathcal{T}_x$ and $\mathcal{A}_x$ accordingly, i.e., all nodes are within the communication range of each other; e) at the end of each frame, all contending nodes are informed whether or not their attempts to access a time slot during this frame were successful. Based on this information, each colliding node, x, randomly chooses an available time slot from the updated $\mathcal{A}_x$ set, and attempts to access this slot during the coming frame.

Let N be the number of initially available time slots in a frame, and X_n be the total number of nodes which acquired a time slot within n frames. Under the assumptions, X_n is a stationary discrete-time Markov chain with the following transition probabilities.

If $K \leq N$,

$$p_{ij} = \begin{cases} \frac{W(j-i,K-i,N-i)}{(N-i)^{K-i}}, & 0 \leq i \leq K-1, \\ & i \leq j \leq K \\ 1, & i = j = K \\ 0, & \text{elsewhere} \end{cases}$$

where $W(l, u, v)$ is the number of ways by which l nodes can acquire a time slot given that there are u contending nodes each randomly choosing a time slot among v available time slots. A node acquires a time slot if no other nodes choose to access the same slot. The Markov chain is illustrated in Fig. 3.6.

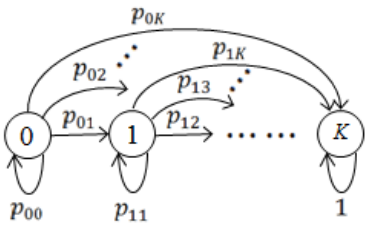

Figure 3.6: Markov chain for X_n when $K \leq N$.

If $K > N$,

$$p_{ij} = \begin{cases} \frac{W(j-i,K-i,N-i)}{(N-i)^{K-i}}, & 0 \leq i \leq N-1, \\ & i \leq j \leq N-1 \\ 1, & i = j, N \leq i \leq K \\ 0, & \text{elsewhere.} \end{cases}$$

The Markov chain is illustrated in Fig. 3.7. To calculate $W(l, u, v)$, considering u different

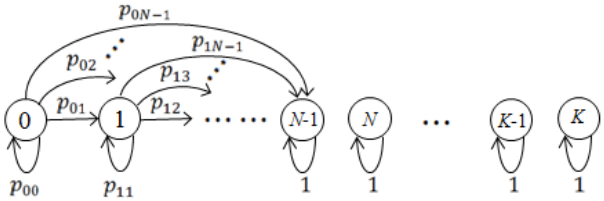

Figure 3.7: Markov chain for X_n when $K > N$.

balls randomly distributed in v different boxes with equal probabilities, $W(l, u, v)$ is the number of ways of having l boxes each containing exactly one ball. This special occupancy problem is solved in a recursive way as follows [47].

If $u \leq v$,

$$W(l, u, v) = \begin{cases} C_l^u A_l^v \left((v-l)^{u-l} - \right. & \\ \left. \sum_{i=1}^{u-l} W(i, u-l, v-l) \right), & 0 \leq l < u \\ A_l^v, & l = u \\ 0, & l > u \end{cases}$$

where $A_l^v = \frac{v!}{(v-l)!}$ and $C_l^u = \frac{A_l^u}{l!}$.

If $u > v$,

$$W(l,u,v) = \begin{cases} C_l^u A_l^v \left((v-l)^{u-l} - \right. \\ \left. \sum_{i=1}^{v-l} W(i, u-l, v-l) \right), & 0 \leq l < v \\ 0, & l \geq v. \end{cases}$$

Let P be the one-step transition probability matrix, and P^n the n-step transition probability matrix. Given that initially all nodes are contending for time slots, i.e., $X_0 = 0$ with probability 1, the unconditional probability distribution of X_n is represented by the first row of P^n. That is,

$$p(X_n = i) = P_{1,i+1}^n, i = 0, \ldots, K$$

where $P_{1,i+1}^n$, denotes the entry of the matrix P^n, located at the first row and $(i+1)^{\text{st}}$ column. The probability that all nodes acquire a time slot within n frames is denoted by F_n^{all}, where

$$F_n^{all} = p(X_n = K) = P_{1,K+1}^n.$$

Let μ_n denote the average number of nodes which acquire a time slot within n frames. Therefore,

$$\mu_n = \sum_{i=0}^{K} i P_{1,i+1}^n.$$

The probability that a specific node, say node x, acquires a time slot within n frames is denoted by F_n, where

$$\begin{aligned} F_n &= \sum_{i=0}^{K} p(\mathcal{E}|X_n = i) p(X_n = i) \\ &= \sum_{i=1}^{K} \frac{C_{i-1}^{K-1}}{C_i^K} P_{1,i+1}^n = \frac{\mu_n}{K} \end{aligned}$$

where $\mathcal{E}$ is the event that node x acquires a time slot within n frames and $p(\mathcal{E}|X_n = i) = \frac{C_{i-1}^{K-1}}{C_i^K} = \frac{i}{K}$ since all nodes have equal chances of acquiring a time slot. Note that, since the VeMAC assumes a fixed number of constant duration time slots in a frame on the CCH, the choice of the L value should always ensure that $K \leq N$. However, the analysis of the protocol for the case $K > N$ can be useful in order to determine an optimal value for L. This analysis gives an indication of how the protocol will behave if the number of nodes in a THS becomes larger than L.

Fig. 3.8 illustrates F_n^{all} for different values of N and K. As shown in Fig. 3.8, in a

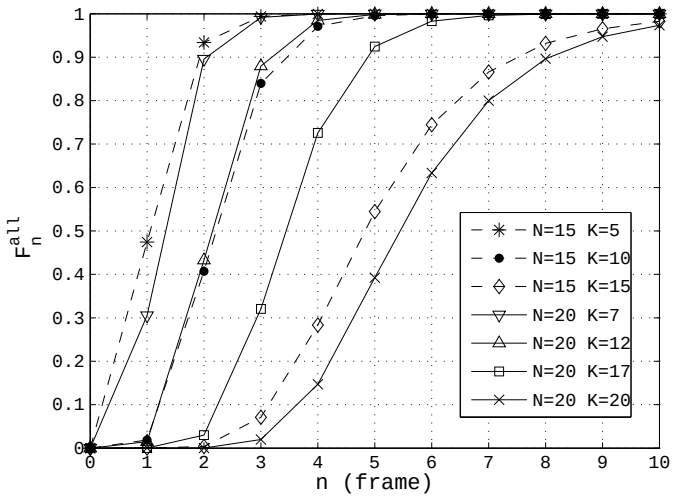

Figure 3.8: Probability that all nodes acquire a time slot within n frames.

dense scenario such as $(N = 15, K = 15)$, there is a probability greater than 0.9 that all the contending nodes acquire a time slot within 8 frames. Hence, given a frame duration around 100 ms (as discussed in Chapter 4), the simplifying assumption of invariant THSs (assumption b) is acceptable, since it is reasonable to assume that the THS configuration remains constant for a sufficiently large time after all the contending nodes acquire a time slot. The analysis presented in this subsection is verified in Subsection 3.5.1 via MATLAB simulations.

3.5 Simulations

This section presents MATLAB simulation results to study the accuracy of the analysis in Subsection 3.4, and evaluate the performance of VeMAC as compared with ADHOC MAC in accessing the CCH in highway and city scenarios.

3.5.1 Analysis Verification

Simulations have been conducted using MATLAB to verify the analysis in Section 3.4. In the simulations, assumption e) is removed, and the average number of nodes which acquire a time slot within n frames is calculated for different K and N, and denoted by μ_n^{sim}. The

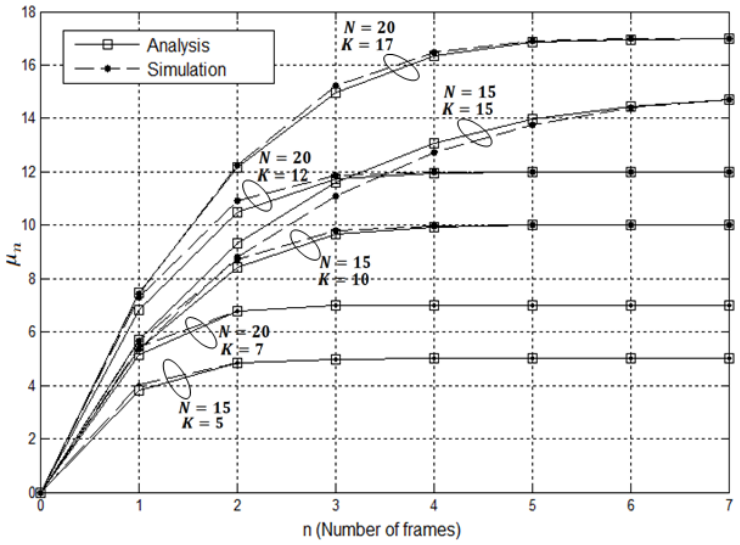

Figure 3.9: Average number of nodes acquiring a time slot within n frames.

98% confidence interval of μ_n^{sim} is less than 0.33 node for all n, K, and N. As shown in Fig. 3.9, the results of μ_n^{sim} obtained from simulations without assumption e) are very close to μ_n obtained from analysis for different K and N.

3.5.2 Simulation Scenarios and Performance Metrics

The first scenario under consideration is a segment of a two-way vehicle traffic highway. A vehicle can communicate with all the vehicles within its communication range, i.e., no obstacles. Each vehicle moves with a constant speed drawn from a normal distribution, and the number of vehicles on the highway segment remains constant during the simulation time. When a vehicle reaches one end of the highway segment, it re-enters the segment from the other end. For this reason, to prevent the unrealistic merging collisions caused by vehicles which jump from one end to the other end, if a vehicle is located at a distance $d \leq R$ from one end of the highway segment, where R denotes the communication range, it can communicate with vehicles located within a distance $R - d$ from the other end of the segment. In this way, for each traffic direction, the vehicles at the end of the segment act as if they are following the vehicles at the start of the segment.

The second scenario is a city grid layout consisting of three horizontal and three vertical two-way vehicle traffic streets. All the streets have the same dimensions, and the horizontal and vertical streets are evenly spaced resulting in four identical square city blocks (a city

Table 3.1: Simulation parameters

Parameter	**Highway**	**City**
Highway length	1 Km	–
# horizontal streets	–	3
# vertical streets	–	3
City street length	–	430 m
# city blocks	–	4
City block edge length	–	200 m
# lanes/direction	2	1
Lane width	5 m	5 m
Speed mean value	100 km/h	50 km/h
Speed standard deviation	20 km/h	10 km/h
Transmission range	150 m	150 m
# slots/frame	100	100
# slots for left directions	50	50
# slots for right directions	50	50
# slots for RSUs	0	0
Slot duration	1 ms	1 ms
Simulation time	2 min.	2 min.
# vehicles	80 to 280 (step = 20)	150 to 600 (step = 50)
THSO	0.24 to 0.96 (step = 0.06)	0.17 to 0.70 (step = 0.06)

block is the smallest area that is surrounded by streets). The area of intersection of a horizontal street with a vertical one is referred to as a junction area. Each vehicle moves with a constant speed drawn from a normal distribution. When a vehicle reaches a junction area, it chooses one of all possible moving directions with equal probability (vehicles are not allowed to leave the simulation area during the simulation time). A vehicle located at a junction area can communicate with vehicles within its communication range located on both streets intersecting at the junction area. On the other hand, a vehicle located at a street but not at a junction area cannot communicate with vehicles located on other streets due to the existence of city blocks which obstruct the wireless signal.

For both scenarios under consideration, all the transmitted packets are broadcast packets, the wireless channel is ideal, and the only source of packet errors is the transmission collision. Table 3.1 summarizes the simulation parameters and Figs. 3.10 and 3.11 show snap shots of the simulated highway and city scenarios respectively, where the black and

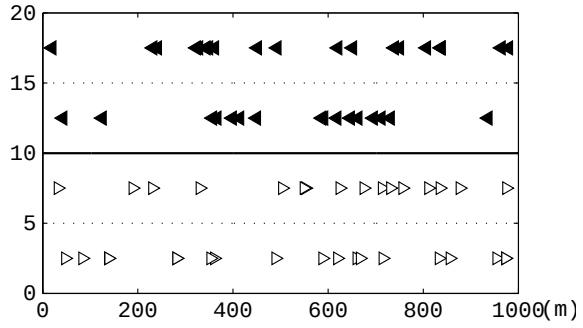

Figure 3.10: A snap shot of the simulated highway segment.

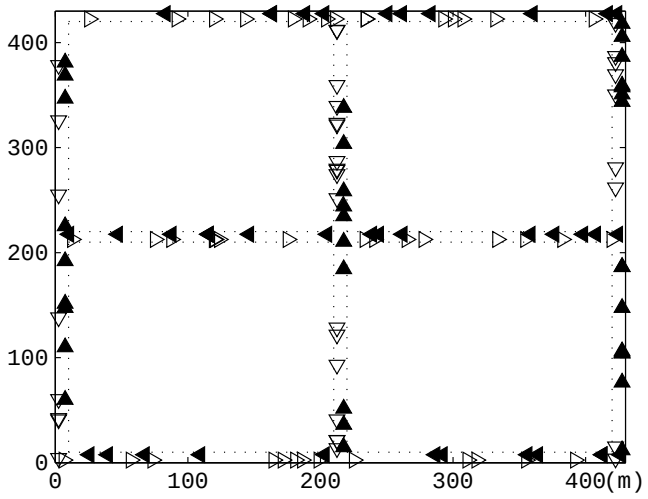

Figure 3.11: A snap shot of the simulated area of the city.

white triangles represent vehicles moving in opposite directions. The same slot duration and total number of time slots per frame are used for all the MAC protocols under consideration (Subsection 3.5.3).

We define a parameter, called the two-hop set occupancy (THSO), equal to $N_v \times \frac{2R}{\text{Length}_h} \times \frac{1}{L}$ or $\frac{N_v}{N_s} \times \frac{2R}{\text{Length}_s} \times \frac{1}{L}$ in the highway and city scenarios respectively, where N_v is the total number of vehicles, N_s is the total number of streets in the city, Length_h is the length of the highway segment, and Length_s is the length of a city street. Note that, the ratio $\frac{N_v}{N_s}$ approximately equals the number of vehicles on a city street, the number L represents the maximum number of time slots available for a THS, and the length $2R$ is the maximum length that a THS can occupy on the highway segment or on a city street. Consequently, the THSO indicates the ratio of the number of time slots required by a THS to the total number of time slots available for a THS. However, the THSO is not guaranteed for each THS in the simulations. The reason is that, if there are N_v moving vehicles, this does not mean that at each instant, each THS on the highway consists of $N_v \times \frac{2R}{\text{Length}_h}$ vehicles or each THS in the city consists of $\frac{N_v}{N_s} \times \frac{2R}{\text{Length}_s}$ vehicles. Also, in the city scenario under consideration, a THS located near a junction area can occupy a length on the streets up to $4R$ ($2R$ on each of the horizontal and vertical street intersecting at the junction area).

The following performance metrics are considered:

a) rate of merging collisions: the average number of merging collisions per frame per THS;

b) rate of access collisions: the average number of access collisions per slot per THS;

c) Tx throughput: the average number of successful transmissions per slot per THS. A transmission by a vehicle x in a certain time slot is considered successful iff no other vehicles in the two-hop neighbourhood of x transmits in the same slot;

d) Rx throughput: the average number of successfully received packets per slot per THS. As mentioned, packet errors only happen due to transmission collision.

Each of the metrics is calculated first for the whole simulation area, and then multiplied by $\frac{2R}{\text{Length}_h}$ or $\frac{1}{N_s} \times \frac{2R}{\text{Length}_s}$ for the highway and city scenarios respectively. Note that, unlike the other three metrics, the rate of merging collisions is calculated per frame not per slot. The reason is that, merging collisions happen due to the movement of the vehicles, which is negligible in the duration of one time slot. The metrics are obtained for each of the MAC protocols mentioned in Subsection 3.5.3. At the beginning of the simulations, the vehicles are randomly (uniformly) placed on the highway segment and on all streets of the

city. The vehicles remain stationary and try to acquire a time slot by using the MAC protocol under consideration. Once no more vehicle can acquire a time slot, the vehicles begin moving and the simulation timer starts. The objective of this process is to quickly bring the system to a steady state where most of the vehicles have acquired a time slot.

3.5.3 Simulated Protocols

Two versions of the VeMAC protocol are considered: VeMAC with $\tau = 0$ (V0) and VeMAC with $\tau = \infty$ (V-inf). As will be shown in Subsection 3.5.4, both versions of the VeMAC protocol significantly outperform the ADHOC MAC protocol in [20]. The poor performance of ADHOC MAC is caused by the following two main reasons. First, due to the lack of a condition similar to the SRP condition in VeMAC, when two vehicles having acquired a time slot enter the communication range of each other, one of them releases its time slot even if no merging collision happens. Second, as mentioned in [20], a node which needs to acquire a time slot should attempt transmission in the next available time slot with probability p_{acc}. For a certain time slot, the optimal probability $p_{opt} = 1/N_c$, where N_c is the number of contending nodes attempting to acquire this time slot [20]. However, since N_c is not known to any of the contending nodes, each contending node x sets $N_c = N_{max} - N^x_{succ}$, where N_{max} is the maximum number of nodes which can exist in a THS and N^x_{succ} is the number of nodes in the two-hop neighbourhood of node x which have successfully acquired a time slot as derived from the framing information received by node x [20]. This estimation of N_c is far from accurate. The reason is that, if a node x detects that N^x_{succ} nodes have successfully acquired a time slot, this does not mean at all that there are $N_{max} - N^x_{succ}$ nodes which need to acquire a time slot in the two-hop neighbourhood of node x. Also, even if there are exactly $N_{max} - N^x_{succ}$ contending nodes, they do not necessarily contend for the same time slots since each of the nodes may belong to a different set of THSs. Additionally, N_{max} is not constant since it depends on parameters such as the inter-vehicle distance and the number of lanes which considerably vary based on the scenario (i.e., highway, city, urban, sub-urban, or rural areas).

In terms of communication over the control channel, the main similarities and differences between the VeMAC and ADHOC MAC protocols can be summarized as follows. Both protocols are based on TDMA, work over the physical layer of different standards (such as the IEEE 802.11), and achieve an efficient multi-hop broadcast service (Subsection 5.2.2) as well as a reliable one-hop broadcast service without the hidden terminal problem. Also, they both require each node to periodically announce the time slots used by all nodes within its one-hop neighbourhood. However, as will be shown in subsection 3.5.4, the VeMAC protocol significantly outperforms the ADHOC MAC protocol, thanks to the

Table 3.2: The simulated protocols

Protocol	**Abbreviation**
VeMAC with $\tau = \infty$	V-inf
VeMAC with $\tau = 0$	V0
ADHOC MAC as in [20]	ADHOC
ADHOC-enhanced	AE
ADHOC-optimal	A-opt

following three main features: the reduction of the access collision rate by using fixed time frames (versus sliding frames in ADHOC MAC) and a new method for the nodes to access the available time slots, the reduction of the merging collision rate by assigning disjoint sets of time slots to vehicles moving in opposite direction and to RSUs, and the SRP condition which prevents the nodes from unnecessarily releasing their time slots when they just enter the communication range of each other. These advantages of VeMAC come in addition to being a multichannel protocol more suitable for the DSRC spectrum as compared to the single channel ADHOC MAC protocol. On the other hand, the VeMAC protocol requires frame synchronization, which is not needed by the ADHOC MAC protocol (due to the use of sliding frames). The frame synchronization can be achieved by using the GPS 1PPS signal with an integer number of frames in each second, as discussed in Subsections 2.2 and 2.4.

Based on the two limitations of the typical ADHOC MAC protocol [20], two more versions of ADHOC MAC are considered in the simulations: the ADHOC-enhanced (AE) and the ADHOC-optimal (A-opt). The AE protocol eliminates the first limitation of ADHOC MAC by using a condition similar to the SRP condition of VeMAC. More precisely, a node x does not release its time slot based on a packet received from a node y unless node x has previously received a packet from node y, i.e., unless node y is included in the framing information [20] constructed by node x. For both ADHOC MAC and AE, the probability of accessing an available time slot by a contending node x is $p_{acc} = \frac{1}{L-N^x_{succ}}$. Note that, N_{max} is replaced by L (i.e., the maximum number of slots available for a THS) as it is not mentioned in [20] how to determine N_{max}. To evaluate the second limitation of ADHOC MAC, the A-opt protocol is implemented. The A-opt is similar to the AE protocol with the difference that, for each time slot, each contending node is aware of the number of contending nodes N_c within its two-hop neighbourhood and sets $p_{acc} = p_{opt} = \frac{1}{N_c}$. Note that this awareness of N_c is provided by the simulator and cannot be achieved in

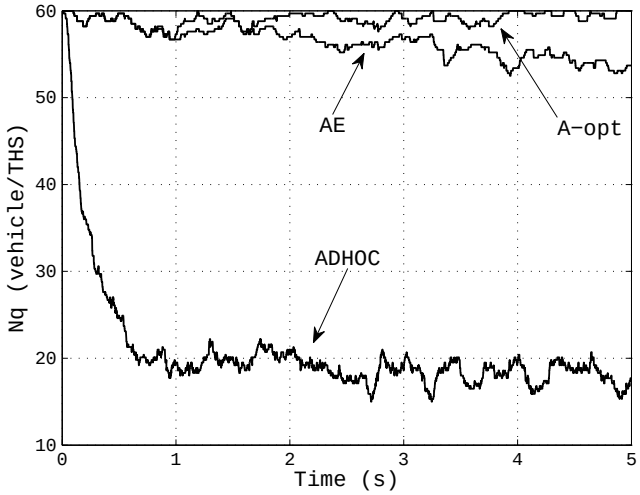

Figure 3.12: The number of vehicles acquiring a time slot for the three ADHOC MAC versions in the highway scenario, at THSO = 0.6 (i.e., 60 vehicle/THS).

reality. Hence, the A-opt is not a realistic protocol, it just represents an upper bound on the performance of ADHOC MAC. The five MAC protocols under consideration are summarized in Table 3.2.

To demonstrate the difference among the three ADHOC MAC versions, Fig. 3.12 shows the total number of vehicles successfully acquiring a time slot, denoted by N_q, in the first five seconds of the simulation in the highway scenario. For the ADHOC protocol, due to the lack of the SRP condition, N_q drops from 60 to 20 vehicle/THS in the first second of the simulation. Also, each vehicle which releases its time slot in the first second cannot quickly acquire a new one due to the inexact probability of accessing an available time slot. For this reason, N_q remains below 20 vehicle/THS at the end of the five seconds. Unlike ADHOC MAC, in the AE protocol, the sudden decrease in N_q is eliminated thanks to the SRP condition. For this protocol, N_q decreases gradually and reaches 54 vehicle/THS at the end of the five seconds. On the other hand, the A-opt protocol does not show any decrease in N_q at the end of the five seconds since it can control the access collisions by using the optimal probability p_{opt} for accessing the available time slots. Similar behaviours of the three ADHOC MAC versions were seen in the city scenario.

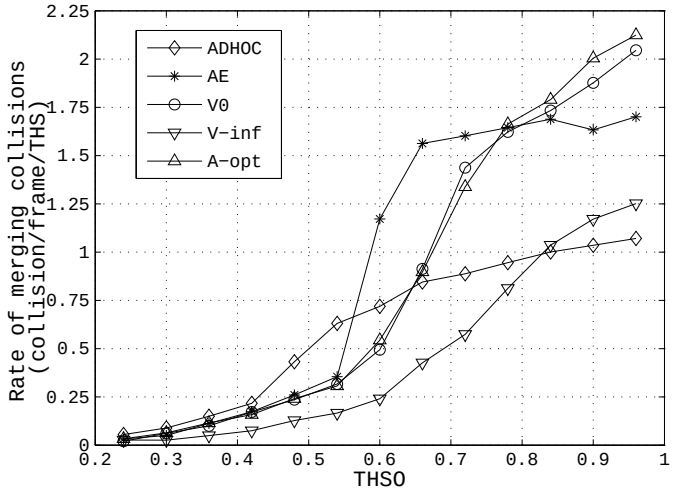

Figure 3.13: The rate of merging collisions in highway.

3.5.4 Simulation Results

3.5.4.1 Highway Scenario

Fig. 3.13 shows the rate of merging collisions for all the MAC protocols under consideration. The V-inf protocol achieves a low rate of merging collisions since it assigns disjoint sets of time slots to vehicles moving in opposite directions. The V0 and A-opt protocols have almost the same rate of merging collisions for different THSO values. Note that for a high THSO, the ADHOC protocol provides a low rate of merging collision, even less than the V-inf protocol, due to a small number of nodes which successfully acquire a time slot as compared to other protocols (recall that, by definition, a merging collision happens only among the nodes which are successfully acquiring a time slot).

The rate of access collisions is shown in Fig. 3.14 for all the protocols. As expected, the A-opt protocol shows a considerably smaller rate of access collisions than both ADHOC and AE protocols, which verifies the inefficiency of both protocols in determining the probability of accessing an available slot. Due to the ability of the V-inf protocol to decrease the rate of merging collisions, as shown in Fig. 3.13, it also achieves a less rate of access collisions than that of the V0 protocol. The reason is that, each merging collision generates access collisions, especially for a high THSO, until each node which released its time slot reacquires a new one. Both VeMAC protocols (V-inf and V0) provide a rate of access collisions which is slightly higher than that of the A-opt protocol but significantly

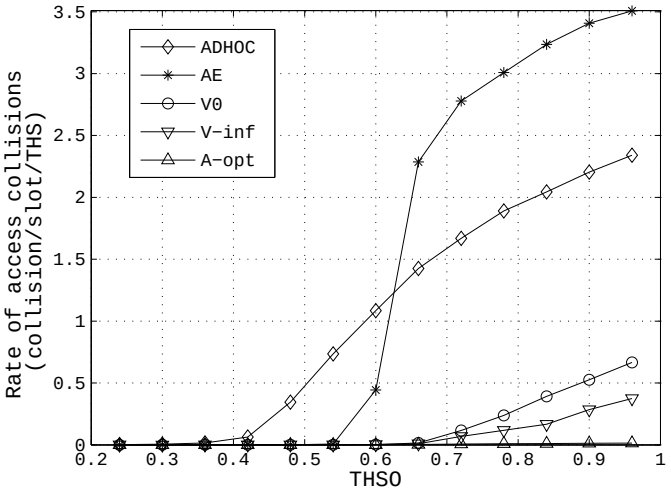

Figure 3.14: The rate of access collisions in highway.

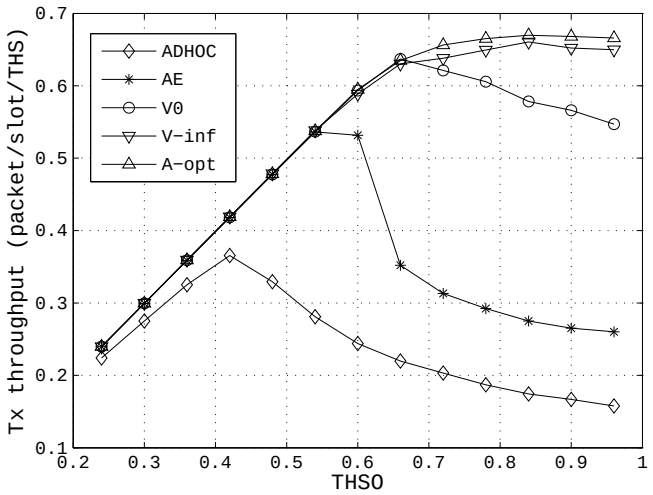

Figure 3.15: The Tx throughput in highway.

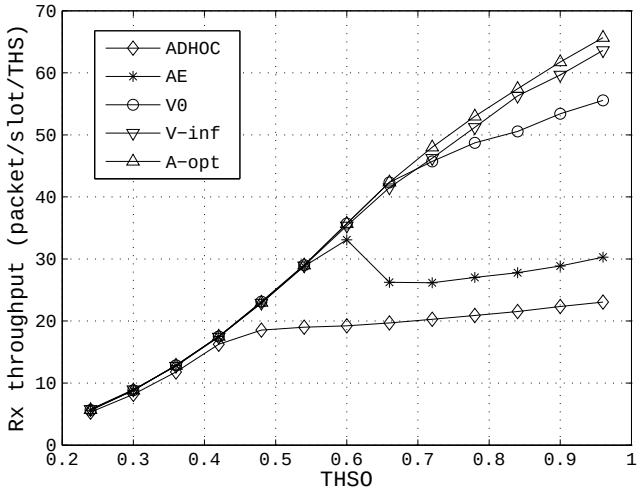

Figure 3.16: The Rx throughput in highway.

lower than the rates provided by the ADHOC and AE protocols especially for a high THSO.

Fig. 3.15 shows the Tx throughput for all the protocols. Because of the limitations discussed in Subsection 3.5.3, the performance of the ADHOC protocol is the lowest among all the MAC protocols for all the THSO values. The AE protocol has better performance than the ADHOC protocol, but its Tx throughput decreases for a high THSO due to its inability to handle the access collisions. For a THSO < 0.7, the V-inf and V0 protocols have almost the same Tx throughput, while for a THSO > 0.7, the V-inf protocol starts to perform better than the V0 protocol. Both protocols outperform the AE and ADHOC protocols for all the THSO values, and the Tx throughput of the V-inf is slightly less than the unrealistic A-opt protocol for a THSO > 0.7.

The Rx throughput is shown in Fig. 3.16. It is clear that, the V-inf and V0 protocols achieve a higher Rx throughput than both of the AE and ADHOC protocols for all the THSO values. For instance, at THSO $= 0.78$, the V-inf protocol provides an Rx throughput of 51 packet/slot/THS as opposed to only 21 packet/slot/THS in the case of the ADHOC protocol (i.e., a 143% increase in the Rx throughput). Note that, for a high THSO, even if the Tx throughput remains constant or slightly decreases, the Rx throughput continues increasing. The reason is that, for the same Tx throughput, when the number of vehicles on the highway segment increases (i.e., when the THSO increases), more vehicles can receive packets since all the packets transmitted are of broadcast type. Similar to the Tx throughput, the V-inf protocol provides a slightly less Rx throughput than the A-

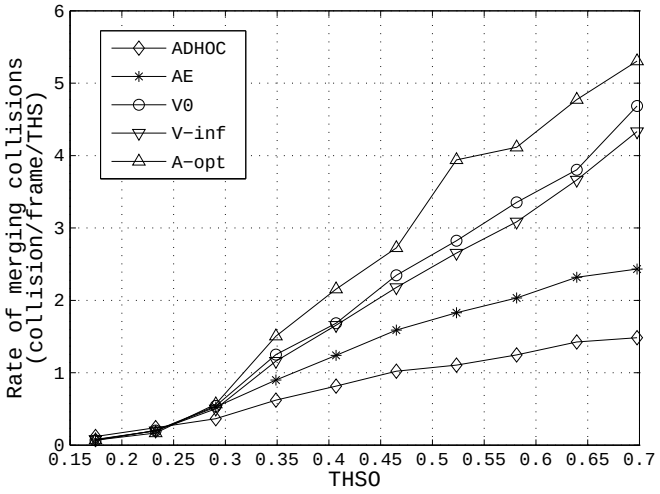

Figure 3.17: The rate of merging collisions in city.

opt protocol. For the range of THSO considered in the highway, the maximum relative difference[3] between the Rx throughput of the V-inf and A-opt protocols is approximately 3.9% (achieved at THSO = 0.72).

3.5.4.2 City Scenario

The rate of merging collision in the city scenario is shown in Fig. 3.17 for all the protocols. It is noted that, the relative difference between the rate of merging collision provided by the V-inf protocol and that provided by the V0 protocol is reduced as compared to the highway scenario. For instance, at a THSO = 0.7 in the highway scenario, the V0 protocol shows approximately 150% higher rate of merging collision than the V-inf protocol, as opposed to only an 8% increase in the city scenario at the same THSO. The reason is that, in the city scenario, the V-inf protocol suffers from the merging collisions near the junction areas due to vehicles which change their moving direction. This kind of merging collision does not exist with the V-inf protocol when employed in the highway scenario (the merging collisions only happens among vehicles moving in the same direction). The close rate of merging collisions of both V-inf and V0 protocols also results in a close rate of access collisions, as shown in Fig. 3.18. Similar to the highway scenario, both V-inf

[3]The relative difference between two values x and y is defined as $\frac{|x-y|}{\min(x,y)}$

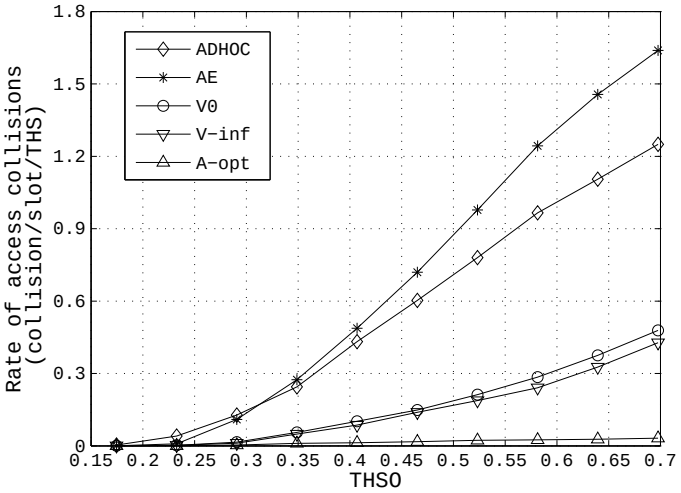

Figure 3.18: The rate of access collisions in city.

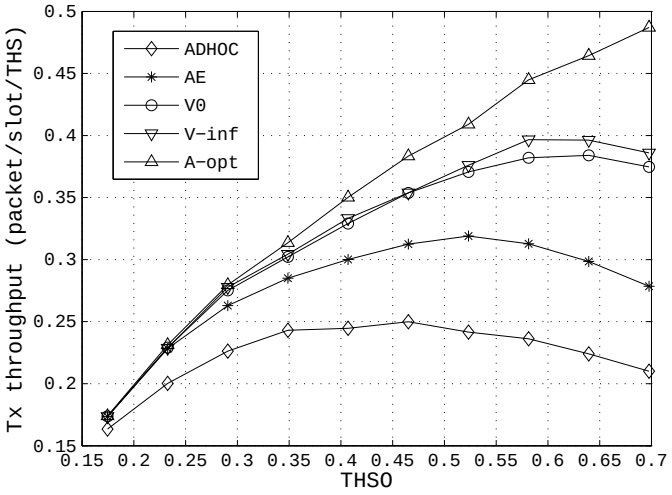

Figure 3.19: The Tx throughput in city.

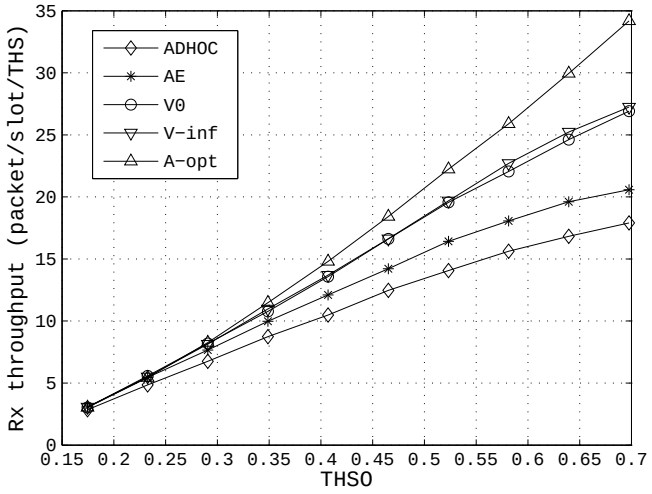

Figure 3.20: The Rx throughput in city.

and V0 protocols provide a rate of access collision which is higher than that of the A-opt protocol but lower than those provided by the AE and ADHOC protocols.

The Tx throughput and Rx throughput are shown in Figs. 3.19 and 3.20 respectively. The V-inf and V0 protocols have the same performance for a THSO < 0.5, while the V-inf protocol performs slightly better for a THSO > 0.5. Unlike the highway scenario, where the A-opt and V-inf protocols have very close Tx and Rx throughputs, in the city scenario the A-opt outperforms the V-inf protocol. This outperforming is a result of the excess merging collisions that the V-inf protocol experiences in the city scenario due to vehicles which change their moving directions. However, similar to the highway scenario, both V-inf and V0 protocols provide higher Tx and Rx throughputs than the AE and ADHOC protocols.

3.6 Summary

This chapter presents VeMAC, a novel multichannel MAC protocol based on TDMA for VANETs. How the periodic and event-driven safety messages are queued and served by the VeMAC protocol is described, and the techniques employed by the protocol for accessing the CCH and SCHs are explained. Mathematical analysis and computer simulations are presented to evaluate the performance of the VeMAC protocol in highway and city

scenarios, in comparison with different versions of the ADHOC MAC protocol. Simulation results show that VeMAC provides a smaller rate of transmission collisions, which results in a significantly higher throughput on the CCH, as compared with that provided by ADHOC MAC. This outperforming of the VeMAC protocol is due to the following three main features: the reduction of the access collision rate by using fixed time frames (versus sliding frames in ADHOC MAC) and a new method for the nodes to access the available time slots, the reduction of the merging collision rate by assigning disjoint sets of time slots to vehicles moving in opposite direction and to RSUs, and the SRP condition which prevents the nodes from unnecessarily releasing their time slots when they just enter the communication range of each other. In addition, the multichannel VeMAC protocol is more suitable for the DSRC spectrum (divided into seven channels) as compared to the single channel ADHOC MAC protocol. Chapter 4 focuses on the delay performance achieved by VeMAC in delivering periodic and event-driven safety messages, and compares its performance with that of the IEEE 802.11p standard via computer simulations in a realistic city scenario.

Chapter 4

Performance Evaluation of VeMAC Supporting VANET Safety Applications

This chapter investigates how the VeMAC protocol can deliver both periodic and event-driven safety messages in VANETs, by presenting a detailed delivery delay analysis, including queueing and service delays, for both types of safety messages [40, 41]. The probability mass function of the service delay is first derived, then the D/G/1 and M/G/1 queueing systems are used to calculate the average queueing delay of the periodic and event-driven safety messages respectively. As well, a comparison between the VeMAC protocol and the IEEE 802.11p standard [21] is presented via extensive simulations using the network simulator ns-2 [48] and the microscopic vehicle traffic simulator VISSIM [49]. A real city scenario is considered and different performance metrics are evaluated, including the network goodput, protocol overhead, channel utilization, protocol fairness, probability of a transmission collision, and message delivery delay. Although the VeMAC is a multichannel protocol, this chapter focuses only on the operation of the VeMAC on the CCH, over which the high priority periodic and event-driven safety messages under consideration are transmitted.

4.1 Delay Analysis

The total delay that a safety message experiences on the CCH before reaching all the one-hop neighbours consists of five components: 1) *upper layers delay* from the time that

a safety message is generated at the application layer until it is assigned to one of the two queues in Fig. 3.1, including the fragmentation time of periodic safety messages; 2) *queueing delay* between the time that a safety message (or a fragment of a safety message) is assigned to one of the queues in Fig. 3.1 and the time that it becomes the head of line (HOL); 3) *access delay* from the time that a safety message (or a fragment of a safety message) becomes the HOL until the start of its transmission. This delay is mainly the time spent by the transmitting node waiting for one of its acquired periodic or event-driven time slots; 4) *transmission duration* of a safety packet; 5) *propagation delay* until the safety packet completely reaches the farthest one-hop neighbour. The *upper layers delay* and *propagation delay* are not considered in the following analysis since they are negligible as compared to the other delay components. The *transmission duration* of any safety packet is assumed to be equal to the duration of one time slot. Note that, the duration of one time slot represents the maximum *transmission duration* which can be experienced by a safety packet on the CCH. However, the difference between the maximum and actual *transmission durations* (fraction of a time slot) is negligible as compared to the *queueing delay* and *access delay* (multiple time slots). The sum of the *access delay* and *transmission duration* is referred to as the *service delay*. To simplify the analysis of the *service delay* and *queueing delay*, denoted by W_s and W_q respectively, we assume that a node releases its periodic or event-driven time slot(s) and acquires a new one(s) after the transmission of each periodic or event-driven safety packet respectively. This assumption guarantees that the *service delays* of the successive periodic and event-driven safety messages assigned to the two queues in Fig. 3.1 form two sequences of independent and identically distributed (i.i.d.) random variables, which is a necessary condition for the application of the D/G/1 and M/G/1 queuing systems in Subsection 4.1.2. The assumption is reasonable in scenarios with high rates of access collisions and merging collisions, where the nodes frequently release their time slots and acquire new ones. The number of periodic and event-driven time slots, k_p and k_e, that a node can access per frame are assumed to be constant. The total delay, denoted by W, is the sum of W_s and W_q, and all delays are represented in the unit of a time slot. For any discrete random variable X, the probability mass function (PMF) and the cumulative distribution function (CDF) are denoted by f_X and F_X respectively, while the first and second moments are denoted by $\overline{X}$ and $\overline{X^2}$ respectively. If random variable X takes only non-negative integer values, its probability generating function (PGF) is denoted by $G_X(z) = \overline{z^X} = \sum_x f_X(x) z^x$, while $G'_X(z)$ denotes $\frac{d}{dz} G_X(z)$. The *service delay* and *queueing delay* are considered separately in Subsections 4.1.1 and 4.1.2 in the following. The accuracy of the analysis in this section under the simplified assumptions is studied via MATLAB simulations in Subsection 4.2.2.

4.1.1 Service Delay

Since the VeMAC protocol serves the two queues in Fig. 3.1 independently using the k_p and k_e time slots, the PMF f_{W_s} is similar for both queues and differs only due to the difference between the k_p and k_e values. Hence, the PMF f_{W_s} is derived in a generic way (i.e., irrespective of the type of the transmitted safety message) given that the transmitting node is accessing k time slots per frame. For the periodic and event-driven safety messages, the PMF f_{W_s} can be calculated just by replacing k in the generic f_{W_s} with k_p and k_e respectively. Let random variable J denote the index of the time slot at the start of which a safety message becomes the HOL. Note that, since the transmission delay is equal to 1, if the inter-arrival time of periodic safety messages is an integer value, and assuming that the first message arrives at the start of a time slot, it is guaranteed that a periodic message always becomes the HOL at the start of a time slot. On the other hand, due to random arrivals of event-driven safety messages with non-integer inter-arrival times, it is possible that, when the queue is empty, an arriving event-driven message becomes the HOL within the duration of a certain time slot. In this case, we neglect a fraction of time slot in the calculation of the *service delay* and assume that the event-driven message becomes the HOL at the start of the next slot. Hence, the *service delay* W_s can take only integer values ranging from 1 to $L-k+1$. The calculation of $f_{W_s}(i), i = 1, ..., L-k+1$, is considered separately for the two extreme values of the split up parameter, $\tau = 0$ and $\tau = \infty$.

4.1.1.1 $\tau = 0$

In this case, if a safety message becomes the HOL at the start of time slot j, the transmitting node can be accessing any k of the L time slots following (and including) time slot j with equal probabilities. Hence,

$$p(W_s = i | J = j) = \frac{C_{k-1}^{L-i}}{C_k^L},$$

$$1 \leq k \leq L, 1 \leq i \leq L-k+1, 0 \leq j \leq L-1$$

where $C_k^n = \frac{n!}{(n-k)!k!}$. The denominator is the number of ways that the transmitting node can access k time slots among the L time slots following (and including) time slot j, while the numerator is the number of ways that one of the k time slots that the node is accessing is the i^{th} time slot starting from j, denoted by $j_a = (j+i-1) \mathrm{mod} S$, and the remaining $k-1$ time slots are among the $L-i$ time slots following time slot j_a. In other words, the numerator is the number of ways that the node is accessing the i^{th} time slot starting from j but not any of the $i-1$ time slots following (and including) time slot j. Note that,

with $\tau = 0$, the probability $p(W_s = i|J = j)$ is independent of the value of j since the transmitting node is allowed to access all the available time slots in a frame with equal probabilities. Hence,

$$f_{W_s}(i) = \sum_{j=0}^{L-1} p(W_s = i|J = j) \times f_J(j) = \sum_{j=0}^{L-1} \frac{C_{k-1}^{L-i}}{C_k^L} \times f_J(j) = \frac{C_{k-1}^{L-i}}{C_k^L},$$

$$1 \leq i \leq L-k+1, 1 \leq k \leq L.$$

4.1.1.2 $\tau = \infty$

Consider that a node is moving in one of the left directions. When a safety message becomes the HOL at the start of time slot j, the transmitting node can be accessing any k time slots in set $\mathcal{L}$ with equal probabilities. There is no probability that the node accesses any of the time slots in sets $\mathcal{R}$ and $\mathcal{F}$. Hence, unlike the $\tau = 0$ case, the probability $p(W_s = i|J = j)$ depends on the value of j.

a) For $|\mathcal{L}| \leq j \leq L-1$, we have

$$p(W_s = i|J = j) = \begin{cases} \frac{C_{k-1}^{|\mathcal{L}|-[i-(L-j)]}}{C_k^{|\mathcal{L}|}}, & L-j+1 \leq i \leq L-j+1+|\mathcal{L}|-k, \\ & 1 \leq k \leq |\mathcal{L}|, \\ 0, & \text{elsewhere.} \end{cases}$$

The denominator represents the total number of ways that the node can access k slots among the $|\mathcal{L}|$ time slots, while the numerator represents the number of ways which result in W_s equal to i. Note that, the smallest possible value of W_s is $L-j+1$, since $j \in \mathcal{R} \cup \mathcal{F}$ while the node cannot access any time slot in set $\mathcal{R} \cup \mathcal{F}$.

b) For $0 \leq j \leq |\mathcal{L}|-1$, we have the following two cases

- If $j < k$, we have $W_s \leq |\mathcal{L}|-k+1$, since at least one of the k time slots that the node is accessing is among the next $|\mathcal{L}|-j$ time slots starting from time slot j. Then

$$p(W_s = i|J = j) = \begin{cases} \frac{C_{k-1}^{|\mathcal{L}|-i}}{C_k^{|\mathcal{L}|}}, & 1 \leq i \leq |\mathcal{L}|-k+1, \\ 0, & \text{elsewhere.} \end{cases}$$

- If $j \geq k$, there is a probability that the k time slots that the node is accessing are all before time slot j, which results in W_s taking values between $L-j+1$ and $L-k+1$. Hence

$$p(W_s = i|J = j) = \begin{cases} \frac{C_{k-1}^{|\mathcal{L}|-i}}{C_k^{|\mathcal{L}|}}, & 1 \leq i \leq |\mathcal{L}| - j, \\ \frac{C_{k-1}^{L-i}}{C_k^{|\mathcal{L}|}}, & L - j + 1 \leq i \leq L - k + 1, \\ 0, & \text{elsewhere.} \end{cases}$$

Given $p(W_s = i|J = j)$ for all $0 \leq j \leq L-1$, we have

$$f_{W_s}(i) = \sum_{j=0}^{L-1} p(W_s = i|J = j) \times f_J(j),$$

$$1 \leq i \leq L - k + 1, 1 \leq k \leq |\mathcal{L}|.$$

For a node moving in a left direction, we assume that

$$f_J(j) = \begin{cases} \frac{1}{|\mathcal{L}|}, & 0 \leq j \leq |\mathcal{L}| - 1, \\ 0, & \text{elsewhere.} \end{cases}$$

This assumption means that, first, a safety message cannot become the HOL at the start of time slots in set $\mathcal{R} \cup \mathcal{F}$ and, second, a safety message becomes the HOL at the start of time slots in set $\mathcal{L}$ equally likely. Note that, although the transmitting node is not allowed to access time slots in set $\mathcal{R} \cup \mathcal{F}$, a safety message still can become the HOL at the start of a time slot belonging to this set, e.g., when a message arrives at the start of a time slot $j \in \mathcal{R} \cup \mathcal{F}$ and finds the queue empty. The same procedure in this subsubsection can be used to derive f_{W_s} for a node moving in a right direction or for an RSU.

4.1.2 Queueing Delay

Although the PMF of the *service delay* is the same for periodic and event-driven safety messages, their *queueing delays* are different due to different arrival patterns for the two different types of safety messages.

4.1.2.1 Event-driven Safety Messages

As mentioned in Chapter 1, the event-driven safety messages are triggered by certain events such as a sudden brake, road feature notification, approaching an emergency vehicle, etc. Given the variety of such events, it is reasonable to assume that their arrival process has independent and stationary increments, with no group arrivals. That is, the numbers of events occurring in disjoint time intervals are independent, the PMF of the number of events occurring in a time interval only depends on the length of the interval, and there is no simultaneous arrival of events. Based on these properties, the arrival process of the event-driven safety messages can be modeled by a Poisson process with rate λ message/slot. Hence, the event-driven safety message queue in Fig. 3.1 is an M/G/1 queue with the *service delay* distribution f_{W_s} as derived in Subsection 4.1.1. Consequently, provided that $\overline{W_s} < \frac{1}{\lambda}$, which is the necessary and sufficient condition for stability of the event-driven safety message queue [50], by applying the P-K formula [51], we have

$$\overline{W_q} = \frac{\lambda \overline{W_s^{\,2}}}{2(1 - \lambda \overline{W_s})}.$$

4.1.2.2 Periodic Safety Messages

Based on the assumption of fixed-size periodic safety messages (Section 2.1), the number of fragments of a periodic safety message is assumed to be fixed for a given node. If n_f denotes the number of fragments of a periodic safety message for a certain node, the arrival of each periodic safety message results in a simultaneous arrival of n_f fragments in the periodic safety message queue in Fig. 3.1. Consequently, this queue can be modeled as a D/G/1 queue with fixed-size batch arrivals. Hence, the *queueing delay* that a tagged fragment of a periodic safety message experiences consists of two components: the delay since the batch (to which the tagged fragment belongs) enters the queue until the first fragment of the batch becomes the HOL, plus the *service delay* of all the fragments queued before the tagged fragment within the batch. The two components of the *queueing delay* are independent and denoted by W_{q_1} and W_{q_2} respectively. Let integer I denote the inter-arrival time of periodic safety messages, i.e., the batch inter-arrival time. The PGF of the *service delay* of one batch, denoted by W_b, is

$$G_{W_b}(z) = \big(G_{W_s}(z)\big)^{n_f}.$$

Hence, provided that $\overline{W_b} = G'_{W_b}(1) < I$, which is the necessary and sufficient condition for stability of the periodic safety message queue [50], the PGF of W_{q_1} can be calculated as

follows [52, 53]

$$G_{W_{q_1}}(z) = \frac{\xi\big[\prod_{i=1}^{I-1}(z-z_i)\big](z-1)}{z^I - G_{W_b}(z)}$$

where

$$\xi = \lim_{z\to 1} \frac{z^I - G_{W_b}(z)}{\big[\prod_{i=1}^{I-1}(z-z_i)\big](z-1)}$$

and complex numbers $z_1, z_2, \ldots, z_{I-1}$ are the roots of the function $z^I - G_{W_b}(z)$, which are on or inside the unit circle but not equal to 1. The PGF, $G_{W_{q_2}}(z)$, can be calculated by noting that $W_{q_2} = \sum_{i=0}^{N_f} W_s$, where N_f is a random variable representing the number of fragments queued before the tagged fragment within the batch. Since the tagged fragment can be any fragment within the batch with equal probabilities, $f_{N_f}(i) = \frac{1}{n_f}, i = 0, \ldots, n_f - 1$, and $G_{N_f}(z) = \frac{1}{n_f}\sum_{i=0}^{n_f-1} z^i$. Hence, by using the law of total expectation,

$$G_{W_{q_2}}(z) = G_{N_f}(G_{W_s}(z)).$$

Consequently,

$$G_{W_q}(z) = G_{W_{q_1}}(z) \times G_{W_{q_2}}(z)$$
$$\overline{W_q} = G'_{W_q}(1).$$

4.2 Numerical Results

4.2.1 Analytical Results

We use MATLAB R2011b and the Symbolic Math Toolbox V5.7 for the calculation of the average delays as described in Section 4.1. Figs. 4.1a and 4.1b show F_{W_s} for a node moving in a left direction with $\tau = 0$ and $\tau = \infty$ respectively. The main difference between the two cases is that, when $\tau = \infty$, $F_{W_s}(n)$ remains constant for a certain range of n. With $\tau = \infty$, the node can only access time slots in set $\mathcal{L}$. As a result, there should be a range of n where $f_{W_s}(n) = 0$. For instance, if $k = 2, L = 100$, and $|\mathcal{L}| = 40$, $f_{W_s}(n) = 0, \forall n \in \{40, \ldots, 61\}$.

Fig. 4.2a shows the average total delay $\overline{W}$ of a periodic safety message with $n_f = 1$ (a typical case for vehicles) for a node moving in a left direction with $k = 1$. Both $\tau = 0$ and $\tau = \infty$ cases are plotted in Fig. 4.2a for various I values. Although the $\tau = 0$ and $\tau = \infty$ cases have different F_{W_s} (in Figs. 4.1a and 4.1b), when $k = 1$, both τ values result in the same $\overline{W_s}$, which is represented by the straight line in Fig. 4.2a. As shown in Fig.

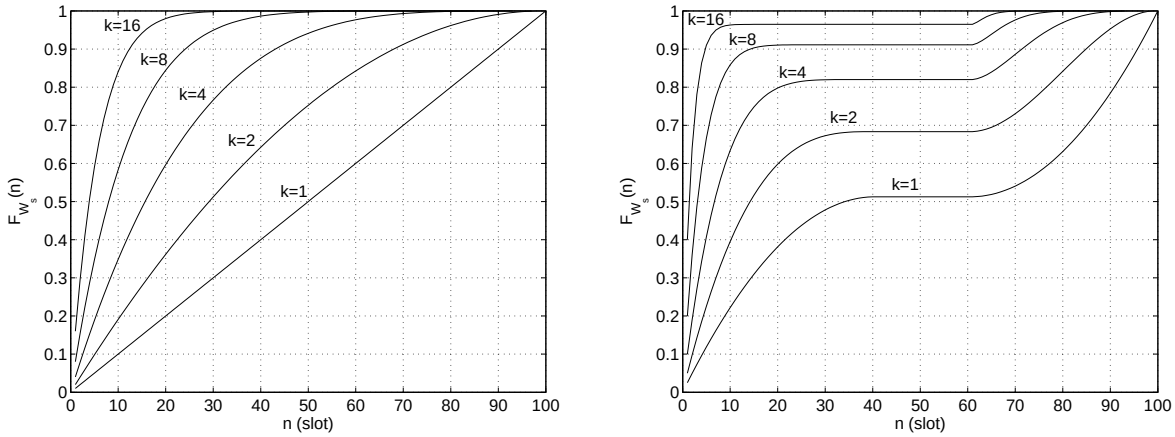

(a) Split up parameter $\tau = 0$

(b) Split up parameter $\tau = \infty$

Figure 4.1: The CDF of the *service delay*, F_{W_s}, for a node moving in a left direction with 100 time slots per frame and 40 time slots associated with the left direction, i.e., $L = 100$ and $|\mathcal{L}| = 40$.

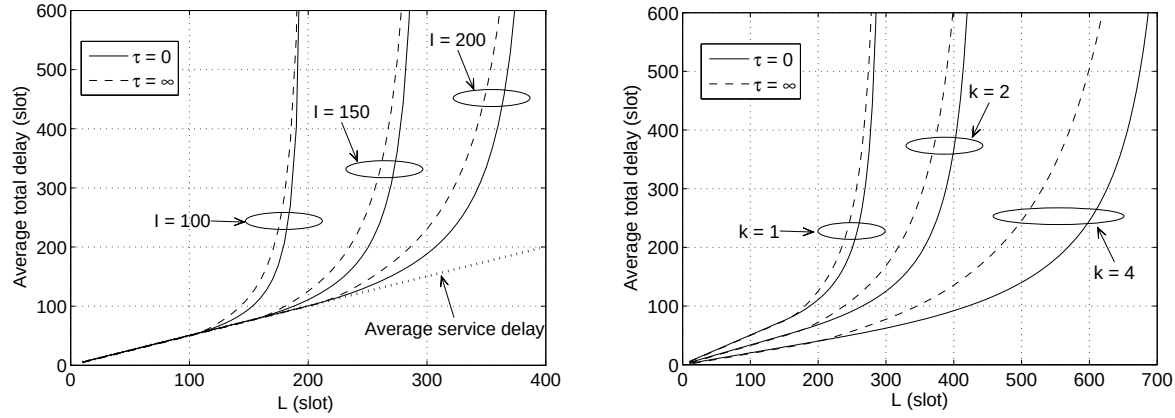

(a) Number of time slots accessed per frame $k = 1$

(b) Periodic message inter-arrival time $I = 150$

Figure 4.2: The average total delay, $\overline{W}$, of a single-fragment periodic message ($n_f = 1$) for a node moving in a left direction with 40 percent of the time slots associated with the left direction, i.e., $|\mathcal{L}| = 0.4L$.

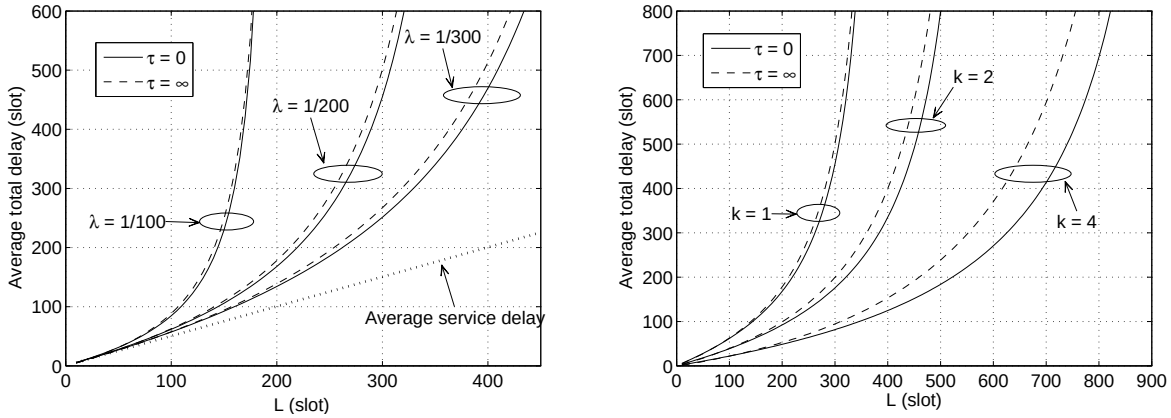

(a) Number of time slots accessed per frame $k = 1$

(b) Event-driven message average arrival rate $\lambda = \frac{1}{200}$ message/slot

Figure 4.3: The average total delay, $\overline{W}$, of an event-driven safety message for a node moving in a left direction with 40 percent of the time slots associated with the left direction, i.e., $|\mathcal{L}| = 0.4L$.

4.2a, if $L \leq I$, $\overline{W}$ is the same as $\overline{W_s}$ since each safety message is served before the next one arrives, i.e., $\overline{W_q} = 0$. When $L > I$, the queueing component W_q is added to the total delay W, and the value of $\overline{W}$ continues to increase with L and approaches ∞ when L tends to the instability value L^* at $\overline{W_s} = I$. Eventually, the value of L^* increases with the number of time slots, k, that the node is allowed to access per frame. To illustrate the effect of k on the total delay W, Fig. 4.2b shows $\overline{W}$ for $I = 150$ and different k values. As shown in Fig. 4.2b, while a frame duration $L = 300$ results in instability for the $k = 1$ case, when k is increased to 2, the value of $\overline{W}$ remains below 200 slots for both $\tau = 0$ and $\tau = \infty$.

Fig. 4.3a illustrates the average total delay $\overline{W}$ of an event-driven safety message for a node moving in a left direction with $k = 1$. Unlike the periodic safety message case in Fig. 4.2a, due to the Poisson arrival of event-driven safety messages, even if $L \leq \frac{1}{\lambda}$, the queueing delay $W_q > 0$ and $\overline{W} > \overline{W_s}$. The effect of k on the total delay of event-driven safety messages is shown in Fig. 4.3b for $\lambda = \frac{1}{200}$ message/slot.

4.2.2 Simulation Results

Computer simulations have been conducted using MATLAB to simulate the two queues in Fig. 3.1. The objectives of the simulations are to study the effect of the assumption on

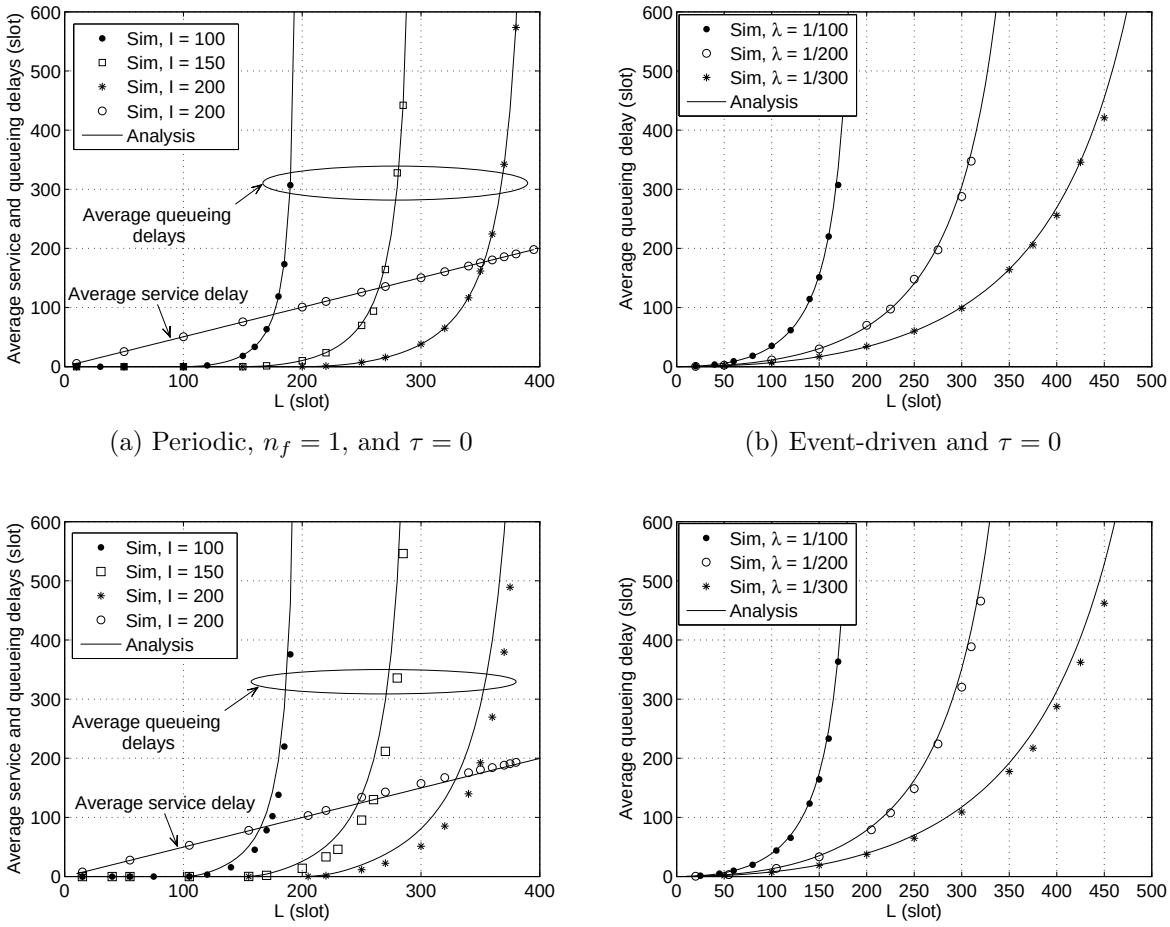

(a) Periodic, $n_f = 1$, and $\tau = 0$

(b) Event-driven and $\tau = 0$

(c) Periodic, $n_f = 1$, and $\tau = \infty$

(d) Event-driven and $\tau = \infty$

Figure 4.4: Analysis and simulation (Sim) results of the average delays for a node moving in a left direction with $k = 1$ and $|\mathcal{L}| = 0.4L$.

f_J for the $\tau = \infty$ case, the impact of neglecting a fraction of time slot in the derivation of f_{W_s} for the event-driven safety messages, and the influence of the numerical errors such as in calculating the roots of $z^I - G_{W_b}(z)$. Fig. 4.4a shows $\overline{W_s}$ and $\overline{W_q}$ of a periodic safety message with $n_f = 1$ for a node moving in a left direction with $k = 1, \tau = 0$, and $|\mathcal{L}| = 0.4L$. The same parameter values are used in Fig. 4.4b to show the average queueing delay $\overline{W_q}$ of an event-driven safety message. Note that, the average service delay $\overline{W_s}$ is not shown in Fig. 4.4b since it is the same as in Fig. 4.4a (W_s is independent of the arrival pattern). As shown in Figs. 4.4a and 4.4b, there is a close match between the analysis and simulation results of the delays of both periodic and event-driven safety messages. The same delays are shown in Figs. 4.4c and 4.4d for $\tau = \infty$. Different from the $\tau = 0$ case, a slight mismatch between the analysis and simulation results appears in Figs. 4.4c and 4.4d, mainly for large I and small λ values, due to the assumption on f_J. The effect of this assumption is worse on the periodic safety messages than on the event-driven safety messages. However, the analysis and simulation results for both types of safety messages are still close to each other in Figs. 4.4c and 4.4d.

To consider a case of large-size periodic safety messages (typically for RSUs), the three delay components $\overline{W_s}$, $\overline{W_{q_1}}$, and $\overline{W_{q_2}}$ of a multi-fragment periodic safety message with $n_f = 4$ are shown respectively in Figs. 4.5a, 4.5b, and 4.5c for an RSU with $\tau = 0$ and different k values. As shown in Figs. 4.5a and 4.5c, there is a close match between the analysis and simulation results of $\overline{W_s}$ and $\overline{W_{q_2}}$. However, some mismatch is noticed for $\overline{W_{q_1}}$ in Fig. 4.5b. This mismatch is the effect of numerical errors, mainly in the calculation of the roots of $z^I - G_{W_b}(z)$. The numerical errors are more significant for large n_f and L due to an increase in the degree of the polynomial $z^I - G_{W_b}(z)$, since $G_{W_b}(z) = \big(G_{W_s}(z)\big)^{n_f}$ and $G_{W_s}(z)$ itself is a polynomial of degree $L - k + 1$.

4.2.3 Discussion

Based on the numerical results in Subsections 4.2.1 and 4.2.2, it is observed that the delay performance of the VeMAC with $\tau = 0$ is better than $\tau = \infty$ for both periodic and event-driven safety messages, especially for large k and I, and small λ values. If the size of the periodic safety messages broadcast by vehicles is 150 bytes, a VeMAC MTU of 675 bytes is suitable to include one periodic safety message and all the VeMAC control information which should be transmitted on the CCH. For a transmission rate of 18 Mbps, which is one of the rates supported by the IEEE 802.11p orthogonal frequency division multiplexing (OFDM) physical layer for the 5 GHz band, the VeMAC MTU transmission time is 0.3 ms. By including guard periods and considering the physical layer overhead, a slot duration of 0.35 ms can be assumed. Given this slot duration, for the periodic safety messages of

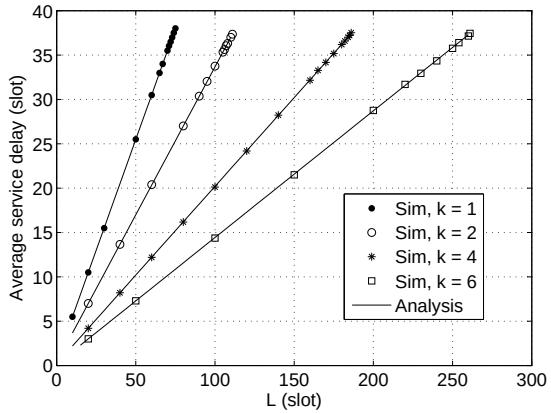

(a) Service delay $\overline{W_s}$ of a fragment

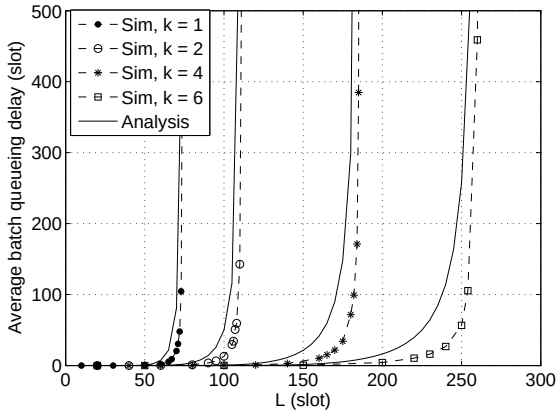

(b) Batch queueing delay $\overline{W_{q_1}}$

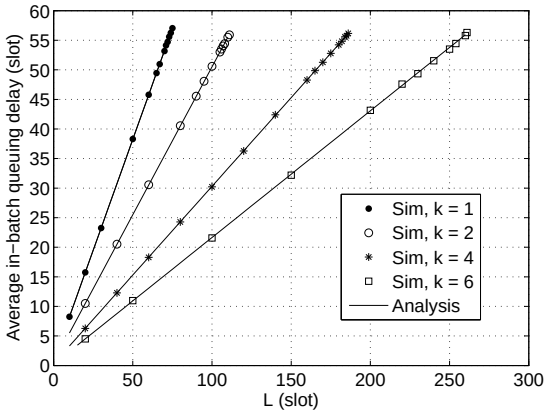

(c) In-batch queueing delay $\overline{W_{q_2}}$

Figure 4.5: Average delays of a periodic safety message with $n_f = 4$ for an RSU when $I = 150$, $|\mathcal{F}| = 0.4L$, and $\tau = 0$.

vehicles, if $I = 200$ slots = 70 ms, and each vehicle is allowed to access one periodic time slot per frame, then from Fig. 4.2a, a frame duration $L = 300$ results in an average total delay around 185 slots (65 ms) for the $\tau = 0$ case. Similarly, for the event-driven safety messages in Fig. 4.3a, if $\lambda = \frac{1}{300}$ message/slot = 9.5 message/s, and if the transmitting node is allowed to access only one event-driven time slot per frame, a frame duration of 300 slots results in an average delay around 250 slots (88 ms). Note that, the frame duration L represents the maximum number of time slots available for any THS in the network. For instance, if $L = 300$ slots and the transmission range is 200 m (corresponding to the maximum length of 400 m occupied by a THS on a road segment), the total number of time slots available for all the nodes on a road segment of any 400 m is equal to 300 slots. The results in this section help to determine the VeMAC parameters, such as $\tau, k_p, k_e,$ and L, used for the comparison with the IEEE 802.11p standard as follows.

4.3 Comparison of VeMAC with IEEE 802.11p

Computer simulations are conducted using the network simulator ns-2 [48] to evaluate the performance of the VeMAC protocol in comparison with the IEEE 802.11p standard in broadcasting the safety messages. Periodic safety messages are generated continuously, while event-driven safety messages are generated according to an exponential ON/OFF model (i.e., the ON and OFF periods are exponentially distributed) at each node in the simulations. For the VeMAC protocol, the periodic and event-driven safety messages are queued and served as specified in Sections 3.1 and 3.2 [1]. On the other hand, for the IEEE 802.11p, we have employed the EDCA scheme, which assigns any MSDU to one of four different access categories (ACs) [22]. The event-driven and periodic safety messages are respectively assigned to the highest and second-highest priority ACs, i.e., AC_VO and AC_VI [21]. Two simulation scenarios are considered: a square network and a realistic city scenario[2]. For both scenarios, the ns-2 parameters are summarized in Table 4.1. The IEEE 802.11p parameter values in Table 4.1 are as specified by the IEEE 802.11p OFDM physical layer for the 5 GHz band [21, 22]. The carrier frequency of 5.89 GHz represents the center frequency of the DSRC channel 178 (the CCH), and the transmission power of 33 dBm is the maximum power allowed on this channel for private OBUs and RSUs as in the ASTM E2213 standard [1]. Given these values of the carrier frequency and the transmission

[1] A website [54] is created in order to upload the ns-2 implementation of the VeMAC protocol, including the periodic and event-driven message queues, for interested researchers.

[2] To the best of our knowledge, currently there is no benchmark vehicle mobility scenarios which can be used for the evaluation of VANET networking protocols.

Table 4.1: ns-2 simulation parameters

Periodic messages		**Event-driven messages**				**Physical layer**			
Parameter	*Value*	*Parameter*	*Value*	*Parameter*	*Value*	*Parameter*	*Value*	*Parameter*	*Value*
Size	150 bytes	Size	450 bytes	Average OFF time	2 s	RXThresh	1.45683×10^{-09} w	CSThresh	8.19468×10^{-10} w
Arrival rate	10 message/s	Average ON time	1 s	Arrival rate during ON time	10 message/s	Carrier frequency	5.89 GHz	Transmission power	33 dBm
						CPThresh	10	Transmission rate	12-18 Mbps
						Antenna	Omni-directional	Channel model	free space
Higher layer protocols		**VeMAC**				**IEEE 802.11p**			
Layer	*Protocol*	*Parameter*	*Value*	*Parameter*	*Value*	*Parameter*	*Value*	*Parameter*	*Value*
Transport layer	UDP	L	275 slots	Slot duration	0.35 ms	aSlotTime	13 μs	SIFS	32 μs
Network layer	dumb agent	k_p	1	k_e	1	AC_VO CW size	3	AC_VO AIFS	58 μs
		τ	0	MTU	450-675 bytes	AC_VI CW size	7	AC_VI AIFS	71 μs
		#bits of a node ID	9	#bits of a slot index	9	Preamble length	32 μs	PLCP header length	8 μs
Simulation time: 1 min. for square network and 5 min. for city						FCS	4 bytes	Header length	32 bytes

power, the receiving threshold (RxThresh) and the carrier sensing threshold (CSThresh) in Table 4.1 result in a communication range of 150 m and a carrier sensing range of 200 m for free space propagation. The capture threshold (CPThresh) is the minimum ratio between the powers of two received signals required for the receiver to capture the signal with the higher power and discard the one with the lower power. The dumb agent used in the network layer just passes the data from the transport layer to the MAC layer while sending, and vice versa while receiving (since all the safety messages under consideration are single-hop broadcast messages).

In addition to the total delay (as defined in Section 4.1), the following performance metrics are considered:

a) goodput: the average rate of safety messages which are successfully delivered to all the one-hop neighbours;

b) channel utilization: the percentage of time that the channel is used for successful transmission of payload data (a transmission is considered successful only if it is correctly received by all the one-hop neighbours);

c) overhead: the percentage of control information relative to the total information transmitted on the channel;

d) probability of a transmission collision: the probability that a transmitted safety message experiences a collision at one or more one-hop neighbours; and

e) fairness indicator: for each node x, a metric denoted by r_x is first calculated, which represents the ratio of the number of safety messages *transmitted* by node x to the total number of safety messages *transmitted* by all nodes. The fairness indicator is the deviation (in percentage) of r_x from a fair share, s_x, that equals the total number of safety messages *generated* at node x normalized by the total number of safety messages *generated* at all nodes. That is, the fairness indicator for a node x is equal to $\mid \frac{r_x - s_x}{s_x} \mid \times 100$.

All the performance metrics, except the overhead and the channel utilization, are calculated separately for the periodic and event-driven safety messages.

4.3.1 Square Network

The first scenario under consideration is a set of stationary nodes uniformly distributed in a square network with side length of 500 m. Fig. 4.6a shows the periodic and event-driven message goodputs of the VeMAC and the IEEE 802.11p protocols using two different physical layer transmission rates. Note that, based on the parameters in Table 4.1, the average rates of periodic and event-driven safety messages generated at each node are 10 messages/s and 3.3 messages/s respectively. As shown in Fig. 4.6a, the VeMAC outperforms the IEEE 802.11p for all the node densities and transmission rates under consideration. For instance, when the number of nodes in the network is 250, the VeMAC protocol can successfully deliver almost all the periodic and event-driven safety messages to all the one-hop neighbours, while the IEEE 802.11p fails to deliver around 50% of the event-driven messages and more than 40% of the periodic messages using a transmission rate of 12 Mbps. This outperforming of the VeMAC protocol in terms of safety message goodput is due to its ability to reduce the probability of a transmission collision as compared with the IEEE 802.11p standard. As shown in Fig. 4.6b, there is a significant difference between the probability of a transmission collision achieved by the two protocols. For the VeMAC protocol, the probability of a transmission collision of an event-driven safety packet is higher than that of a periodic safety packet, especially at high node densities. The reason is that, when the event-driven safety message queue is empty, a node releases its event-driven time slot (i.e., no information is transmitted in the slot) and re-acquires a new one when the next

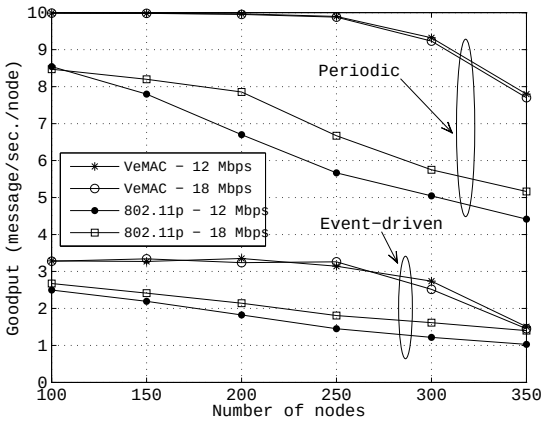

(a) Goodput

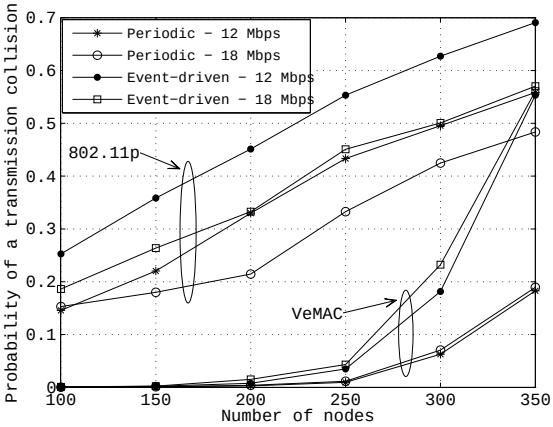

(b) Probability of a transmission collision

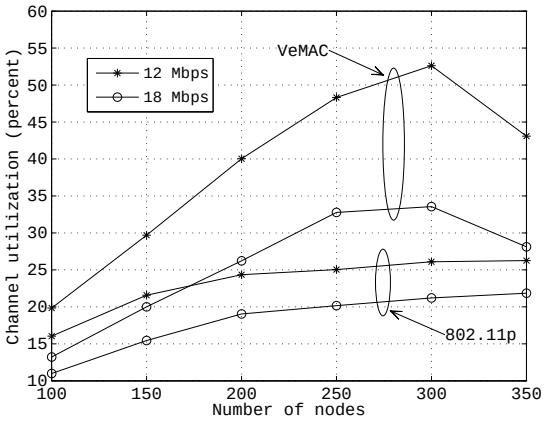

(c) Channel utilization

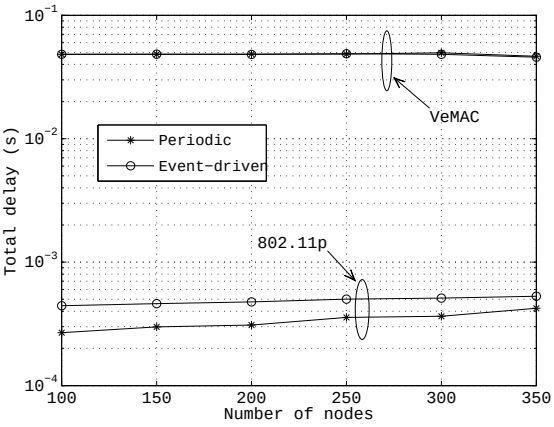

(d) Average delay for a transmission rate of 12 Mbps

Figure 4.6: Simulation results for the square network.

event-driven safety message is generated. This technique relatively increases the rate of access collisions of the event-driven safety packets, as compared with that of the periodic ones. Note that, if the periodic safety message queue is empty, a node must transmit a Type1 packet (including only control information in this case) in its periodic time slot, which allows the node to keep reserving its periodic time slot even when there is no periodic safety packet waiting for transmission. In Figs. 4.6a and 4.6b, the performance of the IEEE 802.11p improves with the higher transmission rate, since the transmission duration of each packet is reduced, which decreases the probability of a transmission collision from the neighbouring nodes. On the other hand, the effect of the channel rate on the performance of the VeMAC in Figs. 4.6a and 4.6b is negligible. As the VeMAC protocol achieves a higher message goodput than the IEEE 802.11p, it also provides a better channel utilization, as illustrated in Fig. 4.6c. The channel utilization in Fig. 4.6c improves with the lower transmission rate, due to an increase in the packet transmission duration, which consequently increases the percentage of time that the channel is used for successful transmissions. When the transmission rate decreases from 18 Mbps to 12 Mbps, the channel utilization of the VeMAC protocol increases by a factor of 1.5 (the same ratio between the two transmission rates), while that of the IEEE 802.11p increases by a factor less than 1.5, as the probability of a transmission collision also increases with the lower transmission rate.

Fig. 4.6d shows the total delay of the VeMAC and the IEEE 802.11p protocols. For both periodic and event-driven safety messages, the total delay of the VeMAC protocol is dominated by the *access delay* component, which is around 48 ms (one half the duration of a frame). At the lowest node density in Fig. 4.6d, the total delay of the periodic safety messages for the IEEE 802.11p protocol is around 280 μs, which is the sum of the durations of one AC_VI arbitrary interframe space (AIFS) (71 μs), one periodic safety packet *transmission duration* (164 μs), and the average backoff time ($\frac{\text{CW size}}{2} \times \text{aSlotTime} =$ 45.5 μs). This delay increases with the node density, due to an increase in the number of backoff cycles that a periodic safety packet encounters. The delay of the event-driven safety messages for the IEEE 802.11p protocol is higher than that of the periodic safety messages, due to a large size of the event-driven messages, which results in a higher *transmission duration*. Although the VeMAC has a higher total delay than the IEEE 802.11p protocol, it is well below the 100 ms delay bound required for most of the safety applications [2].

4.3.2 City Scenario

We consider the city scenario as shown in Fig. 4.7, which consists of a set of roads around the UW campus. To simulate vehicle traffic, the microscopic vehicle traffic simulator VIS-

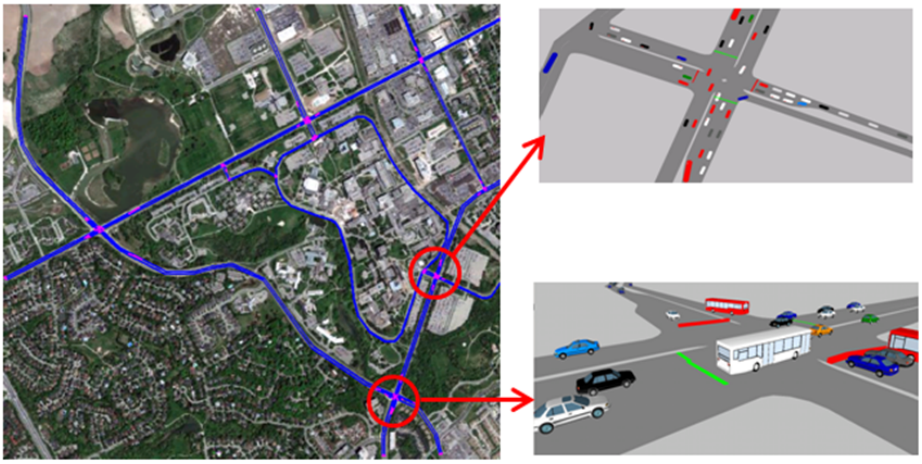

Figure 4.7: A snap shot of the simulations showing the road network with the simulated roads in blue, a 2D view of the intersection of University/Seagram streets, and a 3D view of the intersection of University/Westmount streets.

SIM is employed [49, 55]. The simulator generates a vehicle trace file, which is transformed to an ns-2 scenario file using a MATLAB parser[3]. At the start of the simulation, vehicles enter the road network from every possible entry according to a Poisson process with rate λ_v. After a certain time duration t_{in}, the vehicle input to the road network is stopped, and after an additional warm up period t_w (to reduce transient state effects), the position and speed of each vehicle are recorded at the end of every simulation step. Two types of vehicles are considered: cars and buses. The two vehicle types differ mainly in the vehicle dimensions, as well as the maximum/desired acceleration and deceleration as functions of the vehicle speed. All cars and buses have the same desired speed distribution, which differs from one road to another, and during the left and right turns at intersections. Every intersection in the road network is controlled either by a traffic light, or a stop sign, based on how the intersection is controlled in reality. At signalized intersections, left turns are controlled by the traffic light controller, and right turns are allowed during the red signal phase. Before a vehicle enters an intersection area, it decides whether to turn left, turn right, or not to make any turn, according to a certain probability mass function, which differs from one intersection to another.

The car following model used is the Wiedemann 74 model [58] developed for urban traffic. A vehicle can be in one of four modes: free driving, approaching, following, and

[3]Videos of the VISSIM and ns-2 simulations have been recorded and uploaded to [56] and [57] respectively.

Table 4.2: VISSIM simulation parameters

Vehicle input		**Desired speed (Km/h) distribution**		**Car following (Wiedemann 74)**		**Lane changing**			**Vehicle characteristics**		
Parameter	*Value*	*Location*	*Distribution*	*Parameter*	*Value*	*Parameter*	*Lane changer*	*Trailing vehicle*	*Parameter*	*Car*	*Bus*
λ_v	1000 vehicles/hour	Ring road	$U(32, 48)$	AX	2 m	Maximum deceleration	-4 m/s^2	-3 m/s^2	Average length	4.44 m	11.54 m
t_w	5 min.	All other roads	$U(55, 72)$	BX$_{add}$	2 m	-1m/s^2 per distance	100 m	100 m	Width	1.5 m	2.5 m
t_{in}	2, 4, 6, and 7 min.	Right turns	$U(12, 18)$	BX$_{mult}$	3 m	Accepted deceleration	-1 m/s^2	-1 m/s^2	Percentage of the total # vehicles	95%	5%
# vehicles	292, 603, 839, and 948	Left turns	$U(20, 30)$	**Simulation time:** 5 min.		Default VISSIM maximum/desired acceleration and deceleration functions for cars and buses have been used.					

braking. In each mode, the vehicle acceleration is a function of the vehicle speed, the characteristics of the driver and the vehicle, as well as the distance and the speed difference between the subject vehicle and the vehicle in front [58]. The last two variables also determine the thresholds between the four driving modes of a vehicle. The Wiedemann 74 model uses three parameters: the average standstill distance (AX), the additive part of the safety distance (BX$_{add}$), and the multiplicative part of the safety distance (BX$_{mult}$). The AX parameter is the average desired distance between stationary vehicles, and is used with the BX$_{add}$ and BX$_{mult}$ parameters to determine the desired following distance of a vehicle [58]. A vehicle can perform a lane change, either to turn left or right, or because it has a higher speed than the vehicle in front and there is more space in an adjacent lane. The lane change decision depends on the desired safety distance parameters (i.e., BX$_{add}$ and BX$_{mult}$), as well as on the speeds and decelerations of the vehicle making the lane change and the vehicle coming from behind in the destination lane. The VISSIM simulation parameters are summarized in Table 4.2.

As shown in Figs. 4.8a and 4.8b, for all the vehicle densities under consideration, the VeMAC protocol can successfully deliver almost all the periodic and event-driven safety messages to all the vehicles in the one-hop neighbourhoud. At the highest vehicle density, the VeMAC protocol achieves around 23% and 32% higher goodput respectively in the periodic and event-driven safety message goodputs, as compared to the IEEE 802.11p. Fig. 4.8c shows the significant difference in the probability of a transmission collision achieved by the two protocols. For instance, when the number of vehicles is 839, the probability of a collision of a periodic (event-driven) safety message for the IEEE 802.11p is around 2

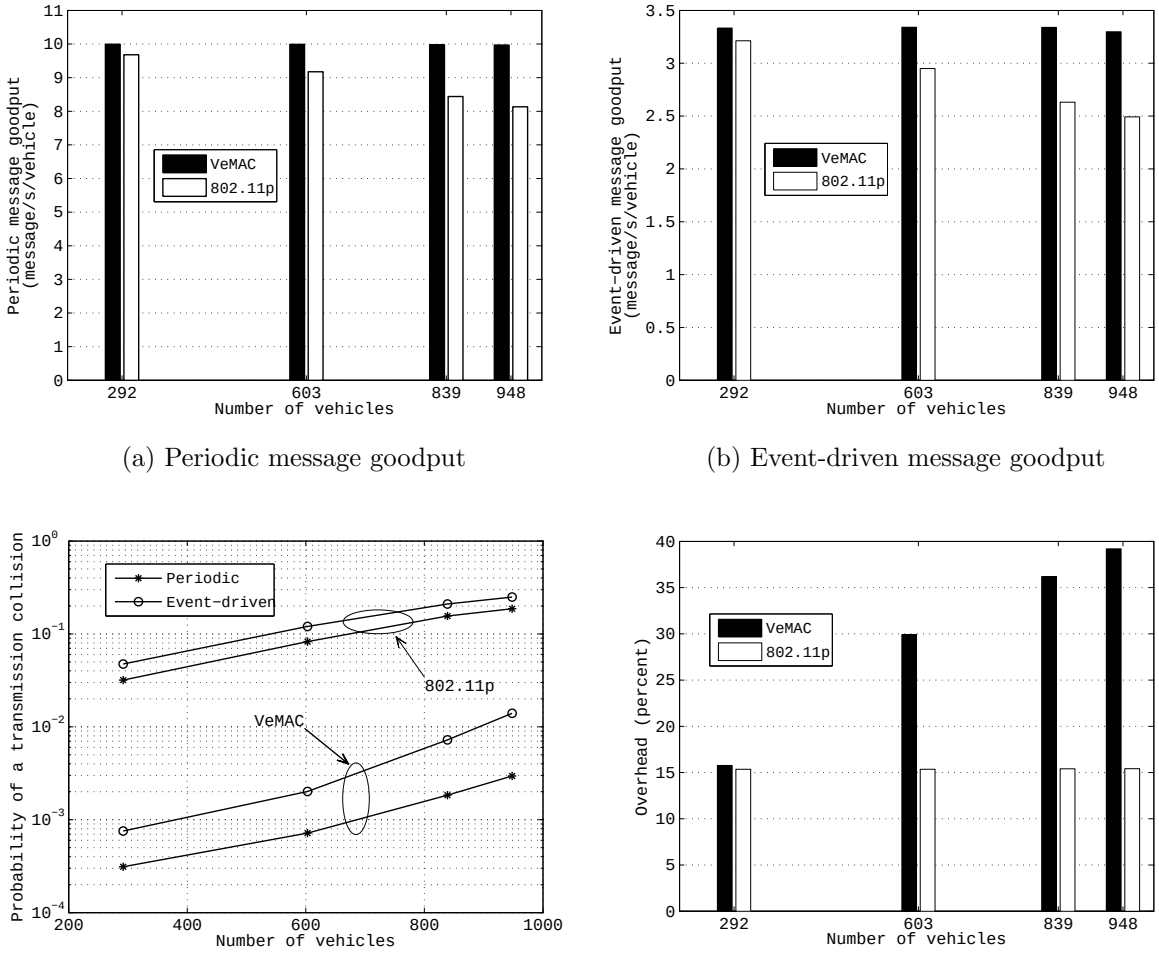

(a) Periodic message goodput

(b) Event-driven message goodput

(c) Probability of a transmission collision

(d) Overhead

Figure 4.8: Simulation results for the city scenario: goodput, probability of a transmission collision, and protocol overhead.

order of magnitude (1.5 order of magnitude) greater than for the VeMAC protocol. One main reason of the high probability of a transmission collision for the IEEE 802.11p is the hidden terminal problem, since for broadcast packets, no handshaking [request-to-send (RTS)/clear-to-send (CTS)] information exchange is used and no acknowledgement is transmitted from any recipient of the packet [22]. Another reason is that, although the small contention window (CW) size assigned to the AC_VO and AC_VI allows the safety packets to be transmitted with small delays, it increases the probability of a transmission collision when multiple vehicles within the same THS are simultaneously trying to broadcast their safety packets. Further, if a transmission collision of a broadcast packet happens, the CW size is not doubled (such as in the unicast case), as there is no collision detection without CTS and acknowledgment packets.

The reduction in the probability of a transmission collision by the VeMAC protocol, which results in the high periodic and event-driven message goodputs in Figs. 4.8a and 4.8b, is achieved at the expense of an increase in the protocol overhead as shown in Fig. 4.8d. The main source of the VeMAC overhead is that every Type1 packet transmitted by a certain vehicle x includes the set of VeMAC IDs (as indicated in Table 4.1), and the corresponding time slot indices, of each one-hop neighbour in $\mathcal{N}_x$. On the other hand, the overhead of the IEEE 802.11p protocol is due to control information such as the frame check sequence (FCS) and the physical layer convergence procedure (PLCP) header. At low vehicle density, the overheads of the VeMAC protocol and IEEE 802.11p are similar, as shown in Fig. 4.8d. However, when the vehicle density increases, the overhead of the IEEE 802.11p remains the same, while that of the VeMAC protocol increases due to a large number of one-hop neighbours of each vehicle, which results in a large amount of control information included in the header of transmitted Type1 packets. Note that, all the VeMAC control information is transmitted on the CCH, which is reserved only for the transmission of safety messages and control information. As well, the VeMAC control information provides each vehicle with knowledge about all the other vehicles in the two-hop neighbourhood. This knowledge can reduce the overhead of some layer 3 protocols, such as the elimination of the Hello messages of position based routing protocols. On the other hand, in a high vehicle density scenario, a large size of the VeMAC control information may increase the number of fragments of each periodic safety message broadcast by an RSU. This excess fragmentation can result in a higher delay of a periodic safety message, unless the RSU accesses more periodic time slots per frame, k_p, to serve the periodic safety message queue. The VeMAC overhead can be significantly reduced if each vehicle, x, broadcasts the VeMAC IDs and the corresponding time slot indices of the nodes in set $\mathcal{N}_x$ once every m frames, instead of once in every frame as described in Section 3.2. However, since the VeMAC IDs of set $\mathcal{N}_x$ and the corresponding time slot indices broadcast by a

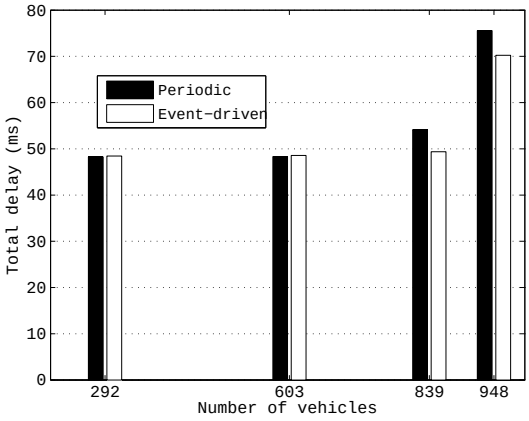

(a) Average total delay for VeMAC

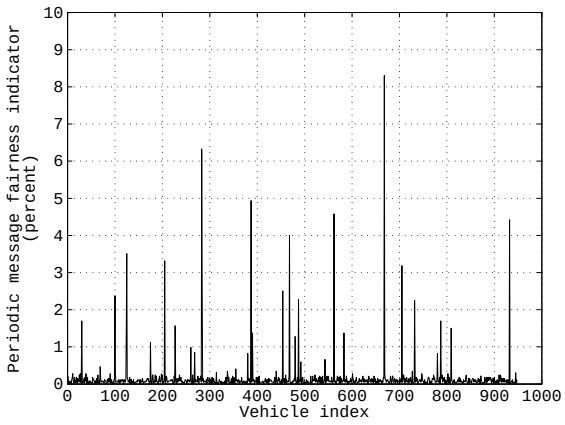

(b) Periodic fairness indicator for VeMAC

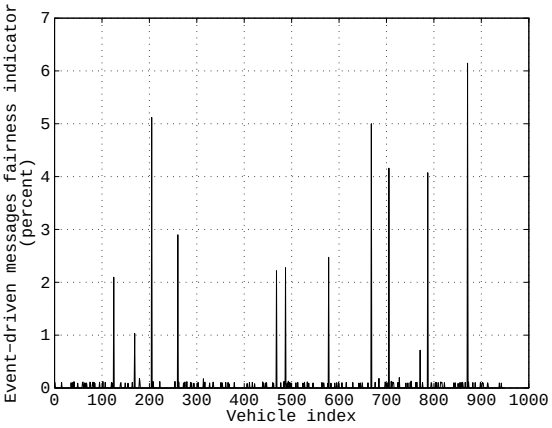

(c) Event-driven fairness indicator for VeMAC

Figure 4.9: Simulation results for the city scenario: total delay and fairness indicators of the VeMAC protocol.

certain node x are required for the one-hop neighbours to detect any transmission collision, as described in Subsection 3.2, the lack of broadcasting this control information in each frame (i.e., $m > 1$) may result in a longer time duration for a colliding node to detect a transmission collision, and consequently to resolve the collision by releasing its time slot and acquiring a new one, a behaviour which can increase the rates of access collisions and merging collisions. The effect of the reduction of the VeMAC overhead when $m > 1$ on the other performance metrics and on the multihop broadcast service (described in Subsection 5.2.2) needs further investigation.

The total delay of the VeMAC protocol for the periodic and event-driven safety messages is shown in Fig. 4.9a. For both types of safety messages, the VeMAC achieves a total delay that is well below 100 ms. One reason of the relative increase in the VeMAC delays at the highest vehicle density is the high contention on the time slots among different vehicles, which may force a vehicle to delay the transmission of a safety packet until a time slot is available. To study the fairness of the VeMAC protocol, Figs. 4.9b and 4.9c show the fairness indicators of the periodic and event-driven messages respectively at the highest vehicle density under consideration. The periodic (event-driven) message fairness indicator is below 0.3% (0.2%) for most of the vehicles, with a maximum value of 8.3% (6.2%). These results indicate that, even in a high vehicle density, the VeMAC protocol allows all the vehicles to transmit their safety messages in a fair way.

4.4 Summary

This chapter presents a detailed delivery delay analysis for VANET safety messages broadcast on the CCH, based on the VeMAC protocol described in Chapter 3. Both queueing and service delays of periodic and event-driven safety messages are analyzed, by taking into consideration the size and the arrival pattern of each type of safety messages. The delay analysis helps to determine the values of VeMAC parameters, such as $\tau, k_p, k_e,$ and L, to satisfy the delay requirement of periodic and event-driven safety applications. These protocol parameter values are used to compare the performance of VeMAC with that of the IEEE 802.11p standard via computer simulations in a square network and in a city scenario consisting of roads around the UW campus. Simulation results show that, the VeMAC protocol has a low probability of a transmission collision, which results in a higher safety message goodput and better channel utilization, as compared with the IEEE 802.11p standard. Also, for both types of safety messages, the VeMAC protocol achieves a total delivery delay that is well below 100 ms, which represents the maximum delay required for most of the safety applications. Additionally, by using suitable values of the VeMAC

parameters, the protocol allows all the vehicles to transmit their safety messages in a fair way, even in a high vehicle density scenario. Chapter 5 shows how some VeMAC features, such as the knowledge of all the nodes which exist in a two-hop neighbourhood, can be exploited for designing an efficient network layer protocol.

Chapter 5

Gateway Placement and Packet Routing For Multihop In-Vehicle Internet Access

As discussed in Section 1.2.2, In-vehicle Internet access is a VANET application which aims at providing the vehicle passengers with a low-cost access to the Internet via on-road gateways. This chapter first develops a new deployment technique to determine the locations of the Internet gateways on the roads and define the maximum number of hops that a gateway can use to communicate with a certain vehicle [43]. The proposed technique minimizes the total cost of gateway deployment, and guarantees that a vehicle can connect to an Internet gateway with a probability greater than a specified threshold. The probability that a vehicle can connect to a certain gateway is the probability of the existence of a network path between them, where the network path consists of a maximum number of hops that is determined by the proposed technique for each deployed gateway. To the best of our knowledge, no previous strategy for gateway placement has considered the existence of network paths among the vehicles and the deployed gateways. Since the existence of a network path mainly depends on the vehicle traffic conditions in the region where the gateways are deployed, the VISSIM vehicle traffic simulator [49] is employed to simulate the vehicle movement in the deployment region. The proposed strategy is evaluated by considering the gateway placement on the roads around the UW campus.

In addition to the deployment strategy of Internet gateways, this chapter introduces a novel packet routing scheme which allows a vehicle to discover the existence of an Internet gateway and to send/receive packets to/from the gateway via multihop communications

[42, 43]. The proposed routing scheme is designed over the VeMAC protocol to exploit some useful VeMAC features, such as the knowledge of all the nodes which exist in a two-hop neighbourhood. This VANET architecture aims at achieving multihop in-vehicle Internet access by using the routing scheme, while satisfying the QoS requirements of the safety applications via the VeMAC protocol. The proposed cross-layer design between the MAC and network layers is evaluated in a highway scenario by studying the end-to-end delay required to deliver a packet from a vehicle to a gateway through multiple relay vehicles. The packet queueing at each relay vehicle is considered in the end-to-end packet delay analysis. Another performance metric under consideration is the percentage of time slots per frame occupied by all the vehicles members of the same THS, required to limit the average packet delay to below a certain threshold at each vehicle. Numerical results are presented to study the effect of different parameters, including the vehicle density and the packet arrival rate, on the performance metrics.

5.1 Gateway Placement

In order to deploy Internet gateways in a certain geographical region, the map of the region is partitioned into equal-size square areas, called cells, by overlaying a uniform square grid over the map. Each cell which cannot be traversed by a vehicle (e.g., a cell with no overlap with any part of the roads) is removed from the set of cells, and the rest of the cells are indexed from 1 to N_{cells}, where N_{cells} denotes the total number of remaining cells. Potential locations for deploying an Internet gateway are defined on the map (e.g., equally spaced along each road) and the total number of potential gateway locations is denoted by N_{gate}. The potential locations are indexed from 1 to N_{gate}, and the cost of deploying a gateway at the j^{th} location is denoted by γ_j. If a gateway is deployed at the j^{th} location, $j = 1, ..., N_{gate}$, let ρ_j denote the maximum number of hops that the gateway can use to connect to a certain vehicle, and ρ_{max} the maximum allowed value of ρ_j for any j. Given the potential gateway locations, it is required to find an optimal set $\mathcal{J}$ of location indices, and determine the values of ρ_j $\forall j \in \mathcal{J}$. Set $\mathcal{J}$ and the corresponding ρ_j values should minimize the total cost of gateway deployment, while ensuring that the number of gateways, which a vehicle located at the i^{th} cell can connect to, is not less than a specified value denoted by ν_i, each with a probability not less than a specified threshold, denoted by $\alpha_i \in (0, 1]$, $i = 1, ..., N_{cells}$. Based on the vehicle traffic conditions in the region where the gateways are deployed, let σ_{ijk} denote the probability that a vehicle at the i^{th} cell can reach a gateway at the j^{th} position within k hops, where $i = 1, ..., N_{cells}$, $j = 1, ..., N_{gate}$, and $k = 1, ..., \rho_{max}$. The values of σ_{ijk} $\forall i, j, k$ can be calculated by using a simulation

model of the vehicle traffic in the region where the gateways are deployed, as described in Subsection 5.4.1. For each cell i, define set β_i as the index set of all gateways which can be reached by a vehicle located in cell i within ρ_{max} hops, i.e., $\beta_i = \{j : \sigma_{ij\rho_{max}} \neq 0\}$.

The gateway deployment is formulated by binary integer programming problem (5.1), which has three sets of decision variables: x_j, y_{jk}, and z_{im}, where $i = 1, ..., N_{cells}$, $j = 1, ..., N_{gate}$, $k = 1, ..., \rho_{max}$, and $m \in \beta_i$ for each i. Let $x_j = 1$ iff a gateway is deployed at the j^{th} potential gateway location, and $y_{jk} = 1$ iff a gateway is deployed at the j^{th} location and has $\rho_j = k$. Therefore, objective function (5.1a) represents the total cost of gateway deployment. For the third set of decision variables, constraints (5.1b)-(5.1d) ensure that, a variable $z_{ij} = 1$ if [only if] a gateway is deployed at the j^{th} location and can reach a vehicle at the i^{th} cell within ρ_j hops with a probability greater than [greater than or equal to] α_i. Given this proposition, constraint (5.1e) guarantees that a vehicle at any cell i can communicate with at least ν_i gateways, each with a probability not less than α_i. To show the validity of the proposition, first suppose that $x_{j'} = 1$ for a certain $j' \in \{1, ..., N_{gate}\}$. Hence, constraint (5.1b) ensures that there exists exactly one value $k' \in \{1, .., \rho_{max}\}$ such that $y_{j'k'} = 1$, which means $\rho_{j'} = k'$. Consequently, for each cell i such that $j' \in \beta_i$, due to constraints (5.1c) and (5.1d), $z_{ij'} = 1$ if $\sigma_{ij'k'} > \alpha_i$, and $z_{ij'} = 0$ if $\sigma_{ij'k'} < \alpha_i$ (note that $\sum_{k=1}^{\rho_{max}} \sigma_{ij'k} y_{j'k} = \sigma_{ij'k'}$). If it happens that $\sigma_{ij'k'} = \alpha_i$, the value of $z_{ij'}$ can be 0 or 1 (more likely the solver let $z_{ij'} = 1$ to satisfy constraint (5.1e)). On the other hand, if $x_{j'} = 0$, then constraint (5.1b) sets $y_{j'k} = 0$ $\forall k$, while constraints (5.1c) and (5.1d) set $z_{ij'} = 0$ $\forall i$ such that $j' \in \beta_i$.

$$\underset{\substack{x_j, y_{jk}, z_{im} \in \{0,1\} \\ \forall i,j,k,m}}{\text{minimize}} \sum_{j=1}^{N_{gate}} \gamma_j x_j \tag{5.1a}$$

$$\text{subject to } \sum_{k=1}^{\rho_{max}} y_{jk} = x_j, \quad j = 1, ..., N_{gate}, \tag{5.1b}$$

$$z_{im} \geq \Big(\sum_{k=1}^{\rho_{max}} \sigma_{imk} y_{mk} \Big) - \alpha_i, \quad i = 1, ..., N_{cells}, m \in \beta_i, \tag{5.1c}$$

$$z_{im} \leq 1 + \Big(\sum_{k=1}^{\rho_{max}} \sigma_{imk} y_{mk} \Big) - \alpha_i, \quad i = 1, ..., N_{cells}, m \in \beta_i, \tag{5.1d}$$

$$\sum_{m \in \beta_i} z_{im} \geq \nu_i, \quad i = 1, ..., N_{cells}. \tag{5.1e}$$

Note that, the solution of problem (5.1) depends on the values of σ_{imk} in constraints (5.1c) and (5.1d), which mainly depend on the vehicle traffic conditions in the region where the gateways are deployed, as will be shown in Subsection 5.4.1. The traffic conditions in different situations (e.g., weekday, weekend, morning, rush hour, etc.) can be simulated by the traffic simulator which generates the σ_{imk} values, by adjusting suitable parameters such as the rate of vehicle arrivals to the road network, the probabilities of a left or right turn at intersections, the schedule of public transit buses, etc. Additionally, special incidences can be introduced in the simulation, such as an accident or a road closure, to simulate the vehicle traffic during such events. Hence, problem (5.1) can be solved by using the σ_{imk} values obtained from the simulator based on target vehicle traffic.

5.2 Packet Routing Scheme

The proposed packet routing scheme consists of two main components: 1. *gateway discovery*, which determines how the vehicles discover the existence of a gateway and how they obtain the information necessary to connect to that gateway; and 2. *packet forwarding*, which defines how a packet is delivered via multihop communications from a vehicle to a gateway and vice versa.

5.2.1 SCH Packet Queueing and Serving

For a certain node, x, let $\mathcal{Q}_x$ denote the set of time slots acquired by node x on the CCH. At each node, the packets which require transmission over the SCHs are queued and served on a first-come-first-served basis as follows. Suppose that node x needs to transmit a packet to its one-hop neighbour y on a SCH. At its first opportunity to access the CCH, node x uses the corresponding time slot in set $\mathcal{Q}_x$ to announce for node y the index of the SCH over which the packet will be transmitted. Following this announcement, both of nodes x and y turn Transceiver2 to the correct SCH and exchange packets (this SCH access scheme is different from the one described in Section 3.3 based on TDMA). In each time slot in $\mathcal{Q}_x$, node x can announce on the CCH for a maximum of b packets to be transmitted on the same SCH (not necessarily to the same one-hop neighbour). At the start of a time slot in $\mathcal{Q}_x$, if the number of queued packets is less than the constant b, referred to as the batch-size, node x does NOT wait until the number of queued packets reaches b, but announces on the CCH to transmit the existing packets on the chosen SCH. Only one SCH index can be announced by node x in a time slot on the CCH, and the batch-size b represents the

maximum number of packets which can be transmitted by node x on the SCH after each announcement.

5.2.2 Gateway Discovery

In order to announce for its service, a gateway, g, periodically broadcasts a gateway discovery packet (GDP) containing the necessary information that a vehicle needs to access the gateway's service, such as the network layer address of gateway g and the maximum number of hops, ρ_g, that it can use to communicate with a certain vehicle, where ρ_g is determined as described in Section 5.1. Before broadcasting a GDP, as mentioned in Section 5.2.1, gateway g first announces on the CCH the index of the SCH over which the GDP will be broadcasted. Accordingly, each one-hop neighbour which receives the announcement turns its Transceiver2 to the correct SCH in order to receive the GDP. Among these one-hop neighbours, a subset is chosen to re-broadcast the GDP, and so on, until the GDP initiated by gateway g propagates ρ_g hops away from the gateway. The propagation of the GDP in the network is controlled via a time-to-live (TTL) field in the GDP header, which is originally set to $\rho_g - 1$ by gateway g and decremented by each vehicle which relays the GDP. Every GDP is identified by a broadcast ID, together with the network layer address of the gateway which initiated the GDP. These two fields are used by a vehicle to discard any duplicate of a previously received GDP. At each hop, the subset of the vehicles which relay the GDP is determined as follows. Suppose that a node, x, announces for a GDP on one of its time slots, t_x, on the CCH. For each node y which receives the announcement, let $\mathcal{D}_y$ denote the set of one-hop neighbours of node y which did not receive the announcement for the GDP sent by node x. Node y does NOT relay the GDP if any of the following conditions holds:

- TTL $= 0$;
- $\mathcal{D}_y = \phi$;
- $\exists\, z \in \mathcal{N}_y \backslash \mathcal{D}_y$ such that $\mathcal{D}_y \subseteq \mathcal{N}_z$ and $|\mathcal{N}_y| < |\mathcal{N}_z|$, where $|\cdot|$ denotes the cardinality of a set;
- $\exists\, z \in \mathcal{N}_y \backslash \mathcal{D}_y$ such that $\mathcal{D}_y \subseteq \mathcal{N}_z$, $|\mathcal{N}_y| = |\mathcal{N}_z|$, and $\min\limits_{t_z \in \mathcal{Q}_z} t_z - t_x + L \times I_{(t_z < t_x)} < \min\limits_{t_y \in \mathcal{Q}_y} t_y - t_x + L \times I_{(t_y < t_x)}$, where the notation $I_{(a<b)}$ equals 1 if $a < b$ and equals 0 otherwise.

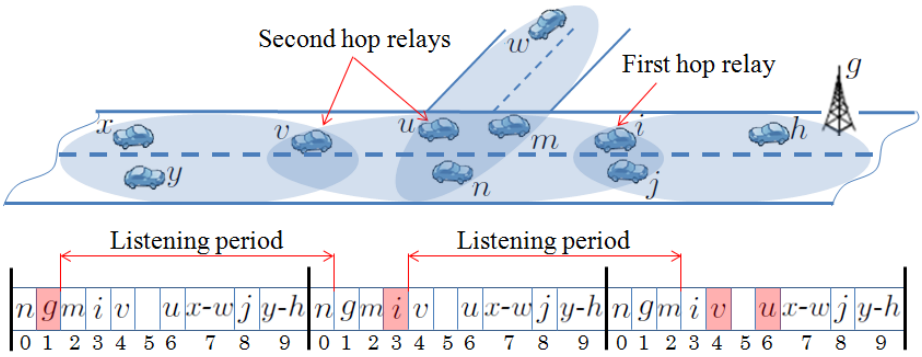

Figure 5.1: The GDP relaying process based on a time slot assignment on the CCH.

When node y receives an announcement for the GDP from node x on time slot t_x, it listens to the CCH for the $L-1$ time slots following t_x. At the end of this listening period, node y can determine sets $\mathcal{Q}_z$ and $\mathcal{N}_z$ for each one-hop neighbour z (recall that, each one-hop neighbour z broadcasts the VeMAC IDs of the nodes in its $\mathcal{N}_z$ set at least once in each frame). Consequently, node y sets $\mathcal{D}_y = \{z \in \mathcal{N}_y : \mathrm{ID}^x_{t_x}$ is not broadcasted by node $z\}$, where ID_{t_x} is the VeMAC ID of node x corresponding to time slot t_x. Consequently, node y relays the GDP if none of the mentioned conditions is true. The last condition means that, node y does not relay the GDP if it has a one-hop neighbour z which satisfies that $\mathcal{D}_y \subseteq \mathcal{N}_z$ and $|\mathcal{N}_y| = |\mathcal{N}_z|$, and which can access the CCH before node y at the end of the listening period following time slot t_x. This condition allows for a faster propagation of the GDP in the network by choosing the relay which can announce for the GDP on the CCH first.

Fig. 5.1 explains how a GDP broadcasted by gateway g is delivered to all the vehicles located within $\rho_g = 3$ hops from the gateway by using a few number of transmissions. In Fig. 5.1, a group of nodes is surrounded by an ellipse iff any two nodes in the group can reach each other in one hop (the same applies to Fig. 5.2). That is, the set of one-hop neighbours of a node, x, consists of all the nodes that are surrounded with node x by a certain ellipse. Fig. 5.1 also shows the time slot assignment on the CCH for all the nodes. Note that, different nodes may access the same time slot if they do not belong to the same THS, e.g., nodes x and w accessing time slot number 7. Each time slot that is highlighted in Fig. 5.1 is a time slot over which an announcement for the GDP is broadcasted. When gateway g announces for the GDP in the first frame, vehicles h, i, and j receive the announcement and listen to the CCH for a duration of 9 time slots ($L = 10$) in order to decide whether or not to relay the GDP. Vehicle h does not relay the GDP because $\mathcal{D}_h = \phi$. Similarly, vehicle j does not relay the GDP since $\mathcal{D}_j = \{m, n, u, v\} \subseteq \mathcal{N}_i$,

$|\mathcal{N}_j| = |\mathcal{N}_i|$, and vehicle i can access the CCH before vehicle j at the end of the listening period. Consequently, vehicle i is the only vehicle which relays the GDP at the first hop. At the second hop, vehicles u, v, m, and n receive the GDP relayed by vehicle i. Vehicle v relays the GDP since none of its one-hop neighbours, u, m, and n (which received the GDP from vehicle i) can reach vehicles x and y in the third hop, i.e., $\nexists\, z \in \mathcal{N}_v \backslash \mathcal{D}_v$ such that $\mathcal{D}_v \subseteq \mathcal{N}_z$. On the other hand, among the three vehicles u, m, and n, only vehicle u relays the GDP, while vehicles m and n do not, for the same reason explained before for vehicle j. At this point, TTL = 0 as it has been decremented by the first and second hop relays. Hence, at the third hop, when vehicles, x, y, and w receive the GDP, none of these vehicles will relay it further. Note that, when a certain relay broadcasts the GDP, every vehicle which has previously received the same GDP can discard the relayed copy by checking the broadcast ID and the address of the initiating gateway, e.g., nodes j and h discard the GDP relayed by node i.

5.2.3 Packet Forwarding

The packet routing from a vehicle to a gateway is done in a proactive way. That is, each vehicle, v, stores a routing table which has an entry corresponding to each gateway g located within ρ_g hops from vehicle v. Each routing table entry at vehicle v consists of the network address of a certain gateway, the number of hops that the gateway can be reached in, and the MAC addresses of the one-hop neighbours of vehicle v which can relay a packet to the gateway. The routing table entry corresponding to a gateway, g, is created/updated during the propagation of each GDP broadcasted by gateway g, as explained in the following. Each vehicle, v, which relays a GDP initiated by gateway g includes in the relayed GDP the VeMAC IDs of a subset of its one-hop neighbours as potential vehicles which can relay a packet to gateway g. This set of potential relays included by vehicle v is denoted by $\mathcal{R}_v$, and the cardinality $|\mathcal{R}_v|$ should be limited to a certain number, denoted by $n_{\mathcal{R}}$. The set $\mathcal{R}_v$ consists of the one-hop neighbours of vehicle v which received the GDP and which can reach (in one hop) the highest number of one-hop neighbours of vehicle v which have not yet received the GDP, i.e., $\mathcal{R}_v = \{z \in \mathcal{N}_v \backslash \mathcal{D}_v : |\mathcal{R}_v| \leq n_{\mathcal{R}}, \mathcal{D}_v \cap \mathcal{N}_z \neq \phi, |\mathcal{D}_v \cap \mathcal{N}_z| \geq |\mathcal{D}_v \cap \mathcal{N}_{z'}| \,\forall\, z' \notin \mathcal{R}_v\}$. If vehicle v has more than one one-hop neighbour $z \in \mathcal{N}_v \backslash \mathcal{D}_v$ that have the same $|\mathcal{D}_v \cap \mathcal{N}_z| > 0$, vehicle v gives priority of inclusion in set $\mathcal{R}_v$ to the one-hop neighbours that are farther from the node from which vehicle v has received the GDP (each vehicle is aware of the positions of all its one-hop neighbours, which are included in the headers of their transmitted Type1 packets). The reason is that, those one-hop neighbours are likely to be closer to the vehicles to which vehicle v is going to relay the GDP. When a vehicle, w, receives the GDP relayed by vehicle v, by calculating $\mathcal{R}_v \cap \mathcal{N}_w$,

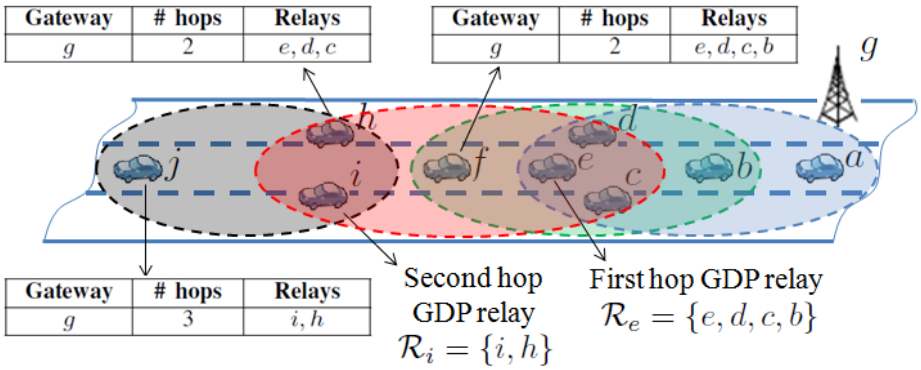

Figure 5.2: Routing tables update during a GDP propagation.

vehicle w determines the set of its one-hop neighbours which can relay a packet to gateway g. Also, by subtracting the TTL field from ρ_g, vehicle w determines the number of hops currently separating it from gateway g. Consequently, vehicle w creates/updates the entry in its routing table corresponding to gateway g. If vehicle w does not receive a GDP from gateway g for a time duration larger than a specified threshold, the entry corresponding to gateway g is removed from the routing table. The GDPs should be broadcasted by each gateway at a broadcast rate which ensures that the routing table at each vehicle is always up-to-date based on the current network topology.

Fig. 5.2 explains how different vehicles update their routing table entries corresponding to gateway g. When the gateway broadcasts a GDP, among all the vehicles which receive the GDP at the first hop (in the blue ellipse), only one vehicle will relay the GDP based on the relaying scheme described in Subsection 5.2.2. If the time slot assignment on the CCH requires that vehicle e is the one to relay the GDP, and if we assume that $n_{\mathcal{R}} = 4$, then vehicle e includes in the relayed GDP set $\mathcal{R}_e = \{e, d, c, b\}$. We have $\mathcal{R}_e = \{e, d, c, b\}$, because $\mathcal{D}_e = \{h, i, f\}$, $\mathcal{N}_e \backslash \mathcal{D}_e = \{e, d, c, b, a\}$, and $\mathcal{D}_e \cap \mathcal{N}_a = \phi$. When the GDP relayed by vehicle e is received by vehicles f, h, and i at the second hop (in the red ellipse), each of these vehicles finds the intersection of its $\mathcal{N}$ set with the $\mathcal{R}_e$ set, and updates the routing table entry corresponding to gateway g accordingly. Vehicle f indicates in its routing table that vehicles e, d, c, and b can relay a packet to gateway g, while each of vehicles i and h only indicates vehicles e, d, and c as potential relays (since vehicle b is not a one-hop neighbour of either vehicle i or h). Similarly, at the second hop, assuming that vehicle i decides to relay the GDP, it includes set $\mathcal{R}_i = \{i, h\}$ in the relayed GDP, which is used by vehicle j at the third hop to determine the set of possible relays to gateway g by calculating $\mathcal{R}_i \cap \mathcal{N}_j = \{i, h\}$.

To deliver a packet from a vehicle to a gateway, the vehicle forwards the packet to a randomly chosen relay among the ones listed in the routing table entry corresponding to the intended gateway. This process is repeated by each relay vehicle until the packet is finally delivered to the destination gateway. For instance, in Fig. 5.2, if vehicle j wants to send a packet to gateway g, by consulting its routing table, vehicle j will forward the packet to either vehicle i or vehicle h equally likely. Then, assuming that vehicle j chooses vehicle h to relay the packet, vehicle h in turn forwards the packet to a randomly chosen relay among vehicles e, d, and c, which delivers the packet directly to gateway g.

Unlike the packet routing from a vehicle to a gateway, which is done on a proactive hop-by-hop basis, packets are routed from a gateway to a vehicle on a reactive source-routing basis. That is, a source gateway includes in the header of each transmitted packet the MAC address of each vehicle which should relay the packet until it reaches the destination vehicle. This information about the whole network path to a certain vehicle, v, is provided to a gateway, g, through the packets that it receives from vehicle v. That is, each relay which forwards a packet from vehicle v to gateway g includes its MAC address in the header of the relayed packet. In this way, gateway g can find a network path to vehicle v by reversing the order of the relays in the header of the most recent packet received from vehicle v. Note that, the way that the routing table at each vehicle is built ensures that all the links on a network path from a vehicle to a gateway are bidirectional. If gateway g does not have information about the network path to a certain vehicle, or if the available network path has not been updated for a time duration larger than a specified threshold, the gateway broadcasts a route-request packet, which propagates in the network as the GDP does, until it reaches the destination vehicle. The vehicle then replies by a route-reply packet which accumulates a network path in its header while propagating back to the gateway.

5.3 Performance Analysis

This section investigates the end-to-end delay required to deliver a packet from a vehicle to a gateway through multiple relay vehicles on a SCH. Another performance metric under consideration is the percentage of time slots per frame occupied by all the vehicles members of the THS, required to limit the average packet delay to below a certain threshold at each vehicle. The total delay that a packet encounters at each vehicle consists of two main components: queueing delay and service delay[1]. The queueing delay is the time duration

[1]The definitions of the queueing and service delays of a packet transmitted over a SCH are different from those mentioned in Section 4.1 for a safety message transmitted over the CCH.

from the instant that a packet arrives to the queue of a certain vehicle to the instant that the vehicle starts to announce for the transmission of the packet on the CCH. This delay includes the time duration that the packet spends in the queue until it becomes in the HOL batch, i.e., among the first b packets, and the duration that the transmitting vehicle spends on waiting for one of its acquired time slots on the CCH (to announce the index of the SCH over which the HOL batch will be transmitted). On the other hand, the service delay of a tagged packet in the HOL batch consists of the duration of one time slot, which is used to transmit the announcement for the HOL batch on the CCH, and the time duration required to deliver the tagged packet in the HOL batch to its destination one-hop neighbour on the announced SCH. The analysis in this section neglects the second component of the packet service delay, which in general is relatively short compared to the packet queueing delay. When "delay" is mentioned solely, it refers to the total delay, which is the sum of the queueing delay and the duration of one time slot. To simplify the delay analysis, we assume that each vehicle, x, releases its time slot(s) in set $\mathcal{Q}_x$ and acquires a new one(s) after each time it accesses the CCH. This assumption guarantees that, at each vehicle, the intervals of time between successive occasions of announcement for an HOL batch on the CCH are i.i.d. random variables. The assumption is appropriate in scenarios with high rates of transmission collisions, where the vehicles repeatedly release their time slots and acquire new ones. Consequently, each vehicle can be modeled as a queueing system with independent time intervals between successive occasions of service, where the packets are served in batches of a maximum batch-size b. In such a queuing system, when the packets arrive according to a Poisson process, we denote the system by $\mathrm{M/G^{(}}b\mathrm{)/1}$. Hence, by considering only the arrival of packets generated at the application layer of a certain vehicle (assuming Poisson arrivals), the vehicle can be modeled as an $\mathrm{M/G^{(}}b\mathrm{)/1}$ queueing system. However, each vehicle not only transmits the packets generated at its own application layer, but also relays the packets arriving from its one-hop neighbours. Therefore, in order to analyze the end-to-end packet delay, a network of $\mathrm{M/G^{(}}b\mathrm{)/1}$ queues should be considered. The exact analysis of such a network of queues is extremely difficult, even when $b = 1$ [51]. Hence, to make the analysis tractable, we approximate the arrival of packets which should be relayed by a vehicle as a single Poisson process with rate parameter equal to the sum of the packet arrival rates coming to the relay vehicle from all its one-hop neighbours. That is, the superposition of the departure processes of a number, N_{input}, of $\mathrm{M/G^{(}}b\mathrm{)/1}$ queues (representing N_{input} one-hop neighbours of a relay vehicle) is approximated by a Poisson process with rate parameter $\Sigma_{i=1}^{N_{\text{input}}}\xi_i$, where ξ_i is the packet arrival rate coming from the i^{th} $\mathrm{M/G^{(}}b\mathrm{)/1}$ queue to the relay vehicle.

To study the accuracy of this approximation, Fig. 5.3 compares the average packet delay at a relay vehicle when the packets arrive to the relay according to a Poisson process

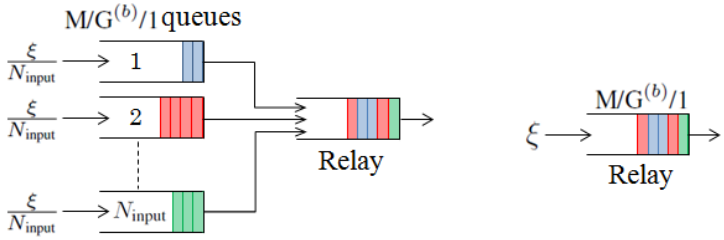

(a) Actual scenario (b) Poisson process approximation

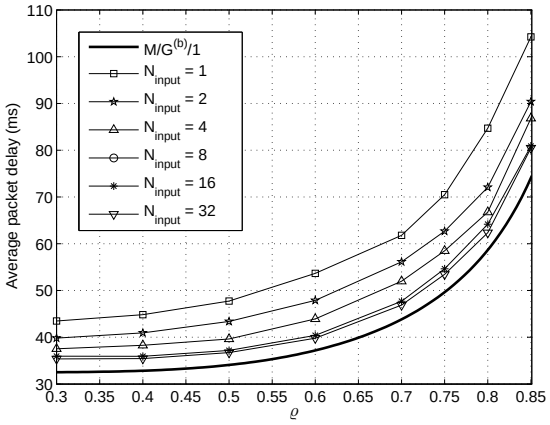

(c) Average packet delay at the relay vehicle vs. the ratio ϱ

Figure 5.3: A relay vehicle with N_{input} one-hop neighbours in comparison with an M/G$^{(b)}$/1 queueing system with $b = 16$.

with rate parameter ξ, as shown in Fig. 5.3b, with that in an actual case when the relay receives packets from the output of N_{input} M/G$^{(b)}$/1 queues, each with a packet arrival rate of $\frac{\xi}{N_{\text{input}}}$, as shown in Fig. 5.3a. For the case in Fig. 5.3b, the average packet delay at the relay vehicle is calculated based on the analysis of the M/G$^{(b)}$/1 queuing system (Subsection 5.3.3), while for that in Fig. 5.3a, the average delay is obtained by using MATLAB simulations, where the packets are served at the relay vehicle and at each of the N_{input} vehicles according to the VeMAC protocol. Fig. 5.3c shows the average packet delay at the relay vehicle versus a ratio, ϱ, which denotes the average number of packet arrivals between two successive occasions of service divided by b. As shown in Fig. 5.3c, for different ϱ values, the average packet delay of the M/G$^{(b)}$/1 queue represents a lower bound on the average delay when the packets arrive to the relay from N_{input} different vehicles.

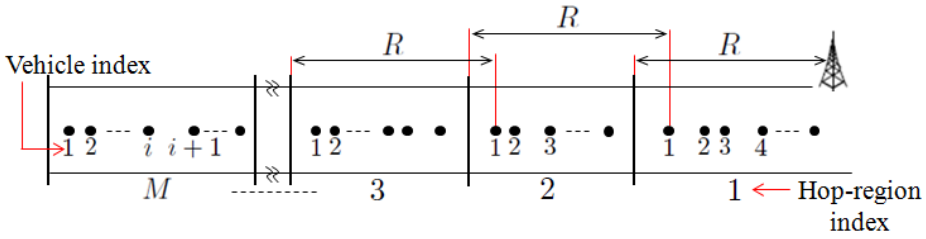

(a) Vehicle and hop-region indexing

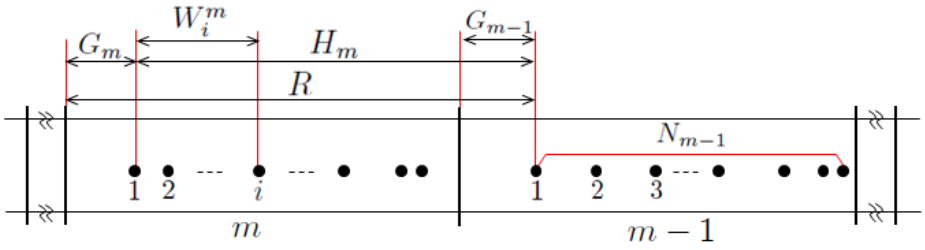

(b) Focus on the m^{th} and $(m-1)^{\text{st}}$ hop-regions

Figure 5.4: Highway segment consisted of M hop-regions.

The lower bound becomes tighter for a large N_{input}, which indicates that the suggested Poisson process approximation is more accurate in a higher vehicle density scenario, when the packets arrive to a relay vehicle from a larger number of one-hop neighbours. Similar results are found for different values of the batch-size b. Based on the Poisson process approximation, the average packet delay at each vehicle is found by using the analysis of the $\text{M/G}^{(b)}/1$ queuing system. However, the main challenge remains in the calculation of the total packet arrival rate at a relay vehicle based on the routing scheme in Section 5.2, which depends mainly on the network topology. In the following, a highway model is first described, then the total packet arrival rate, end-to-end-packet delay, and percentage of occupied time slots per frame are evaluated.

5.3.1 Highway Model

Consider a highway segment consisted of N_{lanes} lanes, where at any time instant the vehicles are distributed in each lane according to a Poisson process with rate parameter η_{lane} (vehicles/mile). By neglecting the width of the highway and the dimensions of a vehicle relative to the communication range, R, the vehicles are distributed along the highway according to a single Poisson process with rate parameter $\eta = N_{\text{lanes}}\,\eta_{\text{lane}}$, as shown in Fig. 5.4a (where the black dots represent vehicles). A gateway is placed at the right end of

the highway segment and serves all the vehicles located within M hops of the gateway. We define M hop-regions, as shown in Fig. 5.4a, and assume that at any time instant there is at least one vehicle in each hop-region, i.e., there exists a network path between the gateway and each vehicle located within M hops of the gateway. The network path from any vehicle to the gateway is always up-to-date, thanks to the periodically broadcasted GDPs (Section 5.2.2). In each of the M hop-regions, the vehicles are indexed in an increasing order starting from the vehicle that is farthest from the gateway, as shown in Fig 5.4a. Based on the routing scheme in Section 5.2, only the first $n_{\mathcal{R}}$ vehicles in each hop-region can relay packets to/from the gateway. As illustrated in Fig. 5.4b, at a certain time instant, N_m denotes the number of vehicles located in the m^{th} hop-region, G_m the gap between the first vehicle in the m^{th} hop-region and the farthest edge of the region with respect to the gateway, H_m the distance separating the first vehicle in the m^{th} hop-region and that in the $(m-1)^{\text{st}}$ hop-region, and W_i^m the distance between the first vehicle in the m^{th} hop-region and the i^{th} vehicle (if exists) in the same region, where all these random variables are defined for $m = 1, ..., M$ and $i = 1, ..., \infty$ (except H_1, which is not defined). The event that N_m takes a value n_m is denoted by $\mathcal{N}_m$, and the same notation applies to all other random variables, i.e., $\mathcal{G}_m$, $\mathcal{H}_m$, and $\mathcal{W}_i^m$. Conditional on the occurrence of an event $\mathcal{E}$, the probability density function (PDF) of a continuous random variable X is denoted by $f_{X|\mathcal{E}}(x)$, the PMF of a discrete random variable Y is denoted by $p(Y = y|\mathcal{E})$, and the probability of the occurrence of another event $\mathcal{E}'$ is denoted by $p(\mathcal{E}'|\mathcal{E})$. The expected value of a random variable Z (discrete or continuous) is denoted by $\mathbb{E}(Z)$. The set of events $\mathcal{U}_{i,r}^m$, $m = 2, ..., M$, $i = 1, ..., \infty$, and $r = 1, ..., \infty$, denotes that the i^{th} vehicle in the m^{th} hop-region exists and its communication range can reach the r^{th} vehicle in the $(m-1)^{\text{st}}$ hop-region. Similarly, the set of events $\mathcal{V}_{i,r}^m$ denotes that the i^{th} vehicle in the m^{th} hop-region exists and uses the r^{th} vehicle in the $(m-1)^{\text{st}}$ hop-region as a relay to the gateway. Indicator random variable $I_{i,r}^m$ is equal to 1 whenever event $\mathcal{V}_{i,r}^m$ occurs, and is equal to 0 otherwise. Packets are generated at the application layer of each vehicle according to a Poisson process with rate parameter λ. At the r^{th} vehicle (if exists) in the m^{th} hop-region, let λ_r^m, Q_r^m, and S_r^m, $m = 1, ..., M$ and $r = 1, ..., \infty$, respectively denote the total packet arrival rate, the packet queueing delay, and the time duration (in the unit of a time slot) between successive occasions of announcement for an HOL batch on the CCH. Let D_{v}^m (D_{r}^m), $m = 1, ..., M$ ($m = 1, ..., M-1$) denote the average packet delay at a randomly chosen vehicle (relay) in the m^{th} hop-region. Also, let E^m, $m = 1, .., M$, denote the average end-to-end delay from a randomly chosen vehicle in the m^{th} hop-region to the gateway.

5.3.2 Total Packet Arrival Rate

The total packet arrival rate, λ_r^m, for the relay and non-relay vehicles is represented respectively by

$$\lambda_r^m = \begin{cases} \lambda + \mathbb{E}(\sum_{i=1}^{\infty} \lambda_i^{m+1} I_{i,r}^{m+1}), & 1 \leq r \leq n_{\mathcal{R}}, \\ & 1 \leq m < M; \\ \lambda, & r > n_{\mathcal{R}} \text{ or } m = M. \end{cases} \tag{5.2}$$

For a relay vehicle ($1 \leq r \leq n_{\mathcal{R}}, 1 \leq m < M$),

$$\begin{aligned} \lambda_r^m &= \lambda + \sum_{i=1}^{\infty} \lambda_i^{m+1} p(I_{i,r}^{m+1} = 1) \\ &= \lambda + \sum_{i=1}^{\infty} \lambda_i^{m+1} p(\mathcal{V}_{i,r}^{m+1}). \end{aligned} \tag{5.3}$$

The probability $p(\mathcal{V}_{i,r}^{m+1})$ can be found by summing the probabilities of the intersection of the event $\mathcal{V}_{i,r}^{m+1}$ with the disjoint events $\mathcal{U}_{i,k}^{m+1}$, $k = r, ..., \infty$, i.e.,

$$\begin{aligned} p(\mathcal{V}_{i,r}^{m+1}) &= p(\bigcup_{k=r}^{\infty} \mathcal{V}_{i,r}^{m+1} \cap \mathcal{U}_{i,k}^{m+1}) \\ &= \sum_{k=r}^{\infty} p(\mathcal{V}_{i,r}^{m+1} \cap \mathcal{U}_{i,k}^{m+1}) \\ &= \sum_{k=r}^{\infty} \frac{1}{\min(k, n_{\mathcal{R}})} p(\mathcal{U}_{i,k}^{m+1}), \end{aligned} \tag{5.4}$$

where $\min(k, n_{\mathcal{R}})$ denotes the minimum of k and $n_{\mathcal{R}}$, and $\frac{1}{\min(k,n_{\mathcal{R}})}$ represents the probability $p(\mathcal{V}_{i,r}^{m+1}|\mathcal{U}_{i,k}^{m+1})$ according to the routing scheme in Section 5.2, since a vehicle in the $(m+1)^{\text{st}}$ hop region is aware of a maximum of $n_{\mathcal{R}}$ relay vehicles in the m^{th} hop region and randomly chooses one among all the relay vehicles that it can reach. The probability $p(\mathcal{U}_{i,k}^{m+1})$ can be calculated for given values of the random variables N_{m+1}, G_m, H_{m+1}, and W_i^{m+1} as follows:

$$p(\mathcal{U}_{1,k}^{m+1}|\mathcal{G}_m \cap \mathcal{H}_{m+1}) = \frac{\big(\eta(R - h_{m+1})\big)^{(k-1)} e^{-\eta(R-h_{m+1})}}{(k-1)!} \tag{5.5a}$$

$$p(\mathcal{U}_{i,k}^{m+1}|\mathcal{N}_{m+1}\cap\mathcal{G}_m\cap\mathcal{H}_{m+1}\cap\mathcal{W}_i^{m+1}) = \frac{\left(\eta(R-h_{m+1}+W_i^{m+1})\right)^{(k-1)}e^{-\eta(R-h_{m+1}+W_i^{m+1})}}{(k-1)!},\ i>1. \tag{5.5b}$$

Equations (5.5a) and (5.5b) are the probabilities of having exactly $k-1$ vehicles in a distance $R-h_{m+1}$ and $R-h_{m+1}+W_i^{m+1}$ respectively. Note that (5.5b) is correct provided that $n_{m+1}\geq i$, otherwise $p(\mathcal{U}_{i,k}^{m+1}|\mathcal{N}_{m+1}\cap\mathcal{G}_m\cap\mathcal{H}_{m+1}\cap\mathcal{W}_i^{m+1})=0$. By using (5.5a), (5.5b), and the law of total probability, we have

$$p(\mathcal{U}_{1,k}^{m+1}) = \int_0^R\int_0^{h_{m+1}} p(\mathcal{U}_{1,k}^{m+1}|\mathcal{G}_m\cap\mathcal{H}_{m+1})\cdot f_{G_m}(g_m)\cdot f_{H_{m+1}|\mathcal{G}_m}(h_{m+1},g_m)\,dg_m\,dh_{m+1} \tag{5.6a}$$

$$\begin{aligned} p(\mathcal{U}_{i,k}^{m+1}) = \sum_{n_{m+1}=i}^{\infty}\int_0^R\int_{W_i^{m+1}}^R\int_0^{h_{m+1}-W_i^{m+1}} & p(\mathcal{U}_{i,k}^{m+1}|\mathcal{N}_{m+1}\cap\mathcal{G}_m\cap\mathcal{H}_{m+1}\cap\mathcal{W}_i^{m+1})\cdot f_{G_m}(g_m) \\ & \cdot f_{H_{m+1}|\mathcal{G}_m}(h_{m+1},g_m)\cdot p(N_{m+1}=n_{m+1}|\mathcal{G}_m\cap\mathcal{H}_{m+1}) \\ & \cdot f_{W_i^{m+1}|\mathcal{G}_m\cap\mathcal{H}_{m+1}\cap\mathcal{N}_{m+1}}(w_i^{m+1},g_m,h_{m+1},n_{m+1})\,dg_m\,dh_{m+1}\,dw_i^{m+1},\ i>1. \end{aligned} \tag{5.6b}$$

The unknown PDFs and PMFs in (5.6) can be found as follows. The PMF $p(N_{m+1}=n_{m+1}|\mathcal{G}_m\cap\mathcal{H}_{m+1})$ is the probability of having exactly $(n_{m+1}-1)$ vehicles in a distance $h_{m+1}-g_m$, i.e.,

$$p(N_{m+1}=n_{m+1}|\mathcal{G}_m\cap\mathcal{H}_{m+1}) = \frac{\left(\eta(h_{m+1}-g_m)\right)^{n_{m+1}-1}e^{-\eta(h_{m+1}-g_m)}}{(n_{m+1}-1)!}. \tag{5.7}$$

The PDF $f_{G_m}(g_m)$, $m=1,...,M-1$, can be found in a recursive way by using [59]:

$$f_{G_1}(g_1) = \frac{\eta e^{-\eta g_1}}{1-e^{-\eta R}},\ 0<g_1<R \tag{5.8a}$$

$$f_{G_m|\mathcal{G}_{m-1}}(g_m,g_{m-1}) = \frac{\eta e^{-\eta g_m}}{1-e^{-\eta(R-g_{m-1})}},\ 0<g_m<R-g_{m-1}, 1<m\leq M \tag{5.8b}$$

$$f_{G_m}(g_m) = \int_0^{R-g_m} f_{G_m|\mathcal{G}_{m-1}}(g_m,g_{m-1})\cdot f_{G_{m-1}}(g_{m-1})\,dg_{m-1},\ 1<m\leq M. \tag{5.8c}$$

The PDF $f_{H_{m+1}|\mathcal{G}_m}(h_{m+1}, g_m)$, $m = 1, ..., M-1$, is calculated by using [59]

$$f_{H_{m+1}|\mathcal{G}_m}(h_{m+1}, g_m) = \frac{\eta e^{-\eta(R-h_{m+1})}}{1 - e^{-\eta(R-g_m)}},\ g_m < h_{m+1} < R. \tag{5.9}$$

Finally, the PDF $f_{W_i^{m+1}|\mathcal{G}_m \cap \mathcal{H}_{m+1} \cap \mathcal{N}_{m+1}}(w_i^{m+1}, g_m, h_{m+1}, n_{m+1})$, $m = 1, ..., M-1$ and $i = 2, ..., \infty$, is the $(i-1)^{\text{st}}$ order statistic of the uniform distribution (conditional on the existence of $n_{m+1} - 1$ vehicles in a distance interval $[0, h_{m+1} - g_m]$, the locations of these vehicles are i.i.d. uniformly distributed random variables), i.e.,

$$\begin{aligned} &f_{W_i^{m+1}|\mathcal{G}_m \cap \mathcal{H}_{m+1} \cap \mathcal{N}_{m+1}}(w_i^{m+1}, g_m, h_{m+1}, n_{m+1}) = \\ &\frac{(w_i^{m+1})^{i-2}(h_{m+1} - g_m - w_i^{m+1})^{n_{m+1}-i}(n_{m+1}-1)!}{(h_{m+1} - g_m)^{n_{m+1}-1}(n_{m+1}-i)!(i-2)!}. \end{aligned} \tag{5.10}$$

Using (5.5), (5.7), (5.9), (5.10), the two equations (5.6a) and (5.6b) can be simplified to:

$$p(\mathcal{U}_{1,k}^{m+1}) = \frac{\eta^k}{(k-1)!} \int_0^R \int_0^{h_{m+1}} (R - h_{m+1})^{(k-1)} \cdot e^{-2\eta(R-h_{m+1})} \cdot \frac{f_{G_m}(g_m)}{1 - e^{-\eta(R-g_m)}}\, dg_m\, dh_{m+1} \tag{5.11a}$$

$$\begin{aligned} p(\mathcal{U}_{i,k}^{m+1}) =& \frac{1}{(k-1)!(i-2)!}\eta^{k+i-1} \int_0^R \int_0^{h_{m+1}} \int_0^{h_{m+1}-g_m} (w_i^{m+1})^{i-2} \cdot\ e^{-2\eta(R-h_{m+1}+w_i^{m+1})} \\ &\cdot (R - h_{m+1} + w_i^{m+1})^{k-1} \cdot \frac{f_{G_m}(g_m)}{1 - e^{-\eta(R-g_m)}}\, dw_i^{m+1}\, dg_m\, dh_{m+1},\ i > 1. \end{aligned} \tag{5.11b}$$

By evaluating the integrals in (5.11) and substituting into (5.4) then (5.3), the total packet arrival rate at each vehicle can be calculated.

5.3.3 End-to-end Packet Delay

At the r^{th} vehicle in the m^{th} hop-region, by using λ_r^m from Subsection 5.3.2, the PGF of the number of packet arrivals during S_r^m is denoted by $K(z)$ and given by

$$\begin{aligned} K(z) &= \sum_{i=0}^{\infty} \Big(\sum_{j=1}^{L} p(S_r^m = j) \frac{e^{-\lambda_r^m jt} (\lambda_r^m jt)^i}{i!} \Big) z^i \\ &= \sum_{j=1}^{L} p(S_r^m = j) e^{-\lambda_r^m jt(1-z)} \end{aligned} \tag{5.12}$$

where PMF $p(S_r^m = j)$ is given by (Subsection 4.1.1.1, only the $\tau = 0$ case is considered)

$$p(S_r^m = j) = \begin{cases} \frac{C_{k_r^m - 1}^{L-j}}{C_{k_r^m}^{L}}, & 1 \le j \le L - k_r^m + 1 \\ 0, & \text{elsewhere} \end{cases} \tag{5.13}$$

with k_r^m being the number of time slots that the r^{th} vehicle in the m^{th} hop-region acquires per frame (over which the vehicle can transmit Type1 packets) and $C_k^n = \frac{n!}{(n-k)!k!}$. By using (5.12) and (5.13), the PGF of the number of packets in the queue just before the start of the service time of an HOL batch is denoted by $\Pi(z)$ and given by [60]

$$\Pi(z) = \frac{\sum_{j=0}^{b-1} \pi_j (z^b - z^j)}{\frac{z^b}{K(z)} - 1} \tag{5.14}$$

where constants π_j, $j = 0, ..., b-1$, should be chosen such that the b zeros of the numerator cancel the b zeros of the denominator on or inside the unit circle. Hence, by using the analysis of the $\text{M/G}^{(b)}/1$ queueing system [60], we have

$$\mathbb{E}(Q_r^m) = \frac{\Pi'(1) - \lambda_r^m t \mathbb{E}(S_r^m)}{\lambda_r^m} + \frac{t\mathbb{E}((S_r^m)^2)}{2\mathbb{E}(S_r^m)} \tag{5.15}$$

where $\Pi'(1) = \frac{d}{dz}\Pi(z)$ evaluated at $z = 1$. Finally, the expected values of D_{v}^m, D_{r}^m, and E^m are given by the following set of equations:

$$\mathbb{E}(D_{\text{v}}^m) = \sum_{i=1}^{\infty} p(N_m = i) \frac{1}{i} \sum_{j=1}^{i} (\mathbb{E}(Q_j^m) + t), \ 1 \le m \le M \tag{5.16}$$

$$\mathbb{E}(D_{\mathrm{r}}^{m}) = \sum_{i=1}^{n_{\mathcal{R}}-1} p(N_m = i)\frac{1}{i}\sum_{j=1}^{i}(\mathbb{E}(Q_j^m)+t) + p(N_m \geq n_{\mathcal{R}})\frac{1}{n_{\mathcal{R}}}\sum_{j=1}^{n_{\mathcal{R}}}(\mathbb{E}(Q_j^m)+t),\ 1 \leq m \leq M \tag{5.17}$$

$$p(N_1 = i) = \frac{(\eta R)^i e^{-\eta R}}{i!(1-e^{-\eta R})},\ i \geq 1 \tag{5.18a}$$

$$\begin{aligned} p(N_m = i) &= \int_0^R \int_0^{h_m} p(N_m = i | \mathcal{G}_{m-1} \cap \mathcal{H}_m) \cdot f_{G_{m-1}}(g_{m-1}) \cdot f_{H_m|\mathcal{G}_{m-1}}(h_m, g_{m-1})\, dg_{m-1}\, dh_m \\ &= \frac{\eta^i}{(i-1)!}\int_0^R \int_0^{h_m} (h_m - g_{m-1})^{i-1} \cdot e^{-\eta(R-g_{m-1})} \cdot \frac{f_{G_{m-1}}(g_{m-1})}{1-e^{-\eta(R-g_{m-1})}}\, dg_{m-1}\, dh_m, \\ &\qquad 1 < m \leq M,\ i \geq 1 \end{aligned} \tag{5.18b}$$

$$\mathbb{E}(E^1) = \mathbb{E}(D_{\mathrm{v}}^1) \tag{5.19a}$$

$$\mathbb{E}(E^m) = \mathbb{E}(D_{\mathrm{v}}^m) + \sum_{i=1}^{m-1}\mathbb{E}(D_{\mathrm{r}}^i),\ 1 < m \leq M. \tag{5.19b}$$

5.3.4 Percentage of Occupied Time Slots

Based on the batch-size b and λ_r^m at the r^{th} vehicle in the m^{th} hop-region, consider that the vehicle adjusts its number of time slots per frame, k_r^m, to guarantee that the average packet delay, $\mathbb{E}(Q_r^m)+t$, is below a threshold, denoted by $d_{\max}$. This subsection studies the number of time slots per frame required by all the vehicles of the same THS in order to limit the average packet delay at each vehicle below $d_{\max}$. This number should not exceed L to avoid any hidden terminal problem and allow each vehicle to acquire a time slot on the CCH. We define $M-1$ two hop (TH) regions. The first TH region contains all the vehicles in the first and second hop-regions, while the m^{th} TH region, $m = 2, ..., M-1$, contains all the vehicles in the m^{th} and $(m+1)^{\text{st}}$ hop-regions, plus all the vehicles in the $(m-1)^{\text{st}}$ hop-region which can reach at least one vehicle in the m^{th} hop-region. Based on this definition, the number of vehicles in each of TH regions 2 to $M-1$ can be larger than the number of vehicles which actually exist in one THS. The reason is that, a vehicle in the $(m-1)^{\text{st}}$ hop-region which can reach some of the vehicles in the m^{th} hop-region is not necessarily a two-hop neighbour of all the vehicles in the $(m+1)^{\text{st}}$ hop-region. Let

O_m, $m = 1, ..., M$ and T_m, $m = 1, ..., M-1$, respectively denote the total number of time slots used by all the vehicles in the m^{th} hop-region and m^{th} TH region. Also, let $\widetilde{N}_m$, $m = 1, ..., M-2$, denote the total number of vehicles in the m^{th} hop-region which can reach at least one vehicle in the $(m+1)^{\text{st}}$ hop-region, and V_m the total number of time slots used by $\widetilde{N}_m$. Hence,

$$\mathbb{E}(O_m) = \sum_{i=1}^{\infty} p(N_m = i) \sum_{j=1}^{i} k_j^m,\ 1 \leq m \leq M \tag{5.20}$$

$$\mathbb{E}(T_1) = \mathbb{E}(O_1) + \mathbb{E}(O_2) \tag{5.21a}$$

$$\mathbb{E}(T_m) = \mathbb{E}(O_{m+1}) + \mathbb{E}(O_m) + \mathbb{E}(V_{m-1}),\ 2 \leq m \leq M-1 \tag{5.21b}$$

$$\mathbb{E}(V_m) = \sum_{i=1}^{\infty} p(\widetilde{N}_m = i) \sum_{j=1}^{i} k_j^m,\ 1 \leq m \leq M-2 \tag{5.22a}$$

$$p(\widetilde{N}_m = i) = \sum_{j=1}^{\infty} p(N_{m+1} = j) p(\mathcal{U}_{j,i}^{m+1}),\ 1 \leq m \leq M-2, 1 \leq i \leq \infty, \tag{5.22b}$$

where $p(N_m = j)$ and $p(\mathcal{U}_{j,i}^{m+1})$ are given by (5.18) and (5.11) respectively.

5.4 Numerical Results

5.4.1 Gateway Placement in a City Scenario

This subsection applies the gateway placement strategy in Section 5.1 for a city scenario consisting of roads around the UW campus. The map is partitioned into square cells with side length of 10 m, and the potential gateway locations are defined along each road with a separation of 10 m between two successive locations. The road network is created in VISSIM, as shown in Fig 4.7, to simulate the movement of the vehicles in low, medium, and high vehicle density scenarios. For each scenario, the VISSIM simulator generates a trace file (listing the location of each vehicle after each simulation step) that is used by a MATLAB script to calculate the probabilities $\sigma_{i,j,k} \forall i, j, k$, as defined in Section 5.1. To determine whether or not a network path exists between a vehicle and gateway,

the MATLAB script assumes that two nodes can communicate iff they are within the communication range of each other. Extending the script to account for the wireless channel effects, such as the shadowing caused by trees and buildings, is left as a future work. At the start of the VISSIM simulations, vehicles arrive to the road network from each possible road entry according to a Poisson process with a rate parameter that differs based on the capacity of the road and the desired vehicle density. The vehicles are left to move for a warm up period of 15 min (to avoid transient effects), then their positions are recorded for another 30 min. The control of each intersection, as well as the left and right turn decisions made by a vehicle are as described in Subsection 4.3.2. Once a vehicle reaches any end of the road network, it is removed from the simulations. The desired speed distributions, car following model, lane changing model, vehicle characteristics, and maximum/desired acceleration and deceleration functions are described in Table 4.2.

After calculating the probabilities $\sigma_{i,j,k}$ from the VISSIM simulations for different vehicle densities, problem (5.1) is solved by using the GUROBI optimizer 5.5 [61] together with the YALMIP modeling language [62]. The GUROBI optimizer combines a branch-and-bound algorithm, cutting-plane methods, and multiple heuristics in order to solve a binary integer programming problem. In problem (5.1), we set $\gamma_j = 1\ \forall j$ (equivalent to minimizing the number of deployed gateways), $\nu_i = 1$, and $\alpha_i = \alpha\ \forall i$, where α is a parameter ranging from 0.6 to 0.9 with step 0.1. A video showing the optimal locations of gateways in a VISSIM simulation can be found at [63].

Fig. 5.5 shows the effect of ρ_{max} and R on the number of deployed gateways in high and low vehicle density scenarios. As shown in Fig. 5.5a, when ρ_{max} is increased from 1 to 3, the number of gateways drops from 35 to 15 and from 19 to only 6 gateways for a communication range of 150 m and 250 m respectively. The effect of increasing ρ_{max} on the reduction of the number of deployed gateways is more significant in the high density scenario due to the existence of more vehicles which can relay packets to/from the gateways. For instance, as shown in Fig. 5.5b, when $R = 150$ m in a low density scenario, increasing ρ_{max} from 1 to 3 results in a 40% reduction of the number of deployed gateways, as compared to around 57% reduction in the high density scenario in Fig. 5.5a. Note that, when $\rho_{max} = 1$, the vehicle traffic density does not have any effect on the number of deployed gateways, which is the case when each cell is required to be within the communication range of at least one gateway.

The effect of the vehicle traffic density and the threshold α on the number of deployed gateways when $R = 150$ m is illustrated in Fig. 5.6 for $\rho_{max} = 2$ and $\rho_{max} = 3$. In each of Figs. 5.6a and 5.6b, for a given α value, the number of gateways decreases when the vehicle density increases. This decrease in the number of gateways deployed in a higher vehicle density is more remarkable when $\rho_{max} = 3$ (Fig. 5.6b), especially for a high α value.

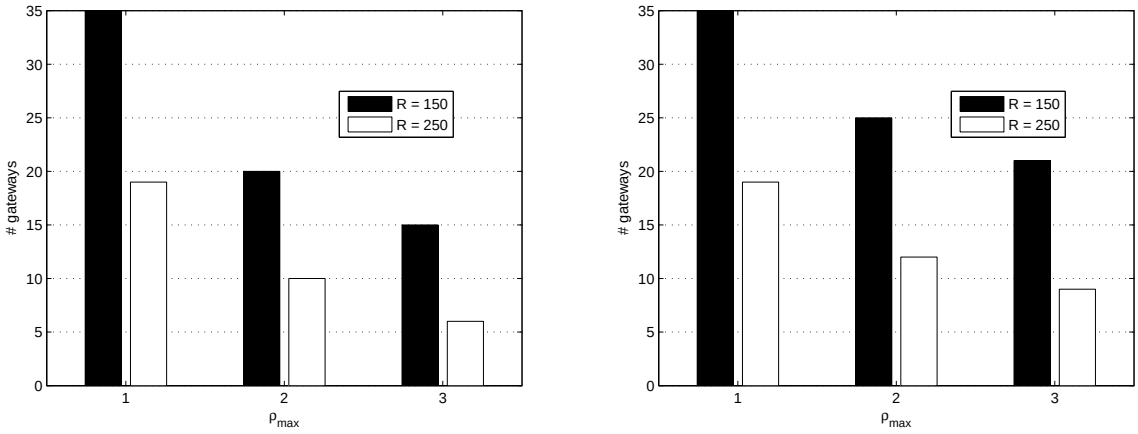

(a) High vehicle density

(b) Low vehicle density

Figure 5.5: The number of deployed gateways versus ρ_{max} for $\alpha = 0.8$ and two different communication ranges.

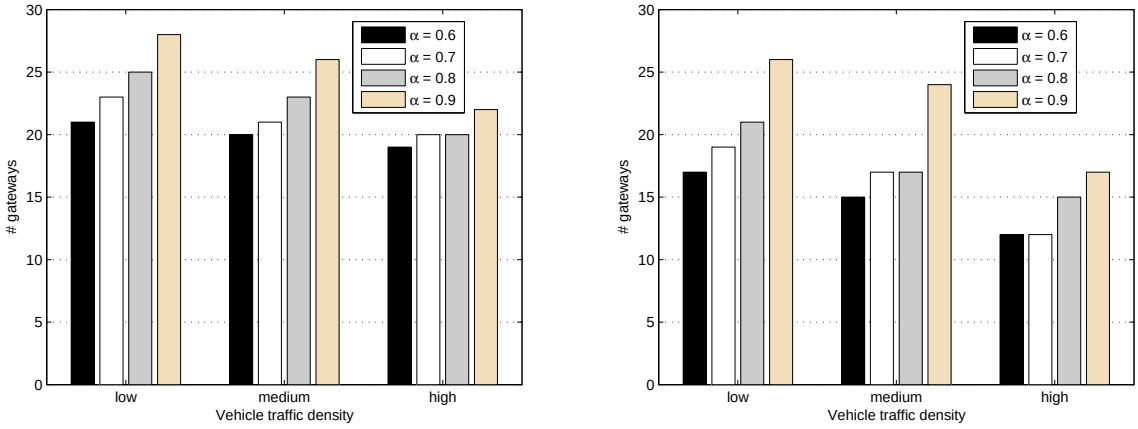

(a) $\rho_{max} = 2$

(b) $\rho_{max} = 3$

Figure 5.6: The number of deployed gateways versus vehicle traffic for $R = 150$ m.

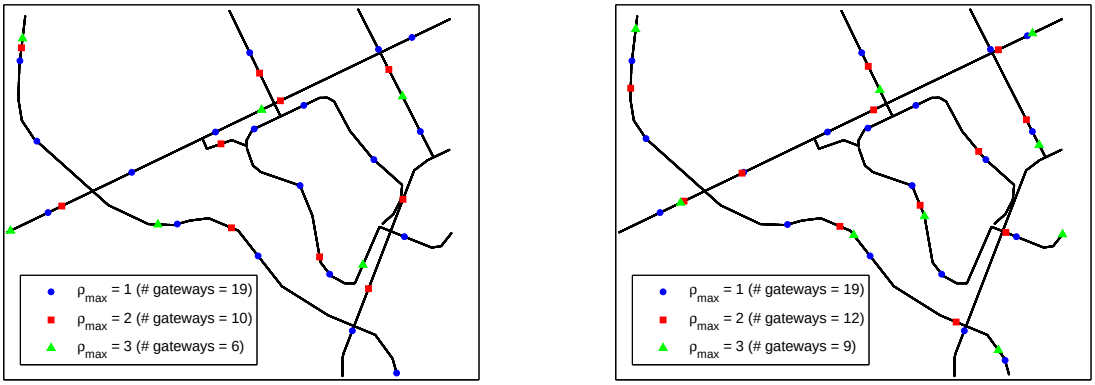

(a) High vehicle density

(b) Low vehicle density

Figure 5.7: The locations of the deployed gateways for $\alpha = 0.8$ and $R = 250$ m.

Similarly, for a certain vehicle density in Fig. 5.6a or 5.6b, increasing α usually requires the deployment of additional gateways. The effect of α on the number of deployed gateways is more significant in a lower vehicle density scenario and for a higher ρ_{max} value. The same results as in Fig. 5.6 are obtained for $R = 250$ m. When $R = 250$ m and $\alpha = 0.8$, Figs. 5.7a and 5.7b illustrate the locations of the gateways on the map for different ρ_{max} values, respectively in high and low vehicle density scenarios. It is obvious from Fig. 5.7 how the vehicle density affects the optimal number and locations of gateways, except when $\rho_{max} = 1$. For a gateway located at position j, the value of ρ_j assigned by the optimizer is equal to ρ_{max} almost for all j.

As the threshold α represents the minimum acceptable probability of reaching a gateway from a certain cell, the average probability (over all cells) of reaching a gateway is eventually greater than α. For instance, as shown in Fig. 5.8a, while $\alpha = 0.7$, for most of the cells, a vehicle can reach a gateway with a probability greater than 0.95. Hence, the average probability of reaching a gateway is around 0.98, as shown in Fig. 5.8b. Note that, in Fig. 5.8b, the cells are indexed by scanning the map from left to right (bottom-up) and, hence, close values of the indices of two cells do not necessarily mean that the cells are located in proximity of each other on the map. The cells having a probability 1 in Fig. 5.8b are those which are located within the communication range of a gateway. The relation between the threshold α and the average probability of reaching a gateway achieved over all cells is shown in Fig. 5.9 for $R = 250$ m. Even when $\alpha = 0.6$, the average probability is above

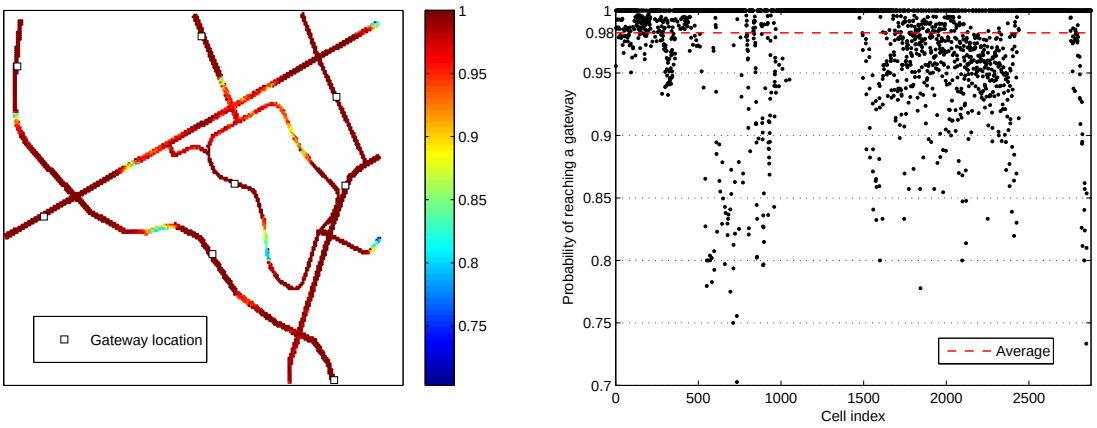

(a) Probability values indicated by the colorbar (b) Probability values versus cell index

Figure 5.8: The probability of reaching a gateway in a low traffic density for $\alpha = 0.7$, $\rho_{max} = 3$, and $R = 250$ m.

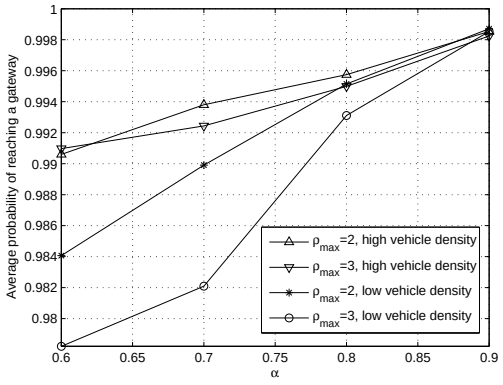

Figure 5.9: The average probability of reaching a gateway versus the threshold α for $R = 250$ m.

0.978 for all vehicle densities and ρ_{max} values. Similar results were found for the other communication range, $R = 150$ m.

To apply the proposed gateway placement strategy in a big deployment region, e.g., in a whole city, the deployment region can be partitioned into smaller regions, in order to avoid solving a single optimization problem with a large number of constraints and decision variables. Also, the choice of the cell size and potential gateway locations should guarantee the feasibility of problem 5.1. For instance, if $\nu_i = 1\ \forall i$, when the cell diagonal is not greater than twice the communication range of a gateway, the feasibility of problem 5.1 is guaranteed by ensuring that for each cell, there is a potential location for a gateway which can entirely cover the cell within its communication range.

5.4.2 Packet Routing in a Highway Scenario

This section presents numerical results for a 4-lane highway segment consisting of 5 hop-regions based on a communication range $R = 150$ m. The average vehicle density per lane, η_{lane}, varies from 12 to 67 vehicles/mile, a range which corresponds to traffic flow conditions varying from a free-flow scenario to a near-capacity one [64]. For the VeMAC protocol, the number of time slots per frame $L = 275$ slots and the slot duration $t = 0.35$ ms, resulting in a frame duration of 96.25 ms [40]. We use MAPLE 17 to calculate the PDFs $f_{G_m}(g_m)$, $m = 1, .., 4$, in (5.8), and MATLAB R2012b for all other calculations including the numerical evaluation of the integrals in (5.18b) and (5.11).

Fig. 5.10a shows λ_r^m, for $r = 1, ..., 10$, $m = 1, ..., 5$, and different λ values. In Fig. 5.10a, with $n_{\mathcal{R}} = 10$, the vehicles under consideration in hop-regions 1 to 4 represent all the potential relay vehicles located in these hop-regions. In the 5^{th} hop-region, $\lambda_r^5 = \lambda\, \forall r$, since the vehicles in this hop-region do not relay any packet. On the other hand, in the m^{th} hop region, $m = 1, ..., 4$, λ_r^m increases when the vehicle index r decreases. The reason is that, when index r is small, a relay vehicle in the m^{th} hop region is more likely to be reached by a higher number of vehicles in the $(m+1)^{\text{st}}$ hop region. Similarly, for a given vehicle index r, λ_r^m increases when the hop-region index m is smaller, i.e., when the r^{th} relay vehicle is in a hop-region closer to the gateway. The reason is that, the relay vehicles located at the m^{th} hop region ($m < 5$) will eventually relay all the packets arriving from all the farther hop-regions (indexed $m+1, ..., 5$) to the gateway. A more focused illustration of the variation of λ_r^m with r and m is shown in Fig. 5.10b, which concentrates only on the first three relay vehicles in each hop-region with a single λ value. The increase in the λ value eventually increases $\lambda_r^m\, \forall r, m$, as shown in Fig. 5.10a. Similarly, if λ remains constant and η_{lane} increases, λ_r^m increases for all the relay vehicles ($m = 1, ..., 4, r = 1, .., 10$), as illustrated in Fig. 5.10c.

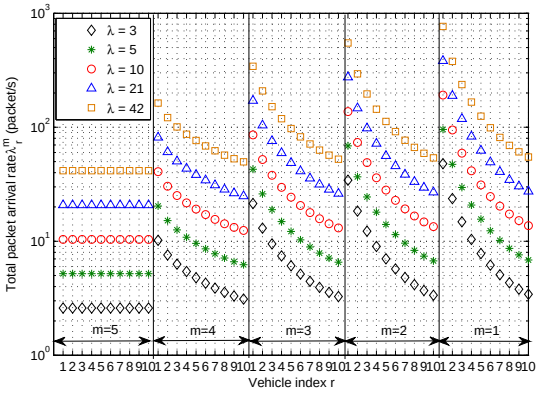

(a) First ten vehicles in each hop region for $n_{\mathcal{R}} = 10$ and $\eta_{\text{lane}} = 30$ vehicles/mile

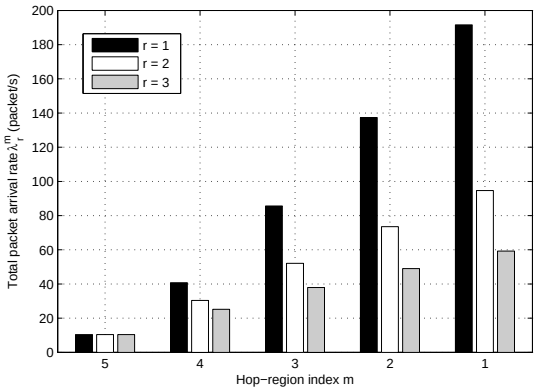

(b) First three vehicles in each hop region for $n_{\mathcal{R}} = 10$, $\eta_{\text{lane}} = 30$ vehicles/mile, and $\lambda = 10$ packet/s

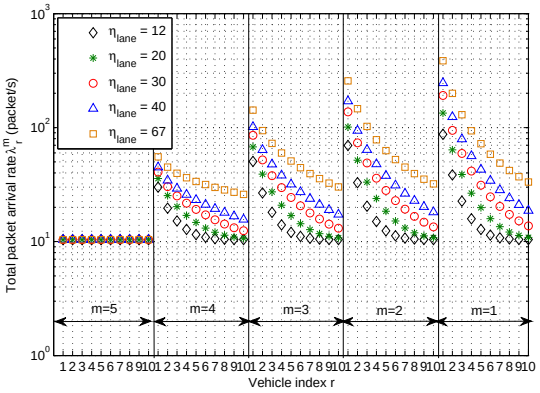

(c) First ten vehicles in each hop region for $n_{\mathcal{R}} = 10$ and $\lambda = 10$ packets/s

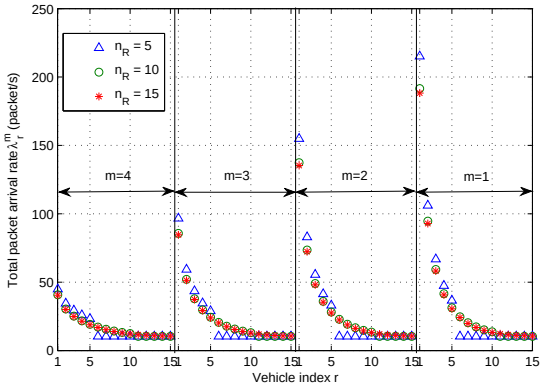

(d) First 15 vehicles in each hop region for $\eta_{\text{lane}} = 30$ vehicles/mile and $\lambda = 10$ packets/s

Figure 5.10: Total packet arrival rate λ_r^m at the vehicles in each hop-region.

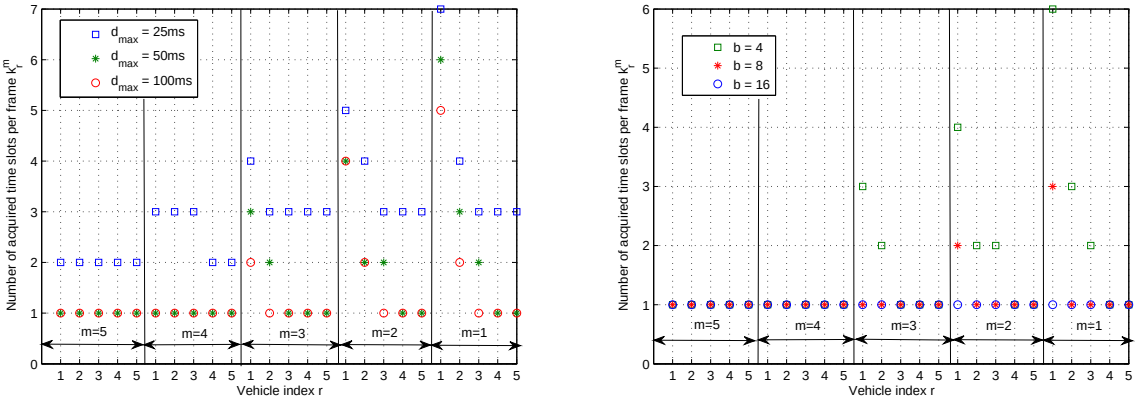

(a) $n_{\mathcal{R}} = 5$ and $b = 4$

(b) $n_{\mathcal{R}} = 5$ and $d_{\max} = 50$ ms

Figure 5.11: Number of acquired time slots per frame k_r^m by each of the first five vehicles in each hop-region for $\eta_{\text{lane}} = 30$ vehicles/mile and $\lambda = 10$ packets/s.

The number $n_{\mathcal{R}}$ of relays included in the GDP defines the number of potential relay vehicles in each hop-region. Consequently, the value of $n_{\mathcal{R}}$ affects λ_r^m for some m and r, as shown in Fig. 5.10d. When $n_{\mathcal{R}} = 5$, only the first 5 vehicles in each hop-region can relay packets, and hence $\forall m$, the value of λ_r^m increases for $r = 1, ..., 5$ and decreases for $r = 6, ..., 15$ as compared to the cases of $n_{\mathcal{R}} = 10$ and $n_{\mathcal{R}} = 15$. On the other hand, no significant difference in $\lambda_r^m \, \forall r, m$ is observed when $n_{\mathcal{R}}$ is changed from 10 to 15. The reason is that, even if there are 15 potential relays included in the GDP broadcast by a vehicle in the m^{th} hop region, not all the 15 relays can be reached by the vehicles in the $(m+1)^{\text{st}}$ hop region, and consequently not all of them will actually relay packets.

The effect of $d_{\max}$ on k_r^m is illustrated in Fig. 5.11a for the first five vehicles in each hop-region. When $d_{\max} = 25$ ms, while the r^{th} vehicle in the 5^{th} hop-region (does not relay packets) has $k_r^5 = 2$ slots $\forall r$, some relay vehicles in the other hop-regions need to acquire a higher number of time slots per frame in order to satisfy this delay requirement, e.g., $k_1^1 = 7$ slots. When $d_{\max}$ is increased to 100 ms, only one time slot per frame is acquired by each vehicle, except the relay vehicles with high packet arrival rates at the hop-regions close to the gateway. Fig. 5.11b shows that, when the bath-size b increases, the number of time slots acquired by a relay vehicle can be significantly reduced, since the vehicle is able to announce for a larger number of packets in each time slot. For instance, as shown in Fig. 5.11b, while a batch-size $b = 4$ requires $k_1^1 = 6$ slots and $k_1^2 = 4$ slots, both values are halved when $b = 8$, and are reduced to only 1 slot when $b = 16$.

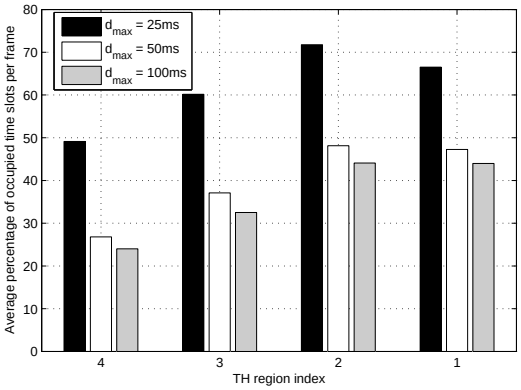

(a) $\lambda = 21$ packets/s, $n_{\mathcal{R}} = 10$, and $b = 4$

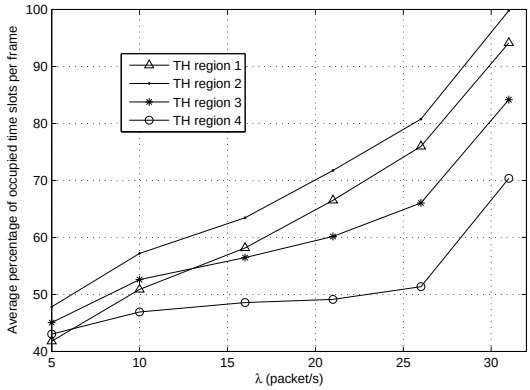

(b) $n_{\mathcal{R}} = 10$, $b = 4$, and $d_{\max} = 25$ ms

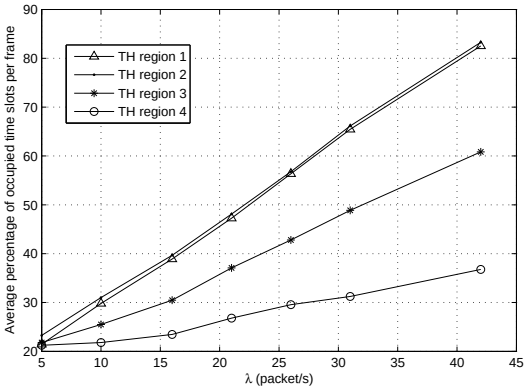

(c) $n_{\mathcal{R}} = 10$, $b = 4$, and $d_{\max} = 50$ ms

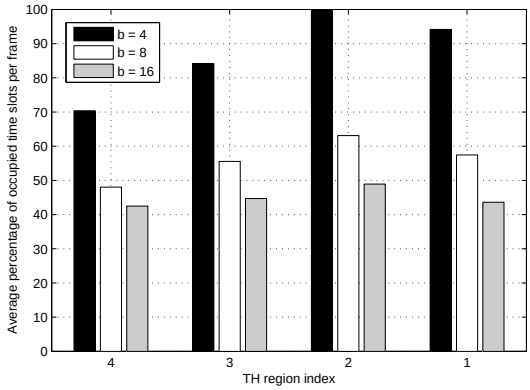

(d) $\lambda = 31$ packets/s, $n_{\mathcal{R}} = 10$, and $d_{\max} = 25$ ms

Figure 5.12: Average percentage of occupied time slots per frame for each TH region for $\eta_{\text{lane}} = 67$ vehicles/mile.

Fig. 5.12a shows the effect of $d_{\max}$ on the average percentage of time slots per frame occupied by all the vehicles in each TH region, i.e., $\frac{\mathbb{E}(T_m)}{L} \times 100, m = 1, ..., 4$. Based on the TH region definition in Subsection 5.3.4, and given the number of time slots acquired by individual vehicles in Fig. 5.11, the second TH region is the most loaded (in terms of time slot occupancy) since it includes all the vehicles in the second and third hop-regions, as well as all the relay vehicles in the first hop-region. As shown in Fig. 5.12a, the second TH region has an average time slot occupancy less than 75%, even for $d_{\max} = 25$ ms and $\eta_{\text{lane}} = 67$ vehicles/mile. In Fig. 5.12a, when $d_{\max} = 25$ ms, each non-relay vehicle needs to acquire three time slots per frame, which results in a significant increase in the average slot occupancy in all TH regions, as compared with the $d_{\max} = 50$ ms and $d_{\max} = 100$ ms cases, in which a non-relay vehicle needs to acquire only two time slots per frame to satisfy the delay threshold. When $d_{\max}$ decreases from 100 ms to 50 ms, the slight increase in the average slot occupancy shown in Fig. 5.12a is because of the extra time slots acquired by some relay vehicles. Fig. 5.12b shows the average percentage slot occupancy for each TH region versus λ. When $\lambda = 31$ packets/s (3 packets/frame), almost 100% average slot occupancy is achieved at the second TH region. Hence, for the highest average vehicle density, $\eta_{\text{lane}} = 67$ vehicles/mile, smallest delay threshold, $d_{\max} = 25$ ms, and smallest batch-size, $b = 4$, under consideration, a frame length of 275 time slots can accommodate all the vehicles in each TH region for a packet arrival rate λ up to 31 packets/s. If $d_{\max}$ is increased to 50 ms, as shown in Fig. 5.12c, then for the same η_{lane} and b values as in Fig. 5.12b, the average percentage of occupied time slots remains below 85% for all TH regions, even for λ as high as 42 packets/sec (4 packets/frame). On the other hand, if $d_{\max} = 25$ ms and b is increased from 4 to 8, the average slot occupancy is reduced by approximately 35% for each TH region, as shown in Fig. 5.12d.

Fig. 5.13a shows the average end-to-end packet delay for each hop-region, $\mathbb{E}(E^m)$, $m = 1, ..., 5$, for different values of $d_{\max}$. A packet sent from a vehicle in the 5^{th} hop-region can be delivered to the gateway with an average end-to-end delay of 110 ms (178 ms) when $d_{\max} = 25$ ms ($d_{\max} = 50$ ms). Note that, the value of $d_{\max}$ represents the delay threshold below which each vehicle limits its average packet delay by acquiring a suitable number of time slots per frame. How much the actual value of the average packet delay at a certain vehicle is below $d_{\max}$ depends mainly on the total packet arrival rate at the vehicle. Fig. 5.13b shows the effect of λ on the average end-to-end packet delay for each hop-region. As shown in Fig. 5.13b, the increase in the average end-to-end packet delay with λ is higher when a hop-region is farther from the gateway. However, the effect of λ on the average end-to-end packet delay is not significant, especially for the first two hop-regions, since when λ increases, each vehicle can access more time slots per frame in order to keep its average packet delay below $d_{\max}$. In other words, increasing λ affects more the percentage

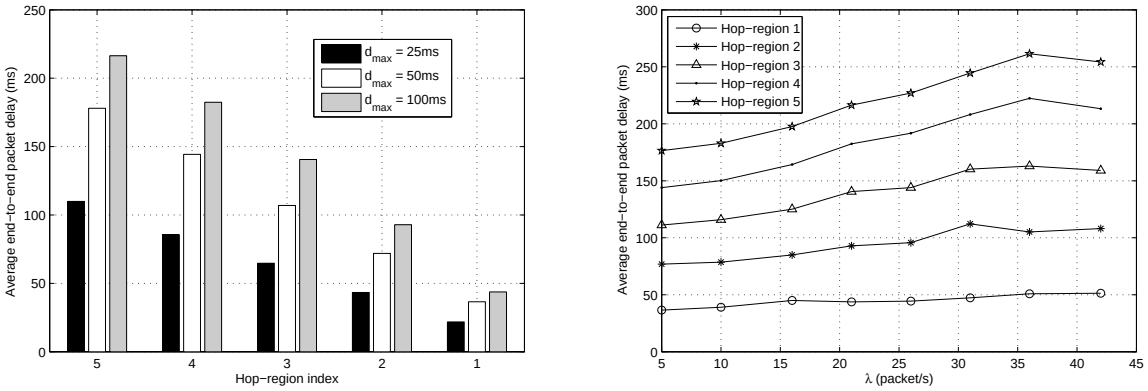

(a) $\lambda = 21$ packets/s and $b = 4$

(b) $b = 4$ and $d_{\max} = 100$ ms

Figure 5.13: Average end-to-end packet delay for each hop-region for $n_{\mathcal{R}} = 10$ and $\eta_{\text{lane}} = 30$ vehicles/mile.

of occupied time slots per frame rather than the end-to-end packet delay as shown in Figs. 5.12b, 5.12c, and 5.13b.

5.5 Summary

This chapter presents a new Internet gateway placement strategy, together with a novel packet routing scheme, in order to provide Internet connectivity to the vehicles by using multihop communications in a multichannel VANET. Based on a target vehicle traffic condition, the Internet gateways are deployed in a way which minimizes the total deployment cost, subject to location-dependant lower bounds on the probability that a vehicle finds a network path to an Internet gateway. This cost minimization problem is formulated by using binary integer programming, and applied for optimal gateway placement in a real city scenario. Numerical results are presented to investigate the effect of different system parameters, including the vehicle density and the communication range, on the number and locations of the deployed gateways. On the other hand, the proposed routing scheme is based on the VeMAC protocol, which is presented and evaluated in Chapters 3 and 4. The routing scheme describes how the vehicles discover the existence of an Internet gateway, and how a vehicle can use the other vehicles to relay packets to/from the gateway. Analysis of the end-to-end packet delivery delay is conducted to evaluate the performance of the proposed routing scheme in a highway scenario, by taking into consideration the packet

queueing delay at each relay vehicle. In addition, the percentage of time slots occupied per frame is evaluated, when each relay vehicle is allowed to access a number of time slots that limits its average packet delay below a certain threshold. Numerical results show that, due to a high total packet arrival rate, a relay vehicle may need to acquire more time slots per frame in order to limit its average packet delay, especially when the relay vehicle is located close to a gateway. By properly adjusting the number of time slots that each vehicle acquires per frame, increasing the packet arrival rate at each vehicle affects more the percentage of occupied time slots per frame rather than the end-to-end packet delay.

Chapter 6

Conclusions and Future Works

6.1 Conclusions

VANETs are an emerging paradigm which is currently receiving significant support from government, academia, and industrial organizations over the globe. By employing V2V and V2R communications, VANETs are expected to realize a variety of advanced applications for road safety, passenger infotainment, and vehicle traffic optimization. The main objectives of this research are to support the QoS requirements of VANET safety applications, and to provide Internet connectivity to the vehicles by using multihop communications in a multichannel VANET. To achieve these objectives, this thesis presents a multichannel MAC protocol (VeMAC), a packet routing scheme, and a strategy for deploying Internet gateways on the roads.

In the TDMA-based VeMAC protocol, the nodes access the time slots on the CCH and SCHs in distributed ways which are designed to avoid any hidden terminal problem. On the CCH, the VeMAC provides a reliable one-hop broadcast service, which is crucial for high priority safety applications supported on this channel. How the periodic and event-driven safety messages are queued and served by the VeMAC protocol is described, and a detailed message delay analysis (including queueing and service delay) is presented by taking into consideration the size and the arrival pattern of each type of safety messages. MATLAB simulations in highway and city scenarios show that, compared with the ADHOC MAC protocol, the VeMAC provides a smaller rate of transmission collisions, which results in a significantly higher throughput on the CCH. Additionally, the network simulator ns-2 and the microscopic vehicle traffic simulator VISSIM are used to evaluate the performance of VeMAC in comparison with the IEEE 802.11p standard in a realistic city scenario.

Simulation results show that, the VeMAC protocol can deliver both types of safety messages to all the nodes in the one-hop neighbouhoud with an acceptable average delivery delay (less than 100 ms). Moreover, it is shown that the VeMAC has a low probability of a transmission collision, which results in a higher safety message goodput and better channel utilization, as compared to the IEEE 802.11p standard. This research sheds light on TDMA as a promising technology for MAC in VANETs, and a suitable replacement of the IEEE 802.11p standard, which have significant limitations in supporting VANET safety applications.

The proposed strategy for deploying Internet gateways on roads minimizes the total cost of gateway deployment based on binary integer programming. This cost minimization is achieved subject to location-dependant lower bounds on the probability that a vehicle finds a network path to a gateway, based on the traffic conditions in the deployment region. To the best of our knowledge, the proposed deployment strategy is the first study to address the probability of existence of multihop network paths among the vehicles and the deployed gateways. The strategy is applied for optimal placement of gateways in a realistic city scenario, and the effects of different system parameters (including the vehicle traffic density) on the number and location of deployed gateways are investigated. How each vehicle discovers the existence of a gateway and how the packets are delivered between a vehicle and a gateway through multiple relay vehicles are both described in the proposed packet routing scheme, which is designed over the VeMAC protocol. To evaluate the performance of this cross-layer design, analysis of the end-to-end packet delivery delay is conducted in a highway scenario, by modeling the system as a network of batch-service queues. The packet arrival rate at each relay vehicle is calculated based on the position of the relay vehicle relative to an Internet gateway. Also, the percentage of time slots occupied per frame is evaluated, when each relay vehicle is allowed to access a number of time slots to limit its average packet delay below a certain threshold. The proposed VANET architecture can achieve multihop in-vehicle Internet access by using the routing scheme, while satisfying the QoS requirements of the safety applications via the VeMAC protocol.

6.2 Further Research Topics

In the future, the performance of the VeMAC protocol using different values of the split up parameter τ, other than $\tau = 0$ and $\tau = \infty$, is worth to be investigated. Another issue which must be examined is how the protocol performance is affected by the existence of asymmetric wireless channels among the nodes, as well as by the packet errors

caused by the channel impairments such as noise, fading, and shadowing. Since each node interprets any packet error as a transmission collision, the packet errors due to a poor wireless channel may result in nodes unnecessarily releasing their time slots on the CCH. Also, since information security is not considered in this thesis, suitable authentication and integrity schemes should be developed to protect the VeMAC protocol against any malicious attack, such as broadcasting of false control information over the CCH, which can affect the VeMAC techniques for distributed time slot assignment and transmission collision detection. Concerning the communications over the SCHs, the proposed scheme for unicast should be evaluated via analysis and simulations, and then extended to support a reliable broadcast service on the SCHs. Finally, a prototype should be created for the VeMAC protocol in order to investigate its implementation complexity and practically test its performance in a real vehicular scenario.

The routing scheme proposed over the VeMAC protocol should be evaluated by using realistic mobility traces of vehicles in highway and city scenarios, in comparison with a bench mark routing protocol, such as the Greedy Perimeter Stateless Routing (GPSR), over the IEEE 802.11p standard. Also, suitable Internet gateway selection and handover schemes should be developed, and results of the presented gateway deployment strategy should be obtained by taking into consideration the effects of the wireless channel.

Another promising research topic is how to support periodic and event-driven safety messages via the Long Term Evolution Advanced (LTE-A) mobile communications standard. To date, very few studies have considered this topic, and there are still many issues which need investigation to determine whether or not the LTE-A standard can be employed for road safety applications.

References

[1] "Specification for Telecommunications and Information Exchange Between Roadside and Vehicle Systems 5 GHz Band Dedicated Short Range Communications (DSRC) Medium Access Control (MAC) and Physical Layer (PHY) Specifications," *ASTM Standard E2213*, 2003 (2010).

[2] "Vehicle safety communications project task 3 final report," The CAMP Vehicle Safety Communications Consortium, Tech. Rep. DOT HS 809 859, Mar. 2005.

[3] W. Zhuang and H. A. Omar, "Vehicular communication netwroks: opportunities and challenges," in *Proc. 5th International Symposium and the 4th Student Organizing International Mini-Conference on Information Electronics Systems*, Feb. 2012.

[4] R. Baldessari, B. Bdekker, A. Brakemeier, M. Deegener, A. Festag, W. Franz, A. Hiller, C. Kellum, T. Kosch, A. Kovacs, M. Lenardi, A. Lbke, C. Menig, T. Peichl, M. Roeckl, D. Seeberger, M. Strassberger, H. Stratil, H.-J. Vgel, B. Weyl, and W. Zhang, "Car-2-car communication consortium manifesto," Tech. Rep. Version 1.1, Aug. 2007.

[5] http://www.car-to-car.org/.

[6] http://www.cvisproject.org/.

[7] http://www.sevecom.org/.

[8] http://evita-project.org/.

[9] http://www.com2react-project.org/.

[10] http://www.ertico.com.

[11] http://www.safespot-eu.org/.

[12] http://www.comesafety.org/.

[13] http://www.geonet-project.eu/.

[14] http://www.ict-itetris.eu/index.htm.

[15] W. Specks, K. Matheus, R. Morich, I. Paulus, C. Menig, A. Lbke, B. Rech, and V. Audi, "Car-to-car communication–market introduction and success factors," in *Proc. 5th European Congress and Exhibition on Intelligent Transport Systems and Services*, 2005.

[16] J. J. Blum and A. Eskandarian, "A reliable link-layer protocol for robust and scalable intervehicle communications," *IEEE Transactions on Intelligent Transportation Systems*, vol. 8, no. 1, pp. 4–13, Mar. 2007.

[17] R. Mangharam, R. Rajkumar, M. Hamilton, P. Mudalige, and F. Bai, "Bounded-latency alerts in vehicular networks," in *Proc. Mobile Networking for Vehicular Environments (MOVE 2007)*, May 2007, pp. 55–60.

[18] F. Watanabe, M. Fujii, M. Itami, and K. Itoh, "An analysis of incident information transmission performance using MCS/CDMA scheme," in *Proc. IEEE Intelligent Vehicles Symposium (IV'05)*, Jun. 2005, pp. 249–254.

[19] H. Nakata, T. Inoue, M. Itami, and K. Itoh, "A study of inter vehicle communication scheme allocating PN codes to the location on the road," in *Proc. IEEE Intelligent Transportation Systems Conference (ITSC 2003)*, vol. 2, Oct. 2003, pp. 1527–1532.

[20] F. Borgonovo, A. Capone, M. Cesana, and L. Fratta, "ADHOC MAC: New MAC architecture for ad hoc networks providing efficient and reliable point-to-point and broadcast services," *Wireless Networks*, vol. 10, pp. 359–366, Jul. 2004. [Online]. Available: http://dx.doi.org/10.1023/B:WINE.0000028540.96160.8a

[21] "IEEE standard for information technology–telecommunications and information exchange between systems–local and metropolitan area networks–specific requirements Part 11: Wireless LAN medium access control (MAC) and physical layer (PHY) specifications Amendment 6: Wireless access in vehicular environments," *IEEE Std 802.11p-2010 (Amendment to IEEE Std 802.11-2007 as amended by IEEE Std 802.11k-2008, IEEE Std 802.11r-2008, IEEE Std 802.11y-2008, IEEE Std 802.11n-2009, and IEEE Std 802.11w-2009)*, pp. 1–51, Jul. 15, 2010.

[22] "IEEE standard for information technology-telecommunications and information exchange between systems-local and metropolitan area networks-specific requirements - Part 11: Wireless LAN medium access control (MAC) and physical layer (PHY) specifications," *IEEE Std 802.11-2012 (Revision of IEEE Std 802.11-2007)*, pp. 1–2793, Mar. 2012.

[23] "IEEE standard for wireless access in vehicular environments (WAVE) - multi-channel operation," *IEEE Std 1609.4-2010 (Revision of IEEE Std 1609.4-2006)*, pp. 1–89, Feb. 2011.

[24] T. Clausen and P. Jacquet, "Optimized link state routing protocol (OLSR)," RFC 3626, Oct. 2003.

[25] C. E. Perkins and P. Bhagwat, "Highly dynamic destination-sequenced distance-vector routing (DSDV) for mobile computers," in *Proc. Conference on Communications Architectures, Protocols and Applications (ACM SIGCOMM '94)*, Sep. 1994, pp. 234–244. [Online]. Available: http://doi.acm.org/10.1145/190314.190336

[26] D. B. Johnson and D. A. Maltz, "Dynamic source routing in ad hoc wireless networks," in *Mobile Computing*, T. Imielinski and H. Korth, Eds. Kluwer Academic Publishers, 1996, pp. 153–181.

[27] Y.-B. Ko and N. H. Vaidya, "Location-aided routing (LAR) in mobile ad hoc networks," *Wireless Networks*, vol. 6, pp. 307–321, Jul. 2000. [Online]. Available: http://dx.doi.org/10.1023/A:1019106118419

[28] C. Perkins and E. Royer, "Ad-hoc on-demand distance vector routing," in *Proc. Second IEEE Workshop on Mobile Computing Systems and Applications (WMCSA '99)*, Feb. 1999, pp. 90–100.

[29] Z. J. Haas and M. R. Pearlman, "ZRP: a hybrid framework for routing in ad hoc networks," in *Ad hoc networking*. Boston, MA, USA: Addison-Wesley Longman Publishing Co., Inc., 2001, pp. 221–253. [Online]. Available: http://portal.acm.org/citation.cfm?id=374547.374554

[30] B. Karp and H. T. Kung, "GPSR: greedy perimeter stateless routing for wireless networks," in *Proc. 6th annual international conference on Mobile computing and networking (MobiCom '00)*, Aug. 2000, pp. 243–254. [Online]. Available: http://dx.doi.org/10.1145/345910.345953

[31] C. Lochert, H. Hartenstein, J. Tian, H. Fuessler, D. Hermann, and M. Mauve, "A routing strategy for vehicular ad hoc networks in city environments," in *Proc. IEEE Intelligent Vehicles Symposium (IV'03)*, Jun. 2003, pp. 156–161.

[32] C. Lochert, M. Mauve, H. Füssler, and H. Hartenstein, "Geographic routing in city scenarios," *SIGMOBILE Mobile Computing and Communications Review*, vol. 9, no. 1, pp. 69–72, Jan. 2005. [Online]. Available: http://dx.doi.org/10.1145/1055959.1055970

[33] R. Morris, J. Jannotti, F. Kaashoek, J. Li, and D. Decouto, "Carnet: a scalable ad hoc wireless network system," in *Proc. 9th ACM SIGOPS European workshop "Beyond the PC: New Challenges for the Operating System" (SIGOPS EW'00)*, Sep. 2000, pp. 61–65. [Online]. Available: http://doi.acm.org/10.1145/566726.566741

[34] S. Basagni, I. Chlamtac, V. R. Syrotiuk, and B. A. Woodward, "A distance routing effect algorithm for mobility (DREAM)," in *Proc. 4th annual ACM/IEEE international conference on Mobile computing and networking (MobiCom '98)*, Oct. 1998, pp. 76–84. [Online]. Available: http://doi.acm.org/10.1145/288235.288254

[35] M. Käsemann, H. Füßler, H. Hartenstein, and M. Mauve, "A reactive location service for mobile ad hoc networks," Department of Computer Science, University of Mannheim, Tech. Rep. TR-02-014, Nov. 2002.

[36] V. Naumov and T. Gross, "Connectivity-aware routing (CAR) in vehicular ad-hoc networks," in *Proc. 26th IEEE International Conference on Computer Communications (INFOCOM 2007)*, May 2007, pp. 1919–1927.

[37] H. A. Omar, W. Zhuang, and L. Li, "VeMAC: A TDMA-based MAC protocol for reliable broadcast in VANETs," *IEEE Transactions on Mobile Computing*, vol. 12, no. 9, pp. 1724-1736, Sept. 2013.

[38] H. A. Omar, W. Zhuang, and L. Li, "Evaluation of VeMAC for V2V and V2R Communications Under Unbalanced Vehicle Traffic," *Proc. IEEE Vehicular Technology Conference (VTC2012-Fall)*, Sept. 2012.

[39] H. A. Omar, W. Zhuang, and L. Li, "VeMAC: a novel multichannel MAC protocol for vehicular ad hoc networks," in *Proc. IEEE International Conference on Computer Communications (INFOCOM) Workshop on Mobility Management in the Networks of the Future World (MobiWorld 2011)*, Apr. 2011, pp. 413-418.

[40] H. A. Omar, W. Zhuang, A. Abdrabou, and L. Li, "Performance evaluation of VeMAC supporting safety applications in vehicular networks," *IEEE Transactions on Emerging Topics in Computing*, vol. 1, no. 1, pp. 69-83, Jun. 2013.

[41] H. A. Omar, W. Zhuang, and L. Li, "Delay analysis of VeMAC supporting periodic and event-driven safety messages in VANETs," in *Proc. IEEE Global Communications Conference (GLOBECOM)*, Dec. 2013.

[42] H. A. Omar, W. Zhuang, and L. Li, "On Multihop Communications For In-Vehicle Internet Access Based On a TDMA MAC Protocol," *Proc. IEEE International Conference on Computer Communications (INFOCOM)*, Apr. 2014.

[43] H. A. Omar, W. Zhuang, and L. Li, "Gateway placement and packet routing for multihop in-vehicle Internet access," *IEEE Transactions on Emerging Topics in Computing*, 2014 (to be submitted).

[44] "Dedicated short range communications (DSRC) message set dictionary," *SAE J2735 Standard*, Nov. 19, 2009.

[45] F. Zaid, F. Bai, S. Bai, C. Basnayake, B. Bellur, S. Brovold, G. Brown, L. Caminiti, D. Cunningham, H. Elzein, J. Ivan, D. Jiang, J. Kenny, H. Krishnan, J. Lovell, M. Maile, D. Masselink, E. McGlohon, P. Mudalige, V. Rai, J. Stinnett, L. Tellis, K. Tirey, and S. VanSickle, "Vehicle safety communications-applications (VSC-A) second annual report," The CAMP Vehicle Safety Communications 2 Consortium, Tech. Rep. DOT HS 811 466, Aug. 2011.

[46] K. Kutzner, J.-J. Tchouto, M. Bechler, L. Wolf, B. Bochow, and T. Luckenbach, "Connecting vehicle scatternets by Internet-connected gateways," in *Proc. Workshop on Multiradio Multimedia Communications (MMC 2003)*, University of Dortmund, Germany, 2003. [Online]. Available: http://i30www.ira.uka.de/research/publications/p2p/

[47] "A recursive solution to an occupancy problem resulting from TDM radio communication application," *Applied Mathematics and Computation*, vol. 101, no. 1, pp. 1–3, Jun. 1999.

[48] http://nsnam.isi.edu/nsnam/index.php/Main_Page.

[49] http://vision-traffic.ptvgroup.com/en-uk/products/ptv-vissim/.

[50] D. V. Lindley, "The theory of queues with a single server," *Mathematical Proceedings of the Cambridge Philosophical Society*, vol. 48, pp. 277–289, 1952.

[51] D. Bertsekas and R. Gallager, *Data networks*. Upper Saddle River, NJ, USA: Prentice-Hall, Inc., 1987.

[52] L. D. Servi, "D/G/1 queues with vacations," *Operations Research*, vol. 34, no. 4, pp. 619–629, 1986.

[53] W. Song and W. Zhuang, "Performance analysis of probabilistic multipath transmission of video streaming traffic over multi-radio wireless devices," *IEEE Transactions on Wireless Communications*, vol. 11, no. 4, pp. 1554 –1564, Apr. 2012.

[54] https://code.google.com/p/vemac/.

[55] PTV Planung Transport Verkehr AG, *VISSIM 5.40-User Manual*, 2012.

[56] http://youtu.be/48daRU6ZpjI.

[57] http://youtu.be/GjYWe7eLJ3s.

[58] R. Wiedemann, "Modeling of RTI-Elements on multi-lane roads," in *Advanced Telematics in Road Transport, Proc. the Drive Conference*, Feb. 1991.

[59] Y.-C. Cheng and T. Robertazzi, "Critical connectivity phenomena in multihop radio models," *IEEE Transactions on Communications*, vol. 37, no. 7, pp. 770–777, 1989.

[60] N. Bailey, "On queueing processes with bulk service," *Journal of the Royal Statistical Society. Series B (Methodological)*, vol. 16, no. 1, pp. 80–87, 1954.

[61] http://www.gurobi.com/.

[62] J. Löfberg, "YALMIP: A toolbox for modeling and optimization in MATLAB," in *Proc. of the CACSD Conference*, Taipei, Taiwan, 2004. [Online]. Available: http://users.isy.liu.se/johanl/yalmip

[63] http://www.youtube.com/watch?v=zaLJWfTHG8s.

[64] A. D. May, *Traffic flow fundamentals*. Englewood Cliffs, N.J: Prentice Hall, 1990.